

Analytical and Numerical Analyses for Rock Slope Stability Using the Generalized Hoek-Brown Criterion

Jiayi Shen

A thesis submitted for the degree of
Doctor of Philosophy



School of Civil, Environmental and Mining Engineering
The University of Adelaide
Australia

July 2013

To my parents

Meihua and Binying

Statement of Originality

I certify that this work contains no material which has been accepted for the award of any other degree or diploma in any university or other tertiary institution and, to the best of my knowledge and belief, contains no material previously published or written by another person, except where due reference has been made in the text. In addition, I certify that no part of this work will, in the future, be used in a submission for any other degree or diploma in any university or other tertiary institution without the prior approval of the University of Adelaide and where applicable, any partner institution responsible for the joint-award of this degree.

I give consent to this copy of my thesis when deposited in the University Library, being made available for loan and photocopying, subject to the provisions of the Copyright Act 1968.

The author acknowledges that copyright of published works contained within this thesis resides with the copyright holder(s) of those works.

I also give permission for the digital version of my thesis to be made available on the web, via the University's digital research repository, the Library catalogue and also through web search engines, unless permission has been granted by the University to restrict access for a period of time.

Name: Jiayi Shen

Signature:

Date: 17th July 2013

Acknowledgments

I gratefully acknowledge my supervisors Dr. Murat Karakus, Associate Prof. Chaoshui Xu and Prof. Stephen Priest, for their invaluable guidance, encouragement and constructive criticism during my candidature period. Without their great contribution this thesis would not be possible. I am particularly grateful to Dr. Murat Karakus for not only gives research supports but also offers encouragement and emotional supports in the past three years.

I would like to sincerely thank the China Scholarship Council and the University of Adelaide for providing the joint PhD scholarship.

I would like to express my gratitude to Mrs Barbara Brougham for editing the submitted and published journal papers which are composed of the thesis.

Many thanks go to Associate Prof. Rafael Jimenez for supervision and cooperation on the rock failure criterion research topic when I was a visiting scholar in the E.T.S.I Caminos, Canales y Puertos at the Universidad Politécnica de Madrid, Spain.

Many thanks go to Prof. Jian Zhao for hosting me as a visiting scholar at Laboratory for Rock Mechanics at the Swiss Federal Institute of Technology Lausanne, Switzerland.

Many thanks go to all the staff of the School of Civil, Environmental and Mining Engineering for their individual help and support. I am especially grateful to Dr. Stephen Carr for helping to install research softwares and for providing IT supports.

Finally, I would also like to thank my parents, for supporting me emotionally during my PhD research.

Introduction

Design of rock slope is one of the major challenges at every stage of open pit mining operations. Providing an optimal excavation design based on a robust analysis in terms of safety, ore recovery and profit is the ultimate goal of any slope design. The rock slope stability is predominantly controlled by the strength and deformation of the rock mass which characteristically consists of intact rock materials and discontinuities. Initially, movement of the slope occurs due to stress relaxation as a result of removal of rocks which used to provide confinement. This behavior of slope can be attributed to linear elastic deformation. In addition to this, sliding along discontinuity surfaces and dilation in consequence of formation of cracks can occur. Ultimately all these instabilities lead to failure of the slopes. Therefore, formulation of slope designs plays critical role in the process of slope stability. In conventional approaches for assessing the stability of a homogeneous slope, such as the limit equilibrium method (LEM) and shear strength reduction (SSR) method, rock mass strength is usually expressed by the linear Mohr-Coulomb (MC) criterion. However, rock mass strength is a non-linear stress function. Therefore, the linear MC criterion generally do not agree with the rock mass failure envelope, especially for slope stability problems where the rock mass is in a state of low confining stresses that make the nonlinearity more dominant.

With the aim of better understanding the fundamental rock slope failure mechanisms and improving the accuracy of the rock slope stability results, this research focuses on the application of the Hoek-Brown (HB) criterion, which can ideally represent the non-linear behavior of a rock mass, on the rock slope stability analysis.

There, three major sections are available in the thesis. The first section, from Chapters 1 to 4, proposes new methods for estimating the intact rock and rock mass properties, which will be

used for slope stability analysis. In the second section studied in Chapter 5, a new non-linear shear strength reduction technique is proposed for the analysis of three-dimensional (3D) slope modeling. In section three (Chapter 6), novel stability charts are proposed, which have the merit of estimating factor of safety (FOS) for a given slope directly from the HB parameters and rock mass properties. These charts can provide a quick and reliable assessment of rock slope stability.

The major research contributions and outcomes of the overall researches are presented in six journal publications which are forming the thesis. The titles of Chapters 1 through 6 reflect the titles of the journal papers.

In Chapter 1, laboratory tests conducted on Hawkesbury sandstone obtained from New South Wales are carried out to investigate the relationship between the HB constant m_i and uniaxial compressive strength (UCS) of intact rock. Based on the analysis of the laboratory tests and the existing database, a new method that can estimate the HB constant m_i values from UCS and rock types is proposed. The proposed method can reliably be used in the HB criterion for intact rock strength estimation when the triaxial tests are not available.

In Chapter 2, an analytical solution for estimating the instantaneous MC shear strength from the HB failure criterion for highly fractured rock mass is presented. The proposed solution is based on the assumption that the HB parameter, s is equal to zero. The proposed solution has the merit of producing very accurate shear strength for highly fractured rock mass where the Geological Strength Index (GSI) is less than 40.

In Chapter 3, an analytical solution, which can calculate the shear strength of rock masses accurately for the whole range GSI values, is proposed as an extension to the work in Chapter 2. The proposed approach is based on a symbolic regression analysis performed by genetic programming (GP). The proposed solution not only can be implemented into the LEM to

calculate the instantaneous shear strength of each slice of a failure surface under a specified normal stress, but also can be implemented into finite element method performed by SSR approach to calculate the instantaneous shear strength of each element under different stress state of a slope.

In Chapter 4, as a part of estimating rock mass strength and elastic properties in the first section, the most widely used empirical equations for the estimation of deformation modulus of rock masses (E_m) are reviewed. Two simplified empirical equations for estimating of E_m are also presented. The proposed empirical equations use the Rock Mass Rating classification system and the deformation modulus of intact rock (E_i) as input parameters. These equations can be used in the numerical modelling for slope stability analysis, which is conducted in Chapter 5.

In Chapter 5, a new non-linear shear strength reduction technique is proposed to analysis the stability of 3D rock slopes satisfying the HB failure criterion. The method for estimating the instantaneous MC shear strength from the HB criterion described in Chapters 2 and 3 are used to estimate shear strength of elements in FLAC^{3D} model. The proposed 3D slope model is used to analyse the influence of boundary condition on the calculation of FOS using 21 real open pit cases where the values of m_i and E_m values are calculated from the methods introduced in Chapters 1 and 4, respectively. Results show that the values of FOS for a given slope will be significantly influenced by the boundary condition, especially the case where the slope angle is less than 50°.

In Chapter 6, extensive slope stability analyses using LEM are carried out. The calculation of FOS is based on estimating the instantaneous MC shear strength of slices of a slip surface from the HB criterion. Based on the analysis results, novel stability charts are proposed. The proposed charts are able to estimate the FOS for a given slope directly from the HB parameters,

slope geometry and rock mass properties. It is suggested that the proposed charts can be used as useful tools for the preliminary rock slope stability assessment.

List of contents

Statement of Originality.....	VI
Acknowledgments.....	VIII
Introduction.....	X
List of Tables	XVI
List of Figures	XVIII
List of Symbols	XXIV
Chapter 1 A New Method for Estimating the Hoek-Brown Constant for Intact Rocks	3
Chapter 2 Determination of Mohr-Coulomb Shear Strength Parameters from Generalized Hoek-Brown Criterion for Slope Stability Analysis	29
Chapter 3 Direct Expressions for Linearization of Shear Strength Envelopes Given by the Generalized Hoek-Brown Criterion Using Genetic Programming.....	51
Chapter 4 A Comparative Study for Empirical Equations in Estimating Deformation Modulus of Rock Masses	81
Chapter 5 Three-Dimensional Numerical Analysis for Rock Slope Stability Using Non-linear Shear Strength Reduction Method	107
Chapter 6 Chart-Based Slope Stability Assessment Using the Generalized Hoek-Brown Criterion	137
Chapter 7 Conclusions and Recommendations for Further Work.....	175

List of Tables

Table A (Table 1 in Chapter 1) Estimated m_i values by regression analysis using triaxial test data at different confining stresses.....	8
Table B (Table 2 in Chapter 1) Best fit m_c and m_d constants to estimate m_{in} using σ_{ci} for specific rock types	15
Table C (Table 3 in Chapter 1) Comparison of the prediction performance of different methods using the sandstone laboratory test data	19
Table D (Table 1 in Chapter 2) Shear stresses obtained from Priest and Bray solutions over a range of GSI.....	35
Table E (Table 2 in Chapter 2) Range of input parameters.....	38
Table F (Table 3 in Chapter 2) Data for validation of the proposed approximate solution.....	39
Table G (Table 4 in Chapter 2) Comparison results of shear strength parameters with different methods.....	43
Table H (Table 1 in Chapter 3) Parameters used in GP analysis.....	63
Table I (Table 2 in Chapter 3) Range of input parameters.....	65
Table J (Table 3 in Chapter 3) Data of HB criterion for GP analysis.....	66
Table K (Table 4 in Chapter 3) Shear stresses obtained from numerical and GP analytical solutions over a range of normal stresses.....	71
Table L (Table 1 in Chapter 4) Empirical equations using RMR and GSI for predicting E_m	85
Table M (Table 1 in Chapter 5) 3D slope stability analysis using different methods.....	109
Table N (Table 2 in Chapter 5) Comparison of failure surfaces corresponding to FOS values using different convergence criteria	119
Table O (Table 3 in Chapter 5) Input parameters of a slope case.....	121

Table P (Table 4 in Chapter 5) Comparison of failure surfaces, contours of c and ϕ and FOS of a slope model under various boundary conditions.....	122
Table Q (Table 5 in Chapter 5) The results of FOS and f_B of the slope with different slope angle.....	124
Table R (Table 6 in Chapter 5) The results of FOS and f_B of real slope cases.....	126
Table S (Table 1 in Chapter 6) Comparison of the factor of safety estimated from different stability charts	145
Table T (Table 2 in Chapter 6) Slope modeling setting in <i>Slide 6.0</i>	146
Table U (Table 3 in Chapter 6) Comparison of the FOS of a given slope with the same value of SR.....	150
Table V (Table 4 in Chapter 6) Comparison of the FOS of a given rock slope with various Hoek-Brown parameters.....	151
Table W (Table 5 in Chapter 6) Three slope examples analyzed using the proposed stability charts.....	169

List of Figures

Figure A (Fig. 1 in Chapter 1) The Hoek-Brown failure envelopes using different m_i values.....	8
Figure B (Fig. 2 in Chapter 1) Comparison of sensitivities to the confining stress range employed for m_i fitting, as indicated by the T parameter	9
Figure C (Fig. 3 in Chapter 1) Distribution of m_i values for sandstone.....	11
Figure D (Fig. 4 in Chapter 1) Correlation between R and m_i , after Read and Richards (2011) ..	12
Figure E (Fig. 5 in Chapter 1) Correlation between m_{in} and σ_{ci} for 28 rock types.....	13
Figure F (Fig. 6 in Chapter 1) Rock strength prediction performance using Eq. 7 for general rock types.....	14
Figure G (Fig. 7 in Chapter 1) Correlation between m_{in} and σ_{ci} for specific rock types corresponding to their rock strength prediction performances.....	16
Figure H (Fig. 8 in Chapter 1) Comparison of experimental rock strength with predicted rock strength using different methods.....	18
Figure I (Fig. 9 in Chapter 1) Cumulative distribution function (CDF) of prediction errors (AAREP) of different methods using five rock types in Table 2.....	21
Figure J (Fig. 1 in Chapter 2) (a) Major and minor principal stresses for the HB criterion, (b) Normal and shear stresses for the HB criterion.....	32
Figure K (Fig. 2 in Chapter 2) Shear stress versus GSI.....	34
Figure L (Fig. 3 in Chapter 2) Priest numerical versus proposed approximate analytical value of ϕ	40
Figure M (Fig. 4 in Chapter 2) Priest numerical versus proposed approximate analytical value of τ/σ_{ci}	41

Figure N (Fig. 5 in Chapter 2) Priest numerical versus proposed approximate analytical value of c/σ_{ci}	42
Figure O (Fig. 6 in Chapter 2) Comparison of angle of friction ϕ results	44
Figure P (Fig. 7 in Chapter 2) Comparison of cohesion c results.....	45
Figure Q (Fig. 8 in Chapter 2) Comparison of shear stress τ results.....	46
Figure R (Fig. 1 in Chapter 3) (a) The basic of method of slices, (b) Forces acting on a given slice.....	52
Figure S (Fig. 2 in Chapter 3) The MC criterion showing shear strength defined by angle of friction ϕ and cohesion c	53
Figure T (Fig. 3 in Chapter 3) (a) Maximum and minimum principal stresses for the GHB criterion, (b) Normal and shear stresses for the GHB criterion [27]	56
Figure U (Fig. 4 in Chapter 3) A typical tree structure of the function of $x*y-\sin(z)$	60
Figure V (Fig. 5 in Chapter 3) A basic flow chart for GP.....	60
Figure W (Fig. 6 in Chapter 3) Crossover operation in genetic programming.....	62
Figure X (Fig. 7 in Chapter 3) Mutation operation in genetic programming.....	62
Figure Y (Fig. 8 in Chapter 3) Numerical versus GP value of τ/σ_{ci}	68
Figure Z (Fig. 9 in Chapter 3) Discrepancy analysis of the proposed analytical solution.....	69
Figure AA (Fig. 10 in Chapter 3) Discrepancy analysis of the analytical solution which has the lowest value of AAREP.....	70
Figure BB (Fig. 11 in Chapter 3) Hoek-Brown shear strength envelope in shear stress/normal stress space.....	72
Figure CC (Fig. 12 in Chapter 3) Comparison of shear stress τ results.....	73

Figure DD (Fig. 1 in Chapter 4) Empirical equations in Group 1 for estimating E_m compared with <i>in-situ</i> data.....	88
Figure EE (Fig. 2 in Chapter 4) Empirical equations in Group 2 for estimating E_m / E_i compared with <i>in-situ</i> data.....	89
Figure FF (Fig. 3 in Chapter 4) Empirical equations in Group 3 for estimating E_m compared with <i>in-situ</i> data.....	91
Figure GG (Fig. 4 in Chapter 4) Empirical equations in Group 4 for estimating E_m / E_i compared with <i>in-situ</i> data.....	92
Figure HH (Fig. 5 in Chapter 4) Empirical equations in Group 5 for estimating E_m compared with <i>in-situ</i> data, $\sigma_{ci}=80\text{MPa}$	93
Figure II (Fig. 6 in Chapter 4) Plot the Eq. 4 for the <i>in-situ</i> data.....	95
Figure JJ (Fig. 7 in Chapter 4) Estimated E_m values from Eq. 4 versus <i>in-situ</i> data.....	96
Figure KK (Fig. 8 in Chapter 4) Plot the Eq. 5 for the <i>in-situ</i> data.....	97
Figure LL (Fig. 9 in Chapter 4) Estimated E_m / E_i values from Eq. 5 versus <i>in-situ</i> data.....	98
Figure MM (Fig. 10 in Chapter 4) E_m values estimated from Eq. 4 compared with Hoek and Diederichs (2006) <i>in-situ</i> data.....	99
Figure NN (Fig. 11 in Chapter 4) E_m / E_i values estimated from Eq. 5 compared with Hoek and Diederichs (2006) <i>in-situ</i> data.....	100
Figure OO (Fig. 1 in Chapter 5) Instantaneous MC envelope of the HB criterion in the normal and shear stress plane.....	112
Figure PP (Fig. 2 in Chapter 5) The correlations between MC parameters and σ_3	114
Figure QQ (Fig. 3 in Chapter 5) Flow chart of the application of HB criterion into FLAC ^{3D} using non-linear SSR technique.....	116

Figure RR (Fig. 4 in Chapter 5) Boundary conditions for a slope model.....	118
Figure SS (Fig. 5 in Chapter 5) Plot of FOS values versus mesh elements.....	120
Figure TT (Fig. 6 in Chapter 5) The correlations between f_B and β under different boundary conditions for a slope case.....	124
Figure UU (Fig. 7 in Chapter 5) The correlations between f_B and β under different boundary conditions for open pit cases.....	127
Figure VV (Fig. 8 in Chapter 5) The correlations between $f_{B,xy}$ and H, σ_{ci}, GSI, m_i	128
Figure WW (Fig. 1 in Chapter 6) Relationship between HB and equivalent MC envelopes	141
Figure XX (Fig. 2 in Chapter 6) Slope stability chart ($\beta=45^\circ, a=0.5$) [12]	142
Figure YY (Fig. 3 in Chapter 6) (a) Slope stability chart with $D=0$ [13], (b) Slope stability chart with $D=0.7$ [14], (c) Slope stability chart with $D=1.0$ [14]	143
Figure ZZ (Fig. 4 in Chapter 6) (a) The basic of method of slices, (b) Stresses acting on a given slice.....	148
Figure AAA (Fig. 5 in Chapter 6) Proposed stability charts for rock mass slope, $\beta=45^\circ, D=0$ ($5 \leq m_i \leq 35$)	155
Figure BBB (Fig. 6 in Chapter 6) Proposed stability charts for rock mass slope, $\beta=45^\circ, D=0$ (SR=0.1, 1, 10, 40)	156
Figure CCC (Fig. 7 in Chapter 6) (a) Relationship between c/σ_{ci} and GSI for different m_i values [29], (b) Relationship between ϕ and GSI for different m_i values [29]	157
Figure DDD (Fig. 8 in Chapter 6) Alternative form of Fig. 6b using the stability number N ...	158
Figure EEE (Fig. 9 in Chapter 6) Chart for estimating disturbance weighting factor f_D , SR=10, $\beta=45^\circ$	160

Figure FFF (Fig. 10 in Chapter 6) Chart for estimating disturbance weighting factor, f_D ($m_i=5, 15, 25, 35$)	164
Figure GGG (Fig. 11 in Chapter 6) Slope angle weighting factor chart.....	165
Figure HHH (Fig. 12 in Chapter 6) Discrepancy analysis of the proposed rock slope stability charts.....	166

List of Symbols

a	Hoek-Brown input parameter for the rock mass
c	Cohesion
D	Disturbance factor
E_i	Deformation modulus of the intact rock
E_m	Deformation modulus of the rock mass
f_B	Boundary weighting factor
f_D	Disturbance weighting factor
f_β	Slope angle weighting factor
H	Slope height
m_b	Hoek-Brown input parameter for the rock mass
m_i	Hoek-Brown constant for the intact rock
m_{in}	Normalized m_i for the Hoek-Brown criterion
m_c	Constant for calculating m_{in}
m_d	Constant for calculating m_{in}
s	Hoek-Brown input parameter for the rock mass
β	Slope angle
ϕ	Angle of friction
γ	Unit weight of the rock mass
ν	Poisson's ratio
σ_1	Major principal stress
σ_3	Minor principal stress
σ_{ci}	Uniaxial compressive strength of the intact rock

- σ_n Normal stress
- σ_t Tensile strength of the intact rock
- τ Shear stress

Statement of Authorship of Journal paper 1

A New Method for Estimating the Hoek-Brown Constant for Intact Rocks

Jiayi Shen * & Murat Karakus

School of Civil, Environmental and Mining Engineering, The University of Adelaide

Adelaide, South Australia, 5005, Australia

Journal of Geotechnical and Geoenvironmental Engineering (ASCE)

Submitted 18th February 2013

(Under review)

By signing the Statement of Authorship, each author certifies that their stated contribution to the publication is accurate and that permission is granted for the publication to be included in the candidate's thesis.

Jiayi Shen

Performed the analysis, wrote the manuscript and acted as corresponding author.

Signature:

Date: 27th May 2013

Dr. Murat Karakus

Supervised development of work and manuscript evaluation.

Signature:

Date: 27th May 2013

Chapter 1

A New Method for Estimating the Hoek-Brown Constant for Intact Rocks

Abstract

The constant m_i is one of the fundamental parameters required for the Hoek-Brown (HB) criterion to estimate the strength of rock materials. In order to calculate m_i values a range of triaxial tests need to be carried out. However, triaxial tests are time-consuming and expensive, and they are not always routinely conducted at the early stage of a project. In this research, we investigate five common rock types and propose a simplified method that can estimate m_i values using the information of rock types and the uniaxial compressive strength (UCS) of intact rocks. In order to evaluate the reliability of proposed method, m_i values estimated from the proposed method are used in the HB criterion to predict intact rock strength. The predicted intact rock strength is then tested against experimental intact rock strength using 908 sets of triaxial tests together with our laboratory tests. Results from the comparison show that m_i values calculated from the proposed method can reliably be used in the HB criterion for estimation of intact rock strength, with small discrepancies between estimated and experimental strength, when triaxial test data are not available.

1 Introduction

The Hoek-Brown (HB) criterion (see Eq. 1), which was initially proposed by Hoek and Brown (1980) for estimating intact rock strength, requires two intact rock properties, namely, the

uniaxial compressive strength (UCS) of the intact rock σ_{ci} and a constant of the intact rock m_i .

$$\sigma_1 = \sigma_3 + \sigma_{ci} \left(m_i \frac{\sigma_3}{\sigma_{ci}} + 1 \right)^{0.5} \quad (1)$$

Further, it was extended to estimate the rock mass strength by using the Geological Strength Index (GSI) and a disturbance factor D to reduce intact rock properties (Hoek et al. 2002). Currently, the HB criterion, whose input parameters can be directly estimated from the measurement of rock mass fracture characteristics (GSI), disturbance condition (D) and intact rock properties (σ_{ci} and m_i), is widely used in rock engineering (Priest 2005; Jimenez et al. 2008; Shen et al. 2012). The details of application and selection of GSI and D can be found in the papers by Marinos et al. (2005) and Hoek and Diederichs (2006).

For the intact properties, the parameter m_i depends upon the frictional characteristics of the component minerals in the intact rock and it has a significant influence on the rock strength (Hoek and Marinos 2000). Regression analysis of triaxial tests over a range of confining stress σ_3 can be employed to estimate the values of m_i . However, triaxial tests require time-consuming testing procedures, and they are not always routinely conducted at the early stage of a project (Cai 2010). On the other hand, the traditional compressive tests of cylindrical specimens can be carried out easily and economically. The value of σ_{ci} can also be predicted from the point-load index test using unprepared rock cores or non-destructive testing methods, such as the sound velocity tests (Karakus and Tutmez 2004; Karakus et al. 2005). Therefore, it is useful to develop a simplified method that m_i values can be estimated from UCS values in the absence of triaxial tests. Based on the analysis of extensive triaxial tests in the database, here, we propose a simplified method that can estimate m_i values using only UCS and rock types.

In this paper, the database and indicators to assess prediction performance of the available methods that estimate m_i values are introduced in section 2. The existing methods for estimating m_i values are reviewed in section 3. The proposed method and validation are presented in section 4. The prediction performance of the proposed and existing methods is compared in section 5.

2 Database and prediction performance indicators

We collected an extensive database of triaxial tests for intact rocks from Singh et al. (2011) and ‘RocData’ (2012). The database compiled by Singh et al. (2011), without the inclusion of tensile strength tests, includes 1190 sets of triaxial tests corresponding to 158 groups of data. The database we collected from ‘RocData’(2012) includes 908 sets of triaxial and tensile strength tests corresponding to 112 groups of data.

The strategy we used to evaluate the reliability of the existing and proposed methods is that: m_i values calculated from different methods are used in the HB criterion to estimate the values of intact rock strength σ_{1_est} under confining stresses σ_{3_test} for a given group of triaxial test (σ_{1_test} , σ_{3_test}) data. The estimated rock strength σ_{1_est} is then compared with that from the experimental rock strength σ_{1_test} . The coefficient of determination (R^2), discrepancy percentage (D_p) and absolute average relative error percentage (AAREP) are adopted as indicators to assess the rock strength prediction. Their definitions are shown in Eqs. 2 to 4.

$$R^2 = 1 - \frac{\sum_{i=1}^N (\sigma_{1_test}^i - \sigma_{1_est}^i)^2}{\sum_{i=1}^N (\sigma_{1_test}^i - \bar{\sigma}_{1_test})^2} \quad (2)$$

$$D_p = \frac{\sigma_{1_est}^i - \sigma_{1_test}^i}{\sigma_{1_test}^i} \times 100\% \quad (3)$$

$$AAREP = \frac{\sum_{i=1}^N \left| \frac{\sigma_{1_test}^i - \sigma_{1_est}^i}{\sigma_{1_test}^i} \right|}{N} \quad (4)$$

where N is the number of testing data used, $\sigma_{1_test}^i$ and $\sigma_{1_est}^i$ are the intact rock strength, as obtained from the experimental data and derived from the HB failure criterion in which m_i values are calculated from different methods. $\bar{\sigma}_{1_test}$ is the mean value of the experimental σ_{1_test} values. By definition, the smaller the AAREP is, the more reliable the estimation. D_p is the relative difference between predicted and experimental values.

3 The review of existing methods for estimating m_i values

There are three methods (regression analysis, guidelines and R index) commonly used for estimating the Hoek-Brown constant m_i values. The most accurate method that can give best rock strength estimates is to carry out regression analysis of triaxial test data. In the absence of triaxial tests, m_i values can also be obtained from guidelines proposed by Hoek and Brown (1980) and Hoek (2007). The R index, the ratio of σ_{ci} to tensile strength σ_t , was also suggested by many researchers as an alternative way to estimate m_i values when triaxial tests are not available. There is also another new method proposed by Cai (2010) for the prediction of m_i directly from the UCS of the intact rock, in which m_i values depend on the ratio of crack initiation stress obtained using acoustic emission techniques to the peak strength. However, the existing triaxial tests in the database do not include the crack initiation stress of rock samples. Therefore, Cai's method will not be adopted for the comparison study in this research.

3.1 Regression method

In order to obtain the best rock strength prediction, Hoek and Brown (1997) suggested that the values of m_i should be calculated over a confining stress σ_3 range from 0 to $0.5 \sigma_{ci}$ by using

regression methods, and at least five sets of triaxial tests should be included in regression analysis. Read and Richards (2011) suggested that the most accurate method of assessing m_i values is regression analysis (including triaxial, uniaxial compressive and tensile tests) within the confining stress range from σ_i to $0.5\sigma_{ci}$.

Given that m_i values calculated from statistical analysis, the reliability of the calculated m_i values depend on the quantity and quality of testing data used in the regression method. Research by Singh et al. (2011) indicated that the range of confining stress σ_3 can have a significant influence on the calculation of m_i . Table 1 shows a comparison study on the calculation of m_i values from different confining stress σ_3 for limestone conducted by Schwartz (1964). The values of m_i calculated using different combinations of data sets are shown in Table 1. For example, if the first three data sets are selected m_i would be equal to 5.16. However, if all eleven data points are used m_i value will then be 1.21. The value of T in Table 1 represents the ratio of the maximum to the minimum of m_i value, for example, $T=m_{i_max}/m_{i_min}=5.16/1.21=4.26$ in this case. T is equal to 1 means there is no variation in the parameter m_i , although different sets of data are used.

Table 1 Estimated m_i values by regression analysis using triaxial test data at different confining stresses

Data sets (N)	σ_3 [MPa]	σ_1 [MPa]	m_i	R^2	AAREP %
1	0	44	-	-	-
2	6.5	66	-	-	-
3	13.7	85	5.16	0.52	12.65
4*	20.3	99	4.63	0.67	10.58
5	27.9	109	3.53	0.88	7.15
6	34.4	119	2.97	0.93	6.65
7	41.2	128.2	2.54	0.94	6.95
8	48.4	135.1	2.07	0.91	8.30
9	55.4	141.9	1.68	0.84	11.09
10	62.3	149.1	1.40	0.77	13.53
11	68.4	156.5	1.21	0.71	15.17
T			4.26		

*Last test for which $\sigma_3 \leq 0.5\sigma_{ci}$

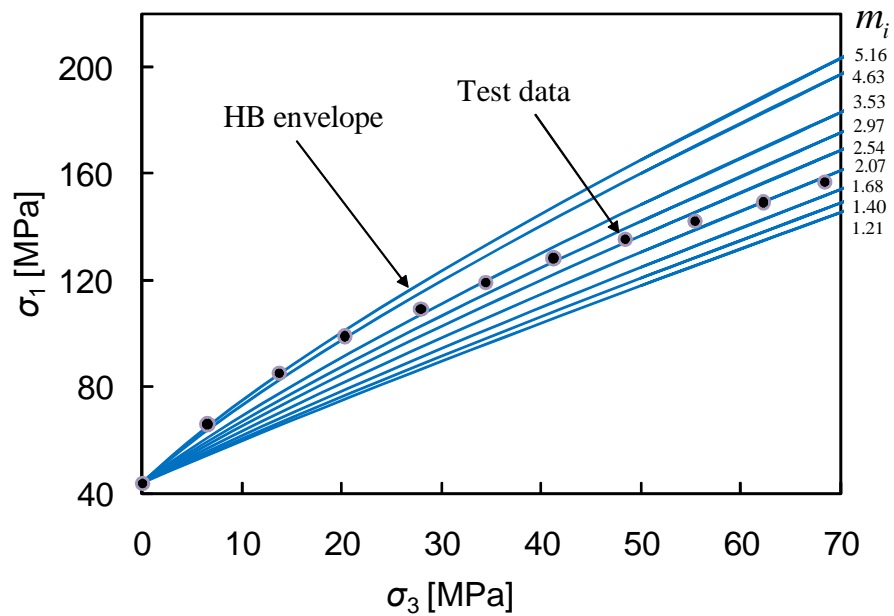


Fig. 1 The Hoek-Brown failure envelopes using different m_i values

The results show that in this case the value of m_i calculated from the regression method over a confining stress σ_3 range from 0 to $0.8\sigma_{ci}$ ($N=6$) gives the best rock strength prediction with AAREP= 6.65%, compared with the suggested range from 0 to $0.5\sigma_{ci}$ ($N=4$) which has AAREP=10.58%. It should be noted that if all the data points ($N=11$) are selected where σ_3 range from 0 to $1.6\sigma_{ci}$ the value of AAREP is up to 15.17%.

To extend the analysis to other triaxial tests for various rock types, the sensitivity of m_i was tested using a large database compiled by Singh et al. (2011). Histogram in Fig. 2 shows T values distribution for a complete comparison.

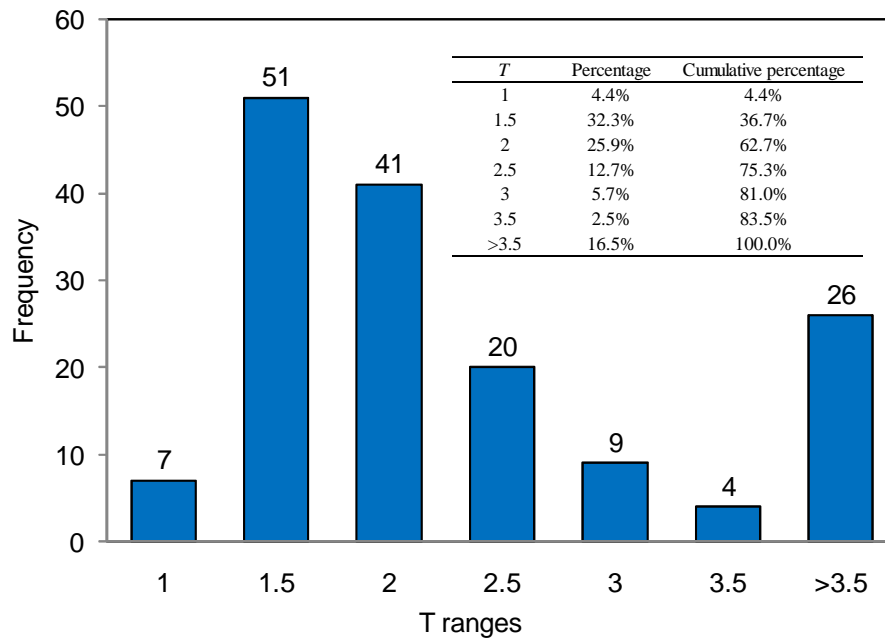


Fig. 2 Comparison of sensitivities to the confining stress range employed for m_i fitting, as indicated by the T parameter

Based on the assessment of T , the results illustrate that the parameter m_i has high sensitivity to variations in confining stress σ_3 . 37.3% of the data sets have T values greater than 2. This

statistical analysis indicates that discrepancies in the predicted values of m_i using different sets of test data can result in reducing confidence in the predicted rock strength values.

3.2 Guidelines method

The m_i values depend on many factors, such as mineral composition, grain size and cementation of rocks. According to some general pattern to the correlation between m_i and rock types, Hoek and Brown (1980) proposed guidelines m_i values for different rock types which can be used for preliminary design when triaxial tests are not available. The latest version of guidelines was proposed by Hoek (2007), associated with a more detailed lithological classification of rocks with the range of m_i values which are dependent upon the accuracy of the geological description of rock types. The relations between guidelines m_i and rock types were extensively evaluated by Mostyn and Douglas (2000) for a variety of rock types. Their comparison results showed that the correlation between guidelines and calculated m_i values is not quite strong; generally the range of calculated m_i values using the regression analysis has a much great spread than those in the guidelines.

For example, Fig. 3 shows a comparison study between m_i from guidelines and that from the regression analysis for 63 groups of data from Singh et al. (2011) and 'RockData' (2012) for sandstone. The results show that compared with the Hoek's (2007) guidelines, $m_i = 17 \pm 4$ for sandstone, only 35% of data lie in the indicated range. The minimum and maximum values of m_i are 3.9 and 36.6, respectively. Such a large variation range presents a major challenge for researchers and engineers to choose an appropriate m_i value for a specific rock type.

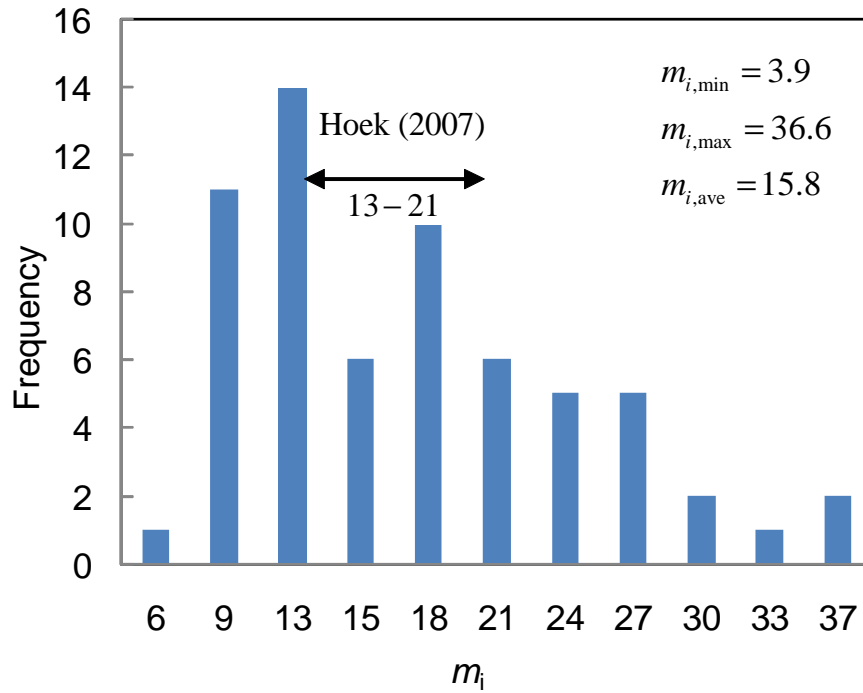


Fig. 3 Distribution of m_i values for sandstone

3.3 R index method

The R index, the ratio of σ_{ci} to tensile strength σ_t , was also suggested by many researchers (Mostyn and Douglas 2000; Douglas 2002; Cai 2010; Read and Richards 2011) as an alternative way to assess m_i values in the absence of triaxial test data. It is known that direct tensile test is not routinely carried out as a standard procedure in many rock testing laboratories because of the difficulty in specimen preparation. Therefore, indirect methods, such as Brazilian tests are widely used to estimate tensile strength in the literature. The relations between m_i and R which are calculated from direct and Brazilian tensile tests are compared as shown in Fig. 4. The solid diagonal line in the figure represents $R=m_i$. The upper and lower dash lines represent the 6 underestimate and over-estimate of the m_i values, respectively. It is found that only 4 out of 57 sets of data fall out the line $m_i = R \pm 6$, which suggested that the absolute error of m_i is ± 6 with a high

level of confidence. Fig. 4 also shows that the use of direct tensile test does not improve the prediction capability of estimating m_i values compared with Brazilian tests.

NOTE:
This figure/table/image has been removed
to comply with copyright regulations.
It is included in the print copy of the thesis
held by the University of Adelaide Library.

Fig. 4 Correlation between R and m_i , after Read and Richards (2011)

4 Proposed method for estimating m_i values

Considering that the UCS of the intact rock is one of the most important rock properties for rock engineering application and can be estimated relatively straightforward in a cost-effective way, we proposed a new method to estimate m_i values directly from the UCS when triaxial test data are not available. The HB criterion can be re-written as follows:

$$\sigma_1 = \sigma_3 + \sigma_{ci} \left(m_m \sigma_3 + 1 \right)^{0.5} \quad (5)$$

where $m_{in} = m_i/\sigma_{ci}$, is the normalized m_i for the HB criterion. Our analysis of the database showed that there is a strong correlation between m_{in} and σ_{ci} (MPa) as shown in Fig. 5.

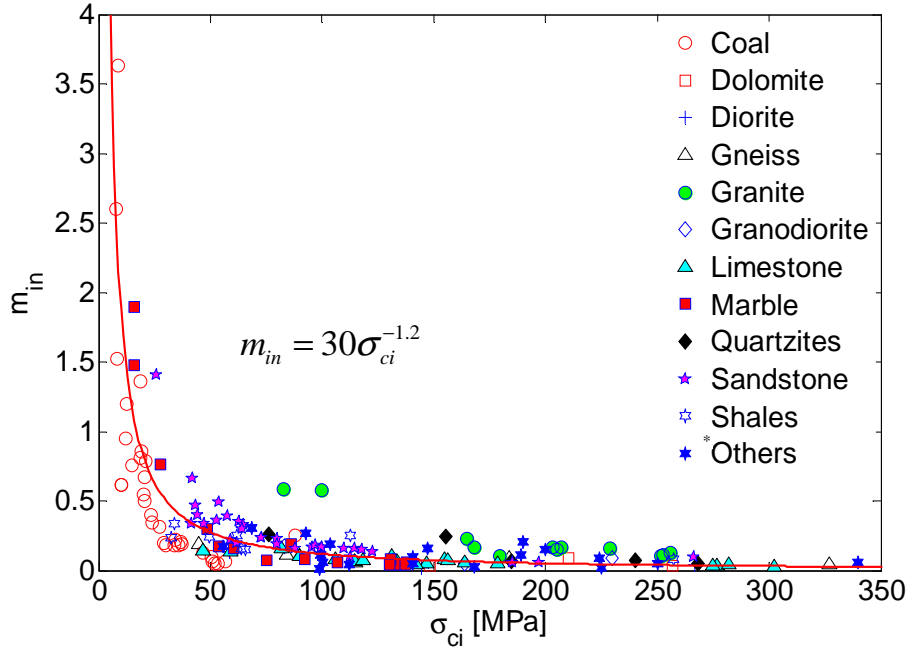


Fig. 5 Correlation between m_{in} and σ_{ci} for 28 rock types

* There are 17 rock types included in the ‘Others’ category.

Most of the data lie along the line which has a trend of decreasing m_{in} with the increase of σ_{ci} . By fitting a regression of the curve, Eq. 6 can be used to estimate m_{in} values from σ_{ci} for different rock types.

$$m_{in} = m_c \sigma_{ci}^{m_d} \quad (6)$$

where m_c and m_d are constants and their values depend on rock types. The best-fit for a general or unspecified rock type is obtained for $m_c=30$ and $m_d= -1.2$.

$$m_{in} = 30\sigma_{ci}^{-1.2} \quad (7)$$

The values of normalized m_i estimated from σ_{ci} can be employed to estimate the strength of intact rock at different confining stresses σ_3 using Eq. 5. The prediction performance of Eq. 7 for

general rock types is shown in Fig. 6 which compares estimated rock strength with experimental rock strength using 1190 sets of triaxial test data. The values of R^2 and AAREP for Eq. 7 are 0.903 and 13.55%, respectively.

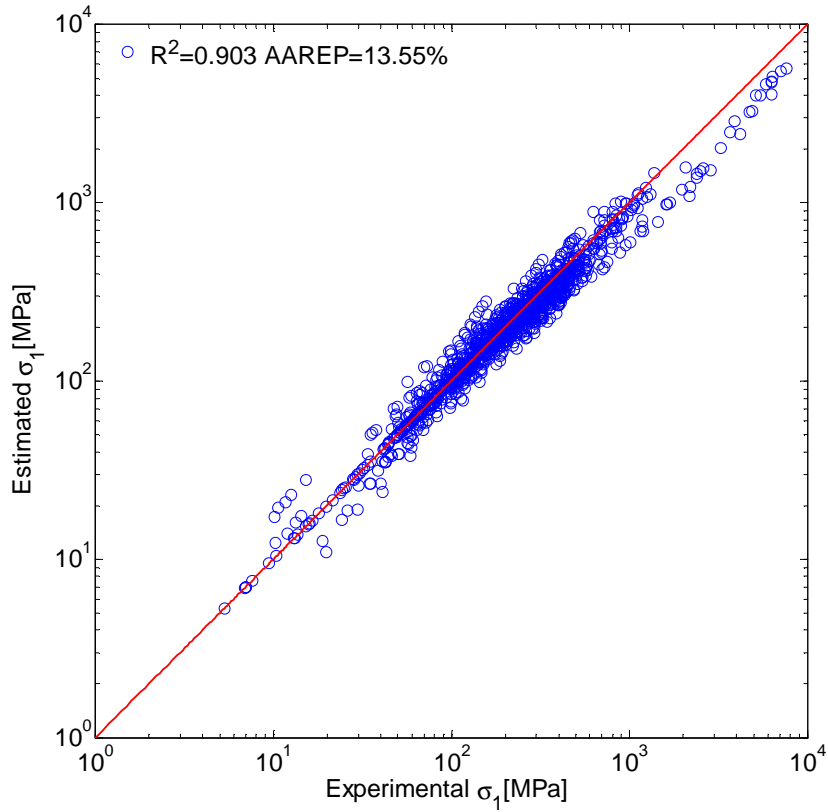


Fig. 6 Rock strength prediction performance using Eq. 7 for general rock types

To produce the correlations for specific rock types, we considered five most common rock types from the database in the ‘RocData’ (2012) in which there are at least 12 groups of data with 115 triaxial tests available. Table 2 lists the number of groups and triaxial tests available, as well as the ranges of σ_3 , σ_1 and σ_{ci} of tests for each rock type. It also presents the best-fit of m_c and m_d that can be used with Eq. 6 to estimate m_{in} for each rock type, corresponding to their rock strength prediction performance (as indicated by R^2 and AAREP values).

Table 2 Best fit m_c and m_d constants to estimate m_{in} using σ_{ci} for specific rock types

Rock Type	Data groups	Data points	σ_{ci} [MPa]		$\sigma_{3, \max}^a$ [MPa]	$\sigma_{1, \max}^b$ [MPa]	m_c	m_d	R^2	AAREP [%]
			(min)	(max)						
Coal	32	208	5.3	92.0	71.4	242.0	120	-1.70	0.92	11.55
Granite	12	115	82.9	256.0	700.0	2700.0	100	-1.20	0.99	7.88
Limestone	21	140	46.9	302.4	56.0	566.3	22	-1.15	0.93	8.38
Marble	15	136	15.8	137.8	165.0	635.0	100	-1.55	0.96	8.84
Sandstone	32	309	26.0	266.5	150.0	739.3	50	-1.26	0.95	6.95
General ^c	158	1190	5.3	507.0	3100.0	7610.0	30	-1.20	0.90	13.55

^a $\sigma_{3, \min}=0$ in all cases. ^b $\sigma_{1, \min}=\sigma_{ci, \min}$ in all cases. ^cTo be used when rock type is unknown or not specified.

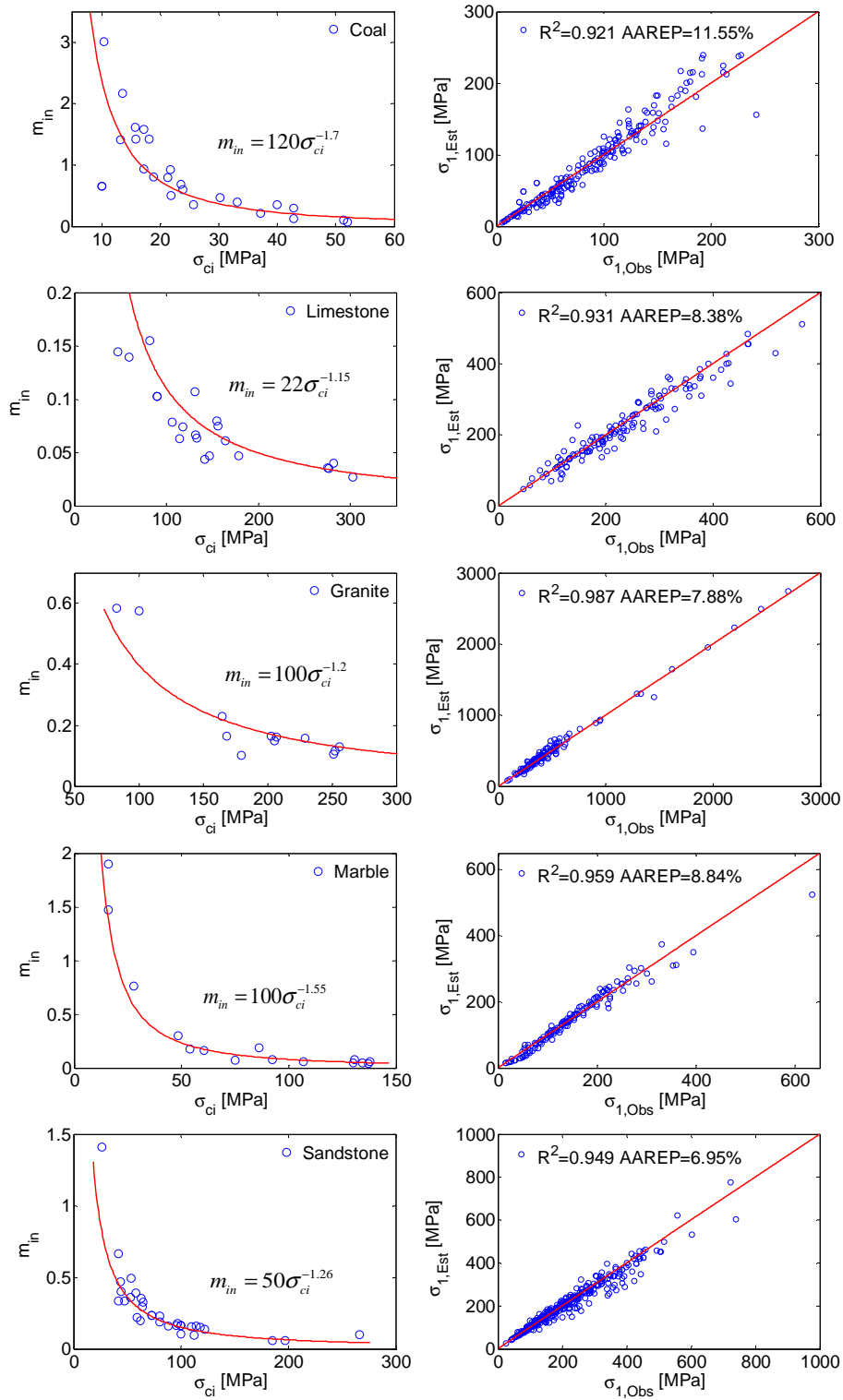


Fig. 7 Correlation between m_{in} and σ_{ci} for specific rock types corresponding to their rock strength prediction performances

Fig. 7 shows the best-fit regression curve (based on Eq. 6) that we obtained for each specified rock type; and it also compares experimental values with those predicted values using σ_{ci} and the best-fit m_c and m_d constants for each rock type.

The results show that there is a close agreement between estimated and experimental rock strength values. The values of R^2 are higher than 0.92 for all rock types, and the values of AAREP for all rock types are less than 9%, excepting coal with AAREP = 11.55%.

5 Comparison of the rock strength prediction performance

Firstly, the prediction performance of the proposed method was compared with that of the existing methods using our laboratory tests conducted on Hawkesbury sandstone obtained from New South Wales. Our laboratory tests include 32 sets of uniaxial compressive tests, 32 sets of Brazilian tensile tests and 39 sets of triaxial compression tests with confining stress σ_3 range from 2 to 21 MPa. The mean values of σ_{ci} and σ_t are 27.20 and 2.02 MPa, respectively. At least two sets of triaxial tests were carried out under a specified confining stress σ_3 , and the mean values of σ_1 for a given value of σ_3 were taken for the calculation as shown in Fig. 8.

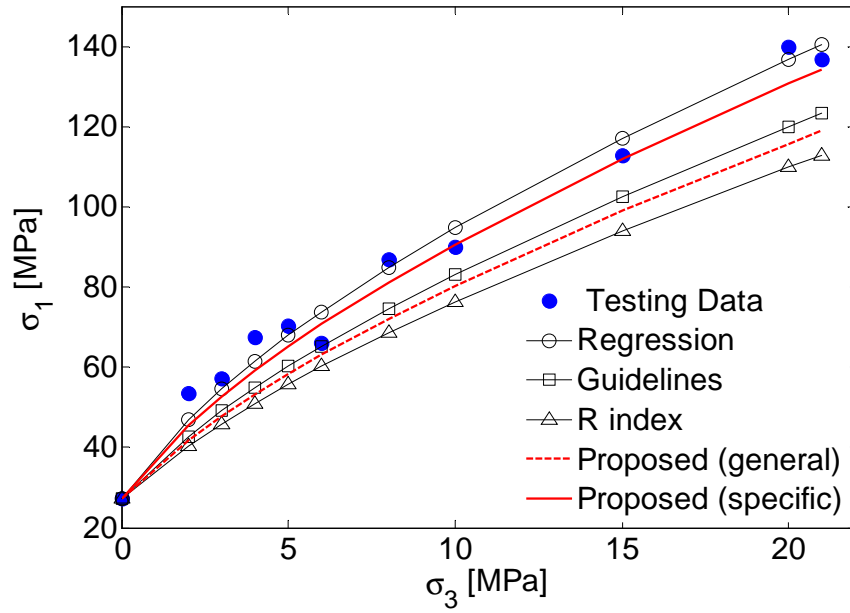


Fig. 8 Comparison of experimental rock strength with predicted rock strength using different methods

We provided two lines to show the predictions of our proposed method: one corresponds to $m_i = 15.50$ using the general rock type $m_c=30$ and $m_d = -1.2$ (see Table 2) and with $\sigma_{ci} = 27.20\text{MPa}$; the other corresponds to a value of $m_i = 21.18$ that would be obtained for a specific rock type, in this case $m_c=50$ and $m_d = -1.26$ for sandstone (see Table 2). We also provided lines for guidelines method with $m_i = 17.0$, R index method with $m_i = 13.47$ and regression method with $m_i = 23.67$ which is calculated over a confining stresses σ_3 from 0 to $0.2\sigma_{ci}$ and can give the best strength prediction. The results of such comparison study on the prediction performance of different methods are shown in Table 3.

Table 3 Comparison of the prediction performance of different methods using the sandstone laboratory test data

Test data		Regression *		Guidelines		<i>R</i> index		Proposed (general)		Proposed (specific)	
σ_3	$\sigma_{1,obs}$	$\sigma_{1,est}$	D_p	$\sigma_{1,est}$	D_p	$\sigma_{1,est}$	D_p	$\sigma_{1,est}$	D_p	$\sigma_{1,est}$	D_p
[MPa]	[MPa]	[MPa]	[%]	[MPa]	[%]	[MPa]	[%]	[MPa]	[%]	[MPa]	[%]
0.0	27.2	27.2	0.00	27.2	0.00	27.2	0.00	27.2	0.00	27.2	0.00
2.0	53.4	47.0	-11.86	42.8	-19.79	40.4	-24.34	41.8	-21.69	45.5	-14.73
3.0	57.2	54.7	-4.44	49.1	-14.17	45.9	-19.83	47.8	-16.53	52.7	-7.95
4.0	67.4	61.6	-8.59	54.9	-18.52	51.0	-24.36	53.3	-20.96	59.2	-12.16
5.0	70.3	67.9	-3.32	60.2	-14.26	55.7	-20.71	58.4	-16.94	65.2	-7.24
6.0	66.1	73.9	11.73	65.3	-1.24	60.2	-8.93	63.2	-4.43	70.8	7.08
8.0	86.8	84.8	-2.38	74.6	-14.04	68.6	-21.01	72.1	-16.93	81.1	-6.54
10.0	90.0	94.7	5.22	83.2	-7.54	76.4	-15.19	80.4	-10.71	90.6	0.67
15.0	112.7	117.0	3.78	102.6	-8.97	94.0	-16.65	99.0	-12.14	111.9	-0.76
20.0	139.8	136.7	-2.19	119.9	-14.18	109.8	-21.43	115.8	-17.17	130.7	-6.45
21.0	136.6	140.4	2.77	123.2	-9.81	112.8	-17.43	118.9	-12.96	134.3	-1.71
AAREP			5.12%	11.14%		17.26%		13.68%		5.94%	

* m_i calculated from regression method ($0 \leq \sigma_3 \leq 0.2\sigma_{ci}$)

The results show that the prediction performance of the proposed method is quite acceptable; the AAREP value for general rock type relations is 13.68%. The value of AAREP for specific rock type relations is equal to 5.94%, which is close to the regression method with AAREP=5.12%. This illustrates that the proposed method can provide good estimates of intact rock strength based on the information of the UCS of intact rock; and that such estimates can be improved with rock specific relations.

The results presented in Fig. 8 and Table 3 only provide one specific example for a sandstone rock. To compare the predictive capabilities of the proposed method with other methods, we

conducted a comprehensive study using the 112 groups of data which includes 908 triaxial and tensile strength tests for five common rock types as indicated in Table 2. (The intermediate m_i values were used for the guidelines method; m_i values for coal, limestone, granite, marble and sandstone are 14.5, 11, 32, 9 and 17, respectively.) The m_i values calculated from different methods are used in the HB criterion for rock strength prediction. For a given group data, the values of AAREP were calculated for different methods.

Fig. 9 presents the results of such comprehensive analysis, in which we adopted the cumulative distribution functions (CDF) of AAREPs values to assess the prediction performance of different methods. (The CDF indicates probabilities are calculated by dividing the number of cases where the value of AAREP is smaller than a threshold by the total number of cases considered.) We included two CDF lines for regression analysis: one for excluding tensile strength ($0 \leq \sigma_3 \leq 0.5\sigma_{ci}$) and one for including tensile strength ($\sigma_t \leq \sigma_3 \leq 0.5\sigma_{ci}$).

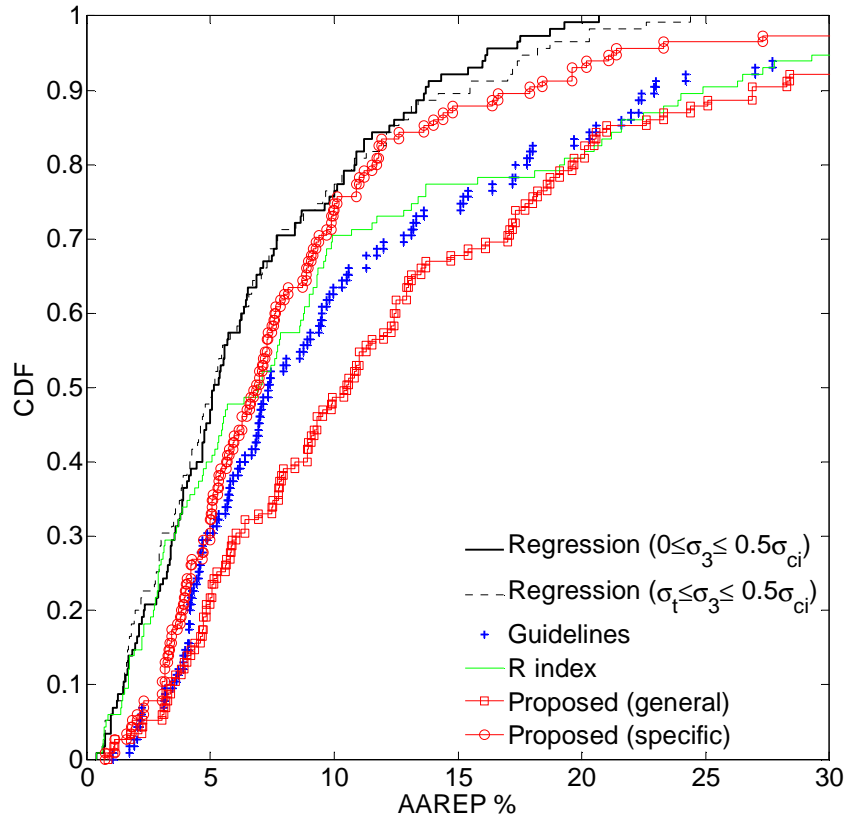


Fig. 9 Cumulative distribution function (CDF) of prediction errors (AAREP) of different methods using five rock types in Table 2

Results indicate that the regression analysis, of course, gives best rock strength prediction. It is also found that the inclusion of tensile strength in the regression analysis to calculate m_i values does not improve the capability of the prediction of rock strength, as shown in Fig. 9. For the proposed method, when no rock specific information is included, the AAREP for 88% of the data sets is less than 25%. However, when rock specific information is included, the proposed method provides the good predictive capabilities; the CDF curve is close to the regression method, and the prediction performance is obviously better than guidelines method. Although R index method gives higher CDF values when $AAREP (\%) < 7$, our proposed method outperforms R index method when $7 < AAREP (\%) < 30$. For example, if the permissible AAREP is 10%, then

the value of CDF within this error by the proposed method is about 75%, slightly lower than that from the regression method at 78% and higher than that from R index and guidelines methods with AAREP are equal to 70 and 62%, respectively.

6 Conclusions

The constant m_i is one of the basic input parameters required for the HB failure criterion. Triaxial tests, which are time-consuming and expensive, can be employed to calculate m_i values using the regression analysis. However, at the early stage of many practical applications, we need to estimate rock strength without having triaxial test data. In those cases, it is useful to estimate rock strength based on simple methods.

We proposed a simplified method (Eq. 6 together with rock specific relations in Table 2) that can estimate m_i (or normalized m_i) values using only UCS and rock types. In order to present the simplified method, we used 112 groups of data for five common rock types in the existing database together with our laboratory tests.

The reliability of the proposed method was evaluated and compared with the existing methods (guidelines and R index), which are commonly used for estimating m_i values when triaxial data are not accessible.

The results show that the proposed method can reliably be used in the HB criterion to estimate intact rock strength, with small discrepancies between estimated and experimental strength. The values of R^2 are greater than 0.92 for all rock types, and the values of AAREP are less than 9%, excluding coal with AAREP = 11.55% (see Fig. 7). Comparison results in Fig. 9 also indicate that the proposed equation for specific rock types yield better intact rock strength prediction compared with that from the guidelines and R index methods.

It should be noted that the proposed normalized m_i and σ_{ci} relations for rock types are based on the analysis of existing triaxial test data and the reliability of estimation of these relations depend on the quality and quantity of triaxial test data. Therefore, the proposed rock specific relations are open to further improvement as more triaxial test data become available.

Acknowledgement

Scholarship supports provided by China Scholarship Council (CSC) is gratefully acknowledged. Many thanks go to Associate Prof. Rafael Jimenez for helpful discussion on the manuscript when the first author was a visiting scholar in the ETSI Caminos C. y P at the Universidad Politécnica de Madrid, Spain. Mrs Barbara Brougham is also acknowledged for editing the manuscript.

References

- Cai, M. (2010). "Practical estimates of tensile strength and Hoek-Brown parameter m_i of brittle rocks." *Rock Mech Rock Eng.*, 43(2), 167-184.
- Douglas, K.J.(2002). "The shear strength of rock masses." PhD thesis, School of Civil and Environmental Engineering, University of New South Wales, Sydney, Australia.
- Jimenez, R., Serrano, A., and Olalla, C. (2008). "Linearization of the Hoek and Brown rock failure criterion for tunnelling in elasto-plastic rock masses." *Int. J. Rock Mech. Min. Sci.*,45, 1153-1163.
- Hoek, E. (2007). "Rock mass properties. Ch 11 in *Practical Rock Engineering*." <http://download.roscience.com/hoek/PracticalRockEngineering.asp>.
- Hoek, E., and Brown, E.T.(1980). "Underground excavations in rock. " *Instn Min Metall.*, London.
- Hoek, E., and Brown, E.T. (1997). "Practical estimates of rock mass strength." *Int. J. Rock Mech. Min. Sci.*, 34(8), 1165-1186.

- Hoek, E., Carranza-Torres, C., and Corkum, B.(2002).“Hoek-Brown failure criterion - 2002 Edition.” In R. Hammah, W. Bawden, J. Curran, and M. Telesnicki (Eds.), Proceedings of NARMS-TAC 2002, Mining Innovation and Technology. Toronto [downloadable for free at Hoek's corner, www.rocscience.com].
- Hoek, E., and Diederichs, M.S.(2006). “Empirical estimation of rock mass modulus.” *Int. J. Rock Mech. Min. Sci.*, 43, 203-215.
- Hoek, E., and Marinos, P. (2000). “ Predicting Tunnel Squeezing. *Tunnels and Tunnelling International.*” Part 1 – November 2000, Part 2 – December, 2000.
- Karakus, M., Kumral, M., and Kilic, O. (2005). “Predicting elastic properties of intact rocks from index tests using multiple regression modeling.” *Int. J. Rock Mech. Min. Sci.*, 42, 323-330.
- Karakus, M., and Tutmez, B. (2006). “Fuzzy and multiple regression modelling for evaluation of intact rock strength based on point load, schmidt hammer and sonic velocity.” *Rock Mech and Rock Eng.*, 39, 45-57.
- Marinos, V., Marinos, P., and Hoek, E.(2005). “The geological strength index: applications and limitations.” *Bull Eng Geol Environ.*, 64, 55-65.
- Mostyn, G., and Douglas, K.J.(2000). “Strength of intact rock and rock masses.” In C. Haberfield et al. (eds.) *GeoEng2000. Proc. intern. conf. geotech. geol. engrg.*, Melbourne, Australia, 19 - 24 November 2000, 1: 1389-1421. Lancaster: Technomic Publishing Company.
- Priest, S.D. (2005). “Determination of shear strength and three-dimensional yield strength for the Hoek-Brown criterion.” *Rock Mech Rock Eng.*, 38(4), 299-327.
- RocData. (2012). www.rocscience.com.
- Read, S.A.L., and Richards, L. (2011).“A comparative study of m_i , the Hoek-Brown constant for intact rock material.” 12th ISRM Congress, Beijing, October 2011.
- Shen, J., Karakus, M., and Xu, C.(2012). “Direct expressions for linearization of shear strength envelopes given by the Generalized Hoek-Brown criterion using genetic programming.” *Comput Geotech.*, 44,139-146.

Shen, J., Priest, S.D., and Karakus, M. (2012). "Determination of Mohr-Coulomb shear strength parameters from generalized Hoek-Brown criterion for slope stability analysis." *Rock Mech and Rock Eng.*, 45, 123-129.

Singh, M., Raj, A., and Singh, B. (2011). "Modified Mohr-Coulomb criterion for non-linear triaxial and polyaxial strength of intact rocks." *Int. J. Rock Mech. Min. Sci.*, 48, 546-555.

Schwartz, A.E.(1964). "Failure of rock in the triaxial shear test. In: *Proceedings of the 6th US rock mechanics symposium.*" Rolla, Mo, pp. 109-135.

Statement of Authorship of Journal paper 2

Determination of Mohr-Coulomb Shear Strength Parameters from Generalized Hoek-Brown Criterion for Slope Stability Analysis

Jiayi Shen*, Stephen Priest & Murat Karakus

School of Civil, Environmental and Mining Engineering, The University of Adelaide

Adelaide, South Australia, 5005, Australia

Rock Mechanics and Rock Engineering 2012, 45:123-129.

By signing the Statement of Authorship, each author certifies that their stated contribution to the publication is accurate and that permission is granted for the publication to be included in the candidate's thesis.

Jiayi Shen

Performed the analysis, wrote the manuscript and acted as corresponding author.

Signature:

Date: 7th May 2013

Prof. Stephen Priest

Supervised development of work and manuscript evaluation.

Signature:

Date: 8th May 2013

Dr. Murat Karakus

Manuscript evaluation.

Signature:

Date: 7th May 2013

Chapter 2

Determination of Mohr-Coulomb Shear Strength

Parameters from Generalized Hoek-Brown Criterion for

Slope Stability Analysis

1 Introduction

Rock slope stability is critical for many aspects of mining and civil engineering projects, such as open pit mining and large dam construction. One of the most popular approaches for estimating the factor of safety (FOS) of a given slope is the limit equilibrium method (LEM) where rock mass strength is usually expressed by the linear Mohr-Coulomb (MC) criterion. Currently, a widely used criterion to estimate rock mass strength is the non-linear Generalized Hoek-Brown failure criterion (GHB) since it is able to estimate the shear strength of various types of intact rock and rock masses (Priest 2005). If the GHB criterion is used in conjunction with LEM for analyzing the rock slope, methods are required to determine the equivalent MC shear strength parameters cohesion c and angle of friction ϕ at the specified normal stress σ_n from the GHB criterion. The determination of reliable shear strength values is a critical step in slope design as small changes in shear strength parameters can result in significant changes in the value of the FOS (Wyllie and Mah 2004). In past decades, methods for the determination of shear strength from the Hoek-Brown criterion for slope stability analysis were proposed by Hoek (1983), Priest and Brown (1983), Londe (1988), Hoek (1990), Hoek and Brown (1997), Kumar (1998), Hoek et al.(2002), Carranza-Torres (2004), Priest (2005), Fu and Liao (2010), Yang and Yin (2010).

Comprehensive review of the literature of estimating shear strength of the Hoek-Brown criterion can be found in the paper by Carranza-Torres (2004). However, as Brown (2008) has noted, deriving exact analytical solutions for estimating the shear strength of a rock mass modeled using the GHB criterion has proven to be a challenging task due to the complexities associated with mathematical derivation.

In the special case of the Hoek-Brown parameter $a=0.5$, an analytical solution proposed by Bray and reported by Hoek (1983) yields accurate results for intact rock with the Geological Strength Index (GSI) is equal to 100. However, in the more general case of $a \neq 0.5$ no accurate analytical solution is available (Carranza-Torres 2004). In this paper, an approximate analytical solution for estimating the equivalent MC parameters for highly fractured rock masses governed by the GHB criterion is proposed. The proposed approximate analytical solution yields fairly good results when $GSI < 40$ and provides great flexibility for the application of the GHB criterion in conjunction with LEM for highly fractured rock mass slope stability analysis.

2 Equivalent MC parameters for GHB criterion

The non-linear Hoek-Brown (HB) criterion, originally presented by Hoek and Brown (1983) has been successfully used in the field of rock engineering for the past three decades to estimate rock mass strength. The latest version is the Generalized Hoek-Brown (GHB) criterion presented by Hoek et al. (2002) is:

$$\sigma_1 = \sigma_3 + \sigma_{ci} \left(\frac{m_b \sigma_3}{\sigma_{ci}} + s \right)^a \quad (1)$$

m_b , s and a are the Hoek-Brown input parameters which can be estimated from the Geological Strength Index (GSI) for the rock mass, given by:

$$m_b = m_i e^{\left(\frac{GSI-100}{28-14D}\right)} \quad (2)$$

$$s = e^{\left(\frac{GSI-100}{9-3D}\right)} \quad (3)$$

$$a = 0.5 + \frac{e^{\left(\frac{-GSI}{15}\right)} - e^{\left(\frac{-20}{3}\right)}}{6} \quad (4)$$

where, σ_1 and σ_3 are the major and minor principal stresses, σ_{ci} is the uniaxial compressive strength of the intact rock mass, m_i is the Hoek-Brown constant for intact rock mass, D is the disturbance factor.

The GHB criterion Eq. 1 can also be expressed in terms of normal stress σ_n and shear stress τ on the failure plane by using Eqs. 5 and 6 which were proposed by Balmer (1952).

$$\sigma_n = \sigma_3 + \frac{(\sigma_1 - \sigma_3)}{\partial\sigma_1/\partial\sigma_3 + 1} \quad (5)$$

$$\tau = (\sigma_n - \sigma_3) \sqrt{\partial\sigma_1/\partial\sigma_3} \quad (6)$$

Taking the derivative of σ_1 with the respect of σ_3 of Eq. 1 and substituting the results into Eqs. (5) and (6) respectively, the GHB criterion can be expressed by the following equations

$$\sigma_n = \sigma_3 + \frac{\sigma_{ci} \left(\frac{m_b \sigma_3}{\sigma_{ci}} + s\right)^a}{2 + am_b \left(\frac{m_b \sigma_3}{\sigma_{ci}} + s\right)^{a-1}} \quad (7)$$

$$\tau = (\sigma_n - \sigma_3) \sqrt{1 + am_b \left(\frac{m_b \sigma_3}{\sigma_{ci}} + s\right)^{a-1}} \quad (8)$$

Fig. 1 gives a graphical representation of the HB criterion expressed by (a) major and minor principal stresses (b) normal and shear stresses.

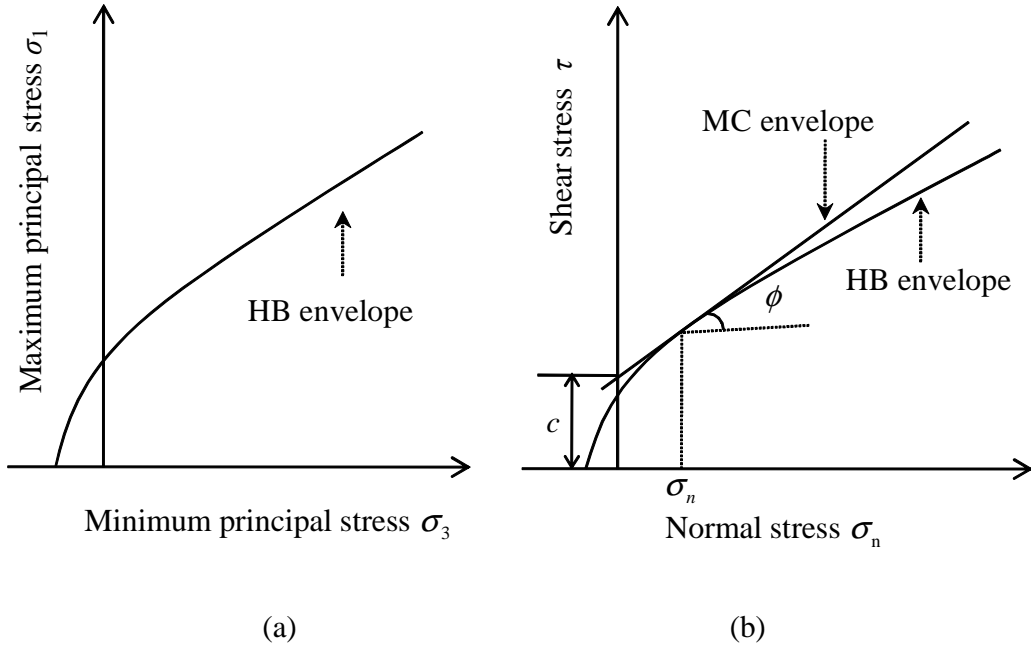


Fig. 1 (a) Major and minor principal stresses for the HB criterion, (b) Normal and shear stresses for the HB criterion

The equivalent MC shear strength parameters can be calculated by locating the tangent of the HB envelope with the specified normal stress σ_n , as illustrated in Fig. 1b. The slope of the tangent to the HB failure envelope gives angle of friction ϕ and the intercept with the shear stress axis gives cohesion c .

Kumar (1998) proposed the general numerical solution for estimating the equivalent MC shear strength parameters from the GHB criterion. Equations are expressed as follows:

$$\frac{2}{m_b a} \left(m_b \frac{\sigma_n}{\sigma_{ci}} + s \right)^{(1-a)} = \frac{(1 - \sin \phi)}{\sin \phi} \left(1 + \frac{\sin \phi}{a} \right)^{(1-a)} \quad (9)$$

$$\tau = \frac{\sigma_{ci} \cos \phi}{2 \left(1 + \frac{\sin \phi}{a} \right)^a} \left(m_b \frac{\sigma_n}{\sigma_{ci}} + s \right)^a \quad (10)$$

$$c = \tau - \sigma_n \tan \phi \quad (11)$$

In the Eqs. 9 to 11, the values of input parameters m_b , s , a and σ_{ci} are known and normal stress σ_n can be estimated by adopting an appropriate stress analysis approach (Hoek and Brown 1997). In general case of $a \neq 0.5$, in order to calculate the shear strength parameters, firstly Eq. 9 is solved iteratively to calculate an angle of friction ϕ value. Having obtained ϕ , shear stress τ and cohesion c can be calculated from Eqs. (10) and (11) respectively. In special case $a=0.5$, the analytical solution derived by Bray and reported by Hoek (1983) can yield the accurate MC shear strength parameters for the Hoek-Brown materials. The equations are expressed as follows:

$$h = 1 + \frac{16(m_b \sigma_n + s \sigma_{ci})}{3m_b^2 \sigma_{ci}} \quad (12)$$

$$\theta = \frac{1}{3} \left(90 + \arctan \frac{1}{\sqrt{h^3 - 1}} \right) \quad (13)$$

$$\phi = \arctan \frac{1}{\sqrt{4h \cos^2 \theta - 1}} \quad (14)$$

$$\tau = (\cot \phi - \cos \phi) \frac{m_b \sigma_{ci}}{8} \quad (15)$$

$$c = \tau - \sigma_n \tan \phi \quad (16)$$

where h and θ are intermediate parameters.

This method provides great flexibility for the use of the original HB criterion ($a=0.5$) in rock slope stability analysis. However, in the GHB criterion, if Eq. 4 is used to calculate a , the value of a can vary from 0.51 when GSI is 40 to 0.5 when GSI is 100. Since the Bray method is based on $a=0.5$, when GSI=100, the equation gives very good results for rock masses where GSI>40. On the other hand, when $0 < \text{GSI} < 40$ the value of a can vary from 0.666 to 0.51. Clearly, this analytical solution can't yield satisfactory results for a geological condition where the value of GSI for a fractured rock mass is relatively low (Priest 2005). Table 1 gives the comparison of shear stress values between the Bray method and the numerical method proposed by Priest (2005)

for a rock mass: $\sigma_{ci}=30000\text{kPa}$, $m_i=20$, $\sigma_n=3000\text{kPa}$, $D=0.8$, $0<\text{GSI}<40$. The results are also plotted in Fig. 2. It is shown that τ values from the Bray method are relatively overestimated compared with the Priest method, and with the decrease of the GSI values the discrepancy of τ can vary from 2.8% when $\text{GSI}=40$ to 98.1% when $\text{GSI}=2$.

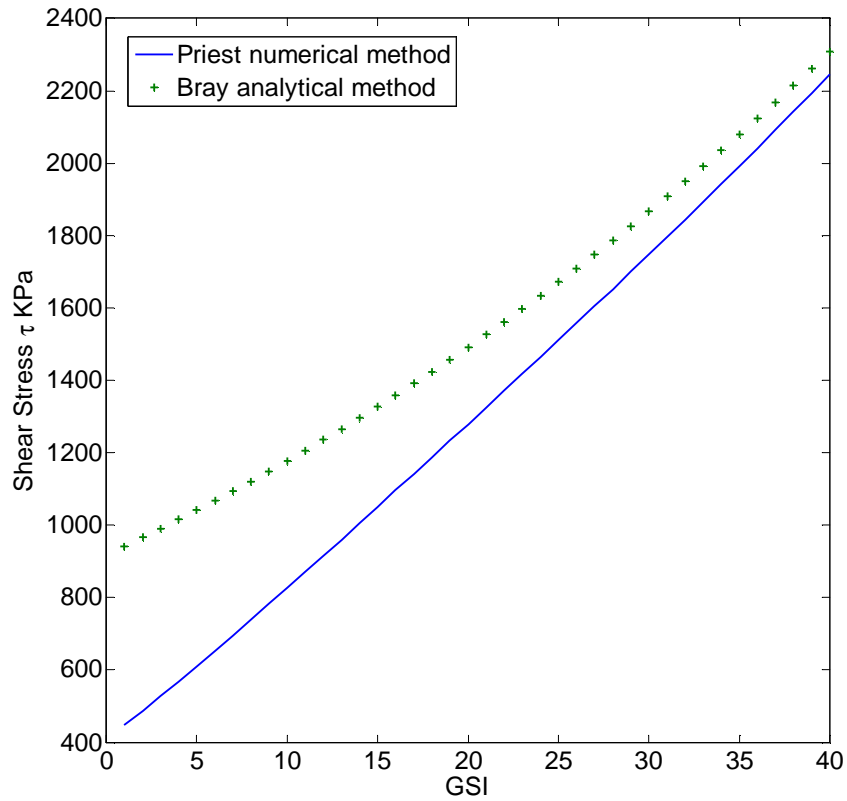


Fig. 2 Shear stress versus GSI

Table 1 Shear stresses obtained from Priest and Bray solutions over a range of GSI

Uniaxial compressive strength, σ_{ci} (kPa)				30000
Hoek-Brown constant for intact rock, m_i				20
Geological Strength Index, GSI				2-40
Normal stress, σ_n (kPa)				3000
Disturbance factor, D				0.8
GSI	Shear stress, τ (kPa)		Discrepancy of Bray method (%)	
	Bray method	Priest method		
2	965.88	487.58	98.1	
4	1015.50	568.38	78.7	
6	1067.30	652.19	63.6	
8	1121.10	738.29	51.9	
10	1177.20	826.08	42.5	
12	1235.40	915.13	35.0	
14	1296.00	1005.10	28.9	
16	1358.80	1095.80	24.0	
18	1424.00	1187.10	20.0	
20	1491.60	1278.90	16.6	
22	1561.70	1371.20	13.9	
24	1634.20	1464.20	11.6	
26	1709.20	1557.90	9.7	
28	1786.80	1652.50	8.1	
30	1866.90	1748.00	6.8	
32	1949.70	1844.60	5.7	
34	2035.20	1942.50	4.8	
36	2123.40	2041.90	4.0	
38	2214.50	2142.80	3.3	
40	2308.40	2245.60	2.8	

3 Proposed method

Based on the numerical method proposed by Kumar (1998) the authors propose a new approximate analytical solution for estimating the MC shear strength parameters from the GHB criterion for a highly fractured rock mass where $0 < \text{GSI} < 40$. The expressions related to the derivations are:

1. After rewriting Eqs. 7 and 9, the angle of friction ϕ can also be expressed by the following equations

$$\phi = \arcsin \left(1 - \frac{2}{2 + am_b \left(\frac{\sigma_3}{\sigma_{ci}} m_b + s \right)^{a-1}} \right) \quad (17)$$

$$\frac{\sigma_3}{\sigma_{ci}} = \frac{\sigma_n}{\sigma_{ci}} - \frac{\left(\frac{m_b \sigma_3}{\sigma_{ci}} + s \right)^a}{2 + am_b \left(\frac{m_b \sigma_3}{\sigma_{ci}} + s \right)^{a-1}} \quad (18)$$

As σ_3/σ_{ci} exists on both sides of Eq. 18, in order to identify an acceptable value for σ_3/σ_{ci} , Eq. 18 must be solved iteratively. Therefore, with the purpose of presenting an approximate analytical solution for estimating the equivalent MC shear strength parameters, the critical step is to present an approximate analytical solution for the intermediate parameter σ_3/σ_{ci} expressed by m_b , s , a and σ_n/σ_{ci} . Having obtained σ_3/σ_{ci} , the angle of friction ϕ , shear stress τ and cohesion c can be directly calculated from Eqs. 17, 10 and 11, respectively.

2. According to Eq. 3, the value of $s < 1.2\text{E-}3$ when $\text{GSI} < 40$. In order to simplify Eq. 18, s is assumed to equal zero and Eq. 18 becomes:

$$\frac{\sigma_n}{\sigma_{ci}} = \frac{\sigma_3}{\sigma_{ci}} \left(1 + \frac{m_b^a}{2 \left(\frac{\sigma_3}{\sigma_{ci}} \right)^{1-a} + a} \right) \quad (19)$$

3. In order to calculate σ_3/σ_{ci} in terms of m_b , a and σ_n/σ_{ci} , a linear function is used to replace the non-linear function $(\sigma_3/\sigma_{ci})^{1-a}$ which is part of Eq. 19.

$$\left(\frac{\sigma_3}{\sigma_{ci}} \right)^{1-a} \approx k \frac{\sigma_3}{\sigma_{ci}} + i \quad (20)$$

Hoek and Brown (1997) recommended that a rock mass stress state of the value of σ_3/σ_{ci} should be in the range of $0 < \sigma_3/\sigma_{ci} < 0.25$ in rock mass slopes. Using the recommended σ_3/σ_{ci} values, the values of k and i are estimated by linear regression analysis, the results are $k=1.81a+1.31$ and $i=0.78a-0.37$.

4. Substituting Eq. 20 into Eq. 19, the following expressions are obtained:

$$\sigma_3 = \frac{\sigma_n - p - q + \sqrt{(p + q - \sigma_n)^2 + 4\sigma_n q}}{2} \quad (21)$$

$$p = \frac{\sigma_{ci} m_b^a}{2k} \quad (22)$$

$$q = \frac{2i\sigma_{ci} + a\sigma_{ci}}{2k} \quad (23)$$

$$k = 1.81a + 1.31 \quad (24)$$

$$i = 0.78a - 0.37 \quad (25)$$

Finally, the angle of friction ϕ can be calculated from Eq. 17, shear stress τ and cohesion c can be directly calculated from Eqs. 10 and 11, respectively.

4 Validation of the approximate analytical solution

One thousand random sets of testing data are generated by the strategy described in the following section. The value of the absolute average relative error percentage (AAREP) is adopted as an

indicator to verify the reliability of the proposed approximate analytical solution. The results from the proposed approximate solution are compared with those from the Priest numerical method. The smaller AAREP is, the more reliable the solution. If the proposed approximate solution has a perfect predictive capacity, the value of AAREP will be zero.

$$AAREP = \frac{\sum_{i=1}^N \left| \frac{x_i - x'_i}{x_i} \right|}{N} \quad (26)$$

where N is the number of testing sets, x_i and x'_i are the results from Priest and the proposed approximate solutions, respectively.

The process of generating testing data for validation is as follows:

1. Selection of input parameters

Table 2 gives the values of input parameters for generating the testing data. The selection σ_3/σ_{ci} is based on Hoek and Brown's (1997) suggestion that the values of σ_3/σ_{ci} should be in the range of $0 < \sigma_3/\sigma_{ci} < 0.25$ in rock mass slopes.

Table 2 Range of input parameters

Input parameters	Range
GSI	0-40
m_i	1-35
D	0-1
σ_3/σ_{ci}	0-0.25

2. Calculation of the Hoek-Brown parameters

For the given values of the input parameters, the Hoek-Brown parameters m_b , s and a can be calculated from Eqs. 2 to 4, respectively.

3. Calculation of the equivalent MC shear strength parameters and σ_n/σ_{ci}

The values of σ_n/σ_{ci} can be calculated from Eq. 18. The angle of friction ϕ , shear stress τ and cohesion c can be calculated from Eqs. 17, 10 and 11, respectively.

Once the strategy is established, the steps outlined above are programmed into ‘*Matlab*’. The programming generates 1000 data sets for testing the reliability of the proposed approximate analytical solution. Table 3 gives the one thousand random sets of data employed for the testing analysis.

Table 3 Data for validation of the proposed approximate solution

Input parameters					Calculated HB parameters			Output parameters			
No	σ_3/σ_{ci}	GSI	m_i	D	m_b	s	a	σ_n/σ_{ci}	ϕ	τ/σ_{ci}	c/σ_{ci}
					Eq. 2	Eq. 3	Eq. 4	Eq. 18	Eq. 17	Eq. 10	Eq. 11
1	0.004	15	8	1.0	0.022	8.8E-07	0.561	0.006	15.7	0.003	0.001
2	0.007	20	36	0.7	0.469	1.0E-05	0.544	0.015	39.4	0.017	0.005
...
1000	0.127	9	26	0.3	0.623	1.6E-05	0.591	0.200	20.0	0.105	0.032

The performance of the proposed approximate analytical solution is shown in Figs. 3 to 5. The solid diagonal line in the figures represents a perfect estimation. Data located under the solid diagonal line represents over estimation, and if located above the solid diagonal line represents under estimation.

The results illustrate that there is close agreement between the proposed approximate analytical solution and the Priest numerical solution as shown in Figs. 3 to 5. Compared with the Priest results, the AAREP of angel of friction ϕ and shear stress τ/σ_{ci} are only 2.2% and 0.7%, respectively, as shown in Figs. 3 and 4. The proposed approximate analytical solution generates

very good results of ϕ and τ , however, it is interesting that the AAREP of c/σ_{ci} is 7.1%, as shown in Fig. 5. The results show that it is inevitable that Eq. 11 will yield relative large discrepancy of cohesion c that is different from the Priest's results because of error transformation: Eq. 11 includes a tangent function that tends to increase the difference between the Priest numerical solution for c and the proposed approximate solution. Even when there is only a small difference in the values of input parameters ϕ and τ , relatively large discrepancy of c occurs.

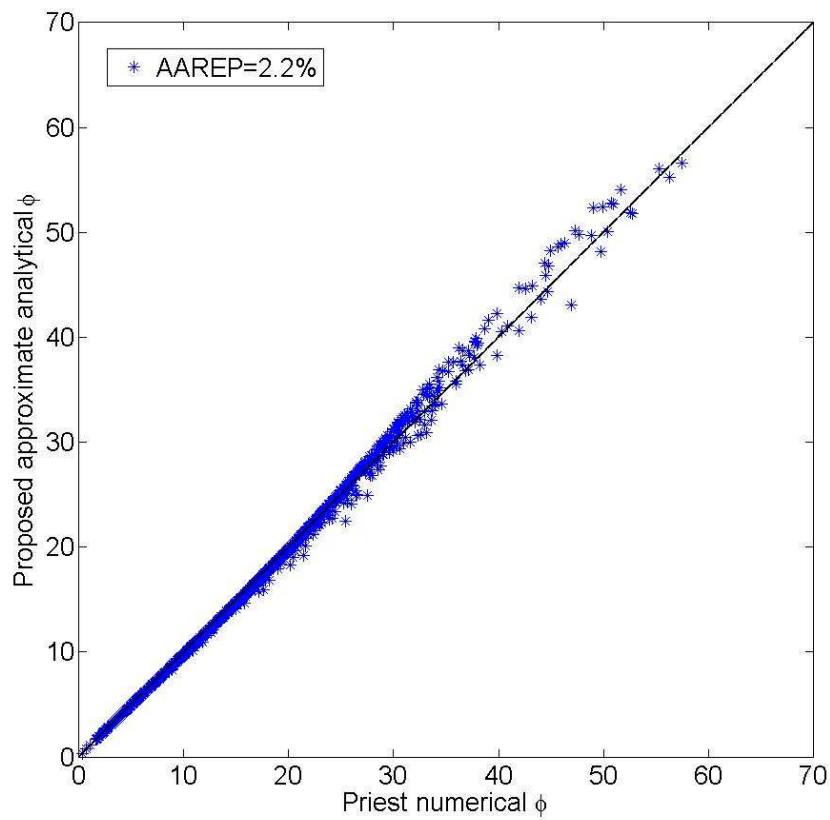


Fig. 3 Priest numerical versus proposed approximate analytical value of ϕ

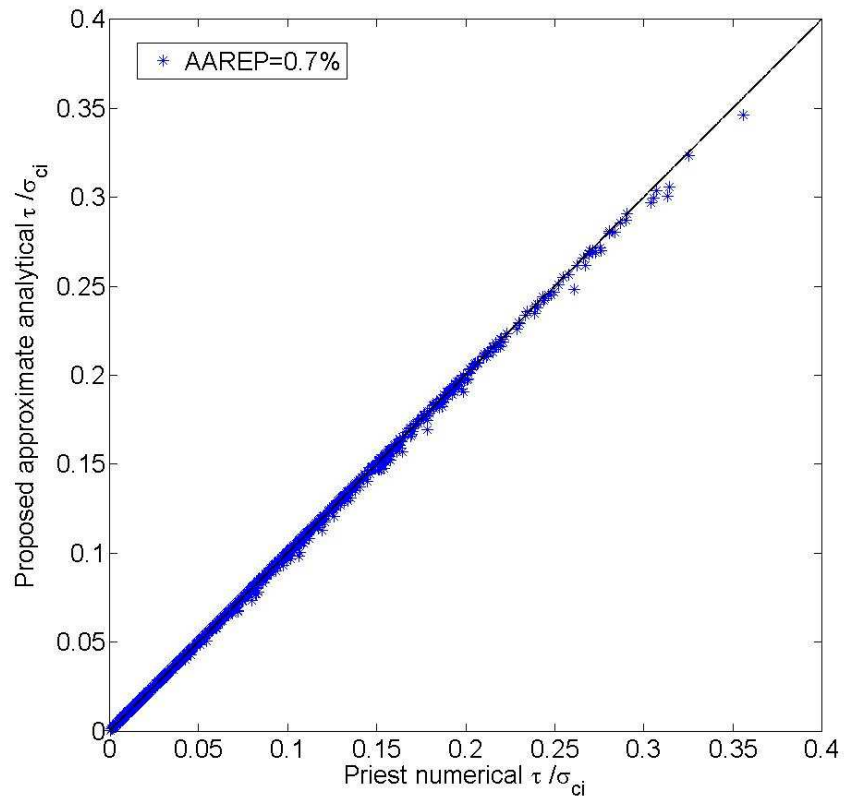


Fig. 4 Priest numerical versus proposed approximate analytical value of τ/σ_{ci}

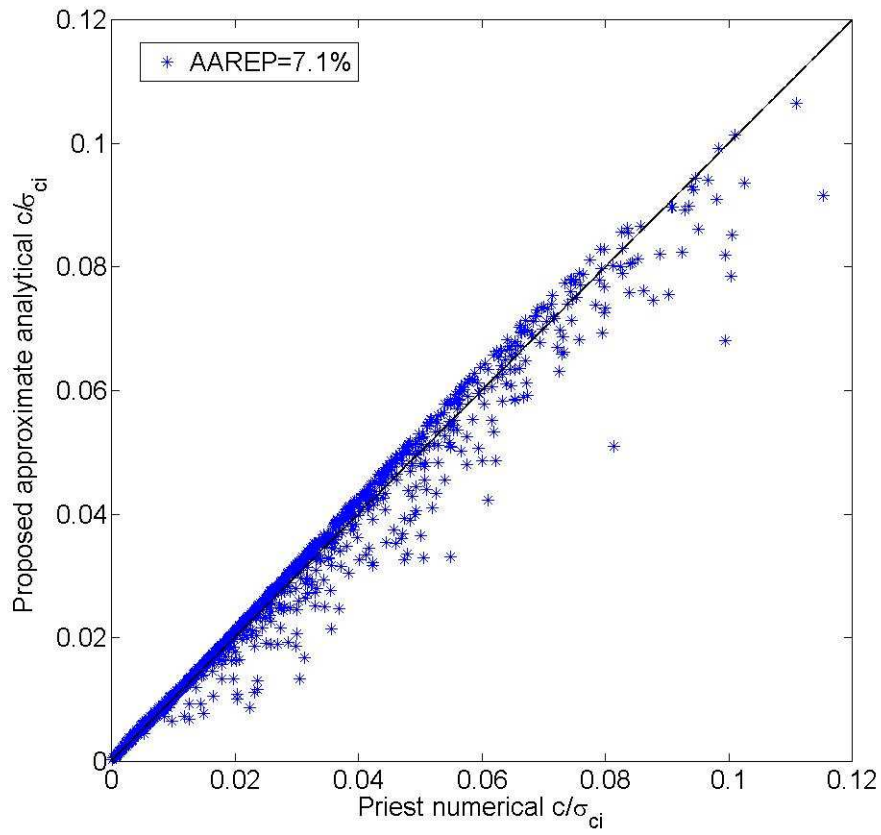


Fig. 5 Priest numerical versus proposed approximate analytical value of c/σ_{ci}

An example of data from the paper by Priest (2005) is used for a final check on the reliability of the proposed approximate analytical solution. The example has the following rock mass parameters: $\sigma_{ci} = 30000\text{kPa}$, $m_i = 16$, $\text{GSI} = 15$, $\sigma_n = 800\text{kPa}$, $D = 0.7$. The results of the comparisons of the equivalent c , ϕ and τ are given in Table 4.

Table 4 Comparison results of shear strength parameters with different methods

Uniaxial compressive strength, σ_{ci} (kPa)	30000					
Hoek-Brown constant for intact rock, m_i	16					
Geological Strength Index, GSI	15					
Normal stress, σ_n (kPa)	800					
Disturbance factor, D	0.7					
Methods	Shear Strength Parameters			Discrepancy		
	c (kPa)	ϕ°	τ (kPa)	Percentage (D_p)%		
Priest Numerical	151.43	21.86	472.37			
Bray analytical	212.65	26.71	615.15	40.43	22.18	30.23
Proposed approximate analytical	173.14	20.96	479.54	14.34	-4.12	1.52

Data in Table 4 show that the proposed approximate analytical method gives slightly different results from the Priest numerical method. The discrepancy percentages (D_p) for c , ϕ and τ are 14.34%, -4.12% and 1.52%, respectively. Compared with the Priest method, the Bray method gives relatively high discrepancy, D_p for c , ϕ and τ are 40.43%, 22.18% and 30.23%, respectively. The results of the comparisons of the equivalent c , ϕ and τ over a range of GSI ($0 < \text{GSI} < 40$) are given in Figs. 6 to 8. The results illustrate that the proposed approximate analytical method yields slightly different results from the Priest method. The AAREP of ϕ , c and τ are found to be 2.9%, 10.8%, and 1.1% respectively. Compared with the Bray methods (AAREP of ϕ , c and τ are 23.8%, 45.4% and 32.3%, respectively) the proposed approximate solution generates much better results.

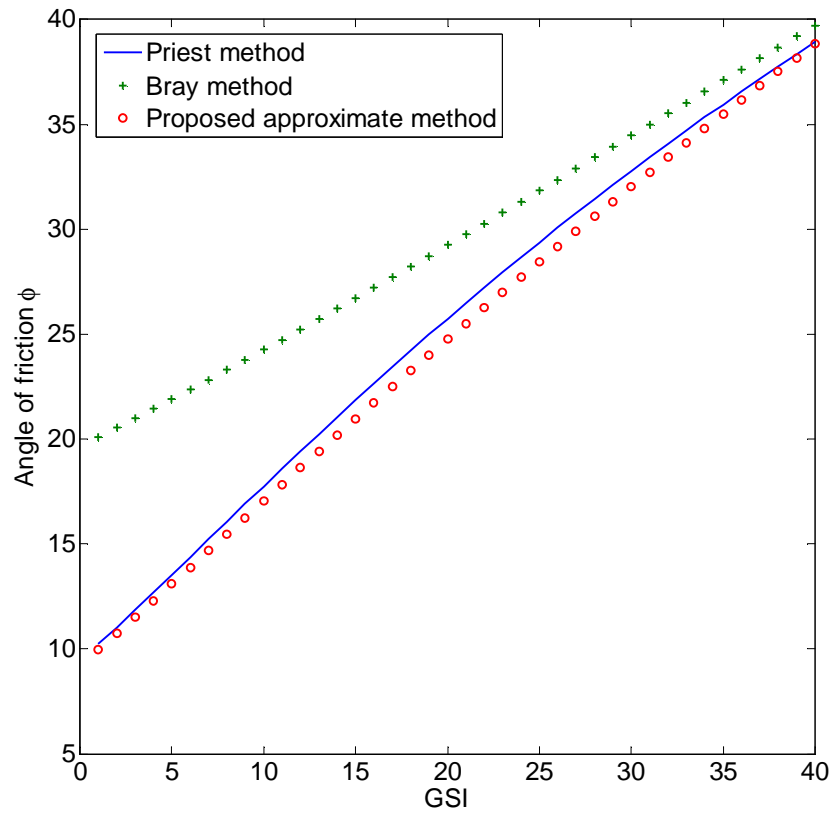


Fig. 6 Comparison of angle of friction ϕ results

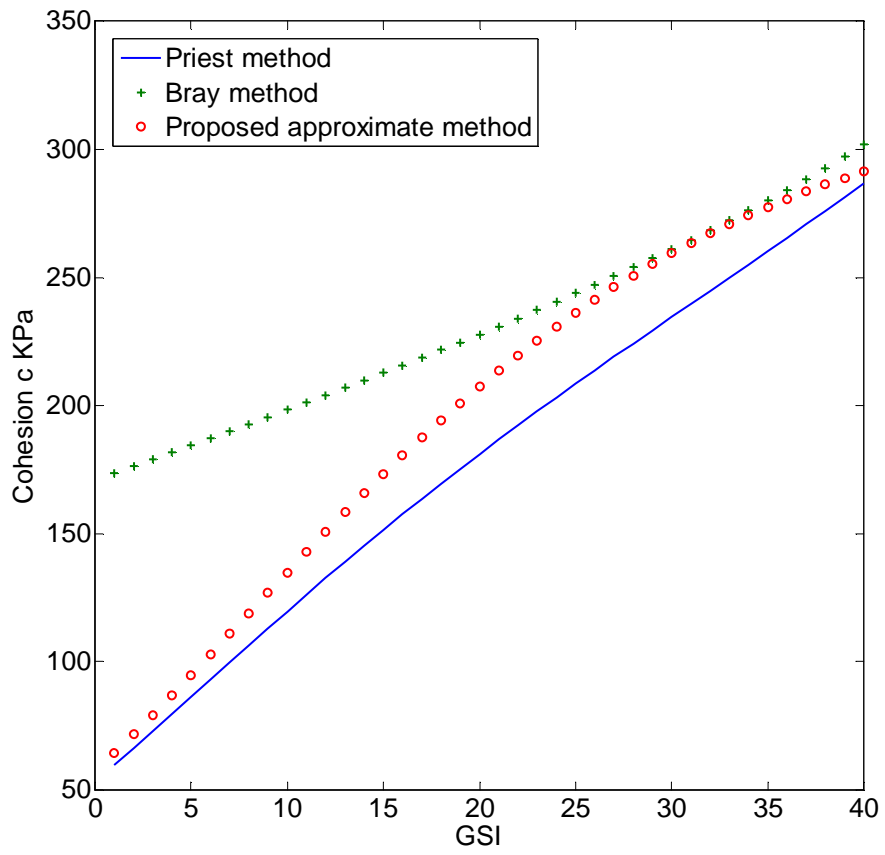


Fig. 7 Comparison of cohesion c results

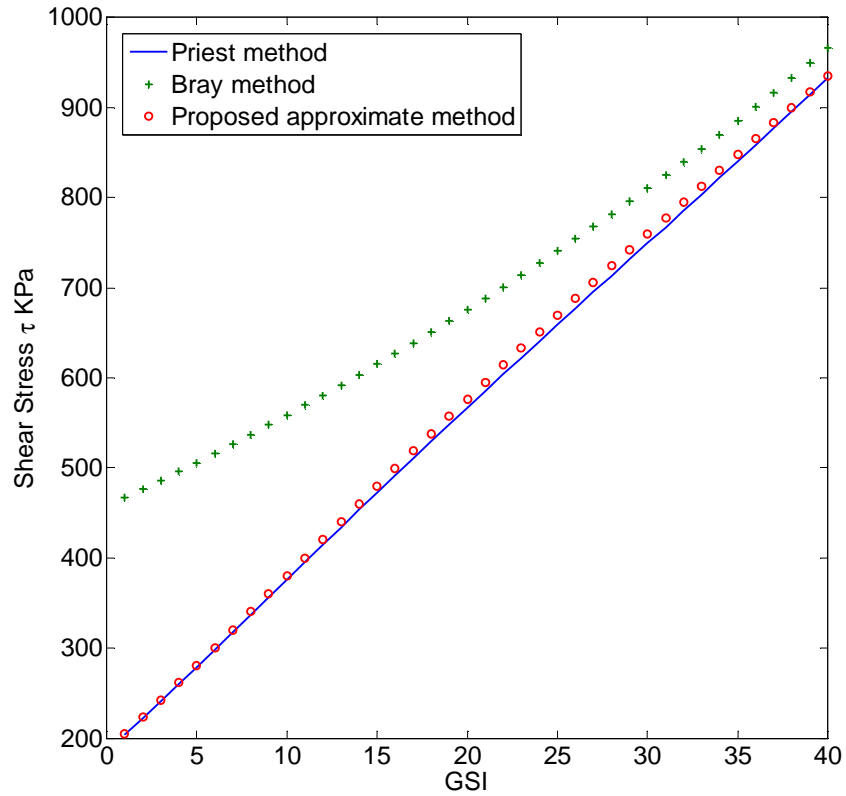


Fig. 8 Comparison of shear stress τ results

5 Conclusions

In this paper, an approximate analytical solution has been proposed for estimating the equivalent Mohr-Coulomb (MC) shear strength parameters from the non-linear Generalized Hoek-Brown failure criterion (GHB) for highly fractured rock mass slope stability analysis.

The proposed approximate analytical solution is based on Eq. 18 to build up an approximate analytical function for the intermediate parameter σ_3/σ_{ci} expressed by input parameters m_b , a and σ_n/σ_{ci} . After finding an explicit solution for σ_3/σ_{ci} , the value of the angle of friction ϕ , cohesion c and shear stress τ can be directly calculated from Eqs. 17, 11 and 10, respectively.

The reliability of the proposed approximate analytical solution has been tested against the Priest numerical solution using 1,000 random sets of data. The results show that there is close

agreement in the values of shear stress τ between the proposed approximate analytical solution and the Priest solution as shown in Fig. 4. In addition, an example of data from the paper by Priest (2005) has been adopted for a final check on the adequacy of the proposed approximate analytical solution. The results show that the proposed approximate analytical solution yields slightly different shear stress τ from the Priest method when $0 < \text{GSI} < 40$, the AAREP of shear stress τ from the proposed approximate analytical solution is only 1.1% (see Fig. 8). This trivial difference is, of course, unimportant in a practical sense. Thus, the proposed approximate analytical solution provides great flexibility for the application of the GHB criterion in conjunction with the limit equilibrium method (LEM) for highly fractured rock mass slope stability analysis.

Acknowledgement

Scholarship supports provided by China Scholarship Council (CSC) is gratefully acknowledged. The authors would like to express their gratitude to the editor Prof. Giovanni Barla and anonymous reviewers for their constructive comments on the draft paper. The authors are grateful to Mrs Barbara Brougham for reviewing the manuscript.

References

- Balmer G (1952) A general analytical solution for Mohr's envelope. *Am Soc Test Mater* 52:1269–1271
- Brown ET (2008) Estimating the mechanical properties of rock masses. In: *Proceedings of the 1st southern hemisphere international rock mechanics symposium: SHIRMS 2008*, vol 1. Perth, Western Australia, pp 3-21
- Carranza-Torres C (2004) Some comments on the application of the Hoek–Brown failure criterion for intact rock and rock masses to the solution of tunnel and slope problems. In:

- Barla G, Barla M (eds) MIR 2004-X Conference on Rock and Engineering Mechanics. 24-25 November, Torino, Italy. Chap 10. Pàtron Editore, Bologna, pp 285-326
- Fu W, Liao Y (2010) Non-linear shear strength reduction technique in slope stability calculation. *Comput Geotech* 37:288-298
- Hoek E (1983) Strength of jointed rock masses. *Géotechnique* 33(3):187-223
- Hoek E (1990) Estimating Mohr–Coulomb friction and cohesion values from the Hoek-Brown failure criterion. *Int J Rock Mech Min Sci* 27:227-229
- Hoek E, Brown ET (1980) *Underground excavations in rock*. Institution of Mining and Metallurgy, London, p 527
- Hoek E, Brown ET (1997) Practical estimates of rock mass strength. *Int J Rock Mech Min Sci* 34(8):1165-1186
- Hoek E, Carranza-Torres C, Corkum B (2002) Hoek-Brown failure criterion-2002 Edition. In: Hammah R, Bawden W, Curran J, Telesnicki M (eds) *Proceedings of NARMS-TAC 2002, Mining Innovation and Technology*. Toronto (downloadable for free at Hoek's corner, <http://www.rocscience.com>)
- Kumar P (1998) Shear failure envelope of Hoek-Brown criterion for rockmass. *Tunn Undergr Space Technol* 13(4):453-458
- Londe P (1988) Determination of the shear stress failure in rock masses. *ASCE J Geotech Eng Div* 114(3):374-376
- Priest SD (2005) Determination of shear strength and three-dimensional yield strength for the Hoek-Brown criterion. *Rock Mech Rock Eng* 38(4):299-327
- Priest SD, Brown ET (1983) Probabilistic stability analysis of variable rock slopes. *Trans Inst Min Metall* 92:A1-A12
- Wyllie DC, Mah C (2004) *Rock slope engineering: civil and mining*, 4th edn. Spon Press, New York
- Yang XL, Yin JH (2010) Slope equivalent Mohr-Coulomb strength parameters for rock masses satisfying the Hoek-Brown criterion. *Rock Mech Rock Eng* 43:505-511

Statement of Authorship of Journal paper 3

Direct Expressions for Linearization of Shear Strength Envelopes Given by the Generalized Hoek-Brown Criterion Using Genetic Programming

Jiayi Shen, Murat Karakus* & Chaoshui Xu

School of Civil, Environmental and Mining Engineering, The University of Adelaide

Adelaide, South Australia, 5005, Australia

Computers and Geotechnics 2012, 44:139-146.

By signing the Statement of Authorship, each author certifies that their stated contribution to the publication is accurate and that permission is granted for the publication to be included in the candidate's thesis.

Jiayi Shen

Performed the analysis and wrote the manuscript.

Signature:

Date: 27th May 2013

Dr. Murat Karakus

Supervised development of work, manuscript evaluation and acted as corresponding author.

Signature:

Date: 27th May 2013

Associate Prof. Chaoshui Xu

Supervised development of work and manuscript evaluation.

Signature:

Date: 27th May 2013

Chapter 3

Direct Expressions for Linearization of Shear Strength Envelopes Given by the Generalized Hoek-Brown Criterion Using Genetic Programming

Abstract

The non-linear Generalized Hoek-Brown (GHB) criterion is one of the most broadly adopted failure criteria used to estimate the strength of a rock mass. However, when limit equilibrium and shear strength reduction methods are used to analyze rock slope stability, the strength of the rock mass is generally expressed by the linear Mohr-Coulomb (MC) criterion. If the GHB criterion is used in conjunction with existing methods for analyzing the rock slope, methods are required to determine the equivalent MC shear strength from the GHB criterion. Deriving precise analytical solutions for the equivalent MC shear strength from the GHB criterion has not proven to be straightforward due to the complexities associated with mathematical derivation. In this paper, an approximate analytical solution for estimating the rock mass shear strength from the GHB criterion is proposed. The proposed approach is based on a symbolic regression (SR) analysis performed by genetic programming (GP). The reliability of the proposed GP solution is tested against numerical solutions. The results show that shear stress estimated from the proposed solution exhibits only 0.97 % average discrepancy from numerical solutions using 2451 random sets of data. The proposed solution offers great flexibility for the application of the GHB criterion with existing methods based on the MC criterion for rock slope stability analysis.

1 Introduction

The stability of rock slopes is significant for various rock engineering projects, such as open pit mining and dam construction. One of the most popular methods for analyzing slope stability is the limit equilibrium method (LEM) where rock mass strength is generally expressed in terms of the linear Mohr-Coulomb (MC) criterion.

The principles of LEM can be applied to determine the factor of safety (FOS) of a given slope by the method of slices as shown in Fig. 1a. The FOS can be defined as a function of resisting force f_R divided by driving force f_D . The forces of f_R and f_D can also be expressed in terms of shear stress τ^i and normal stress σ_n^i acting on the base of an arbitrary element i as shown in Fig. 1b [1].

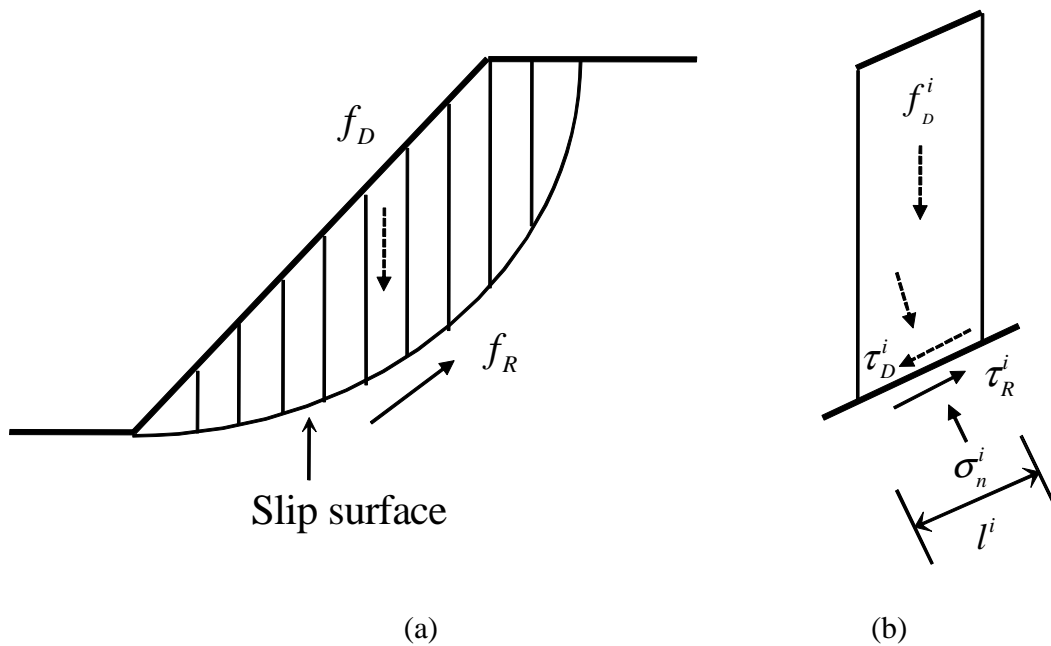


Fig. 1(a) The basic of method of slices, (b) Forces acting on a given slice

Fig. 2 illustrates the MC failure envelope. The slope of the tangent to the MC envelope gives angle of friction ϕ and the intercept with the shear stress axis gives cohesion c . The MC criterion

is linear, therefore the values of shear strength parameters c and ϕ are unchanged under various normal stress σ_n values. Traditional LEM only need unique values of c and ϕ to calculate FOS of a given slope. That means, arbitrary slice (as shown in Fig. 1b) with various normal stress σ_n has the same c and ϕ values.

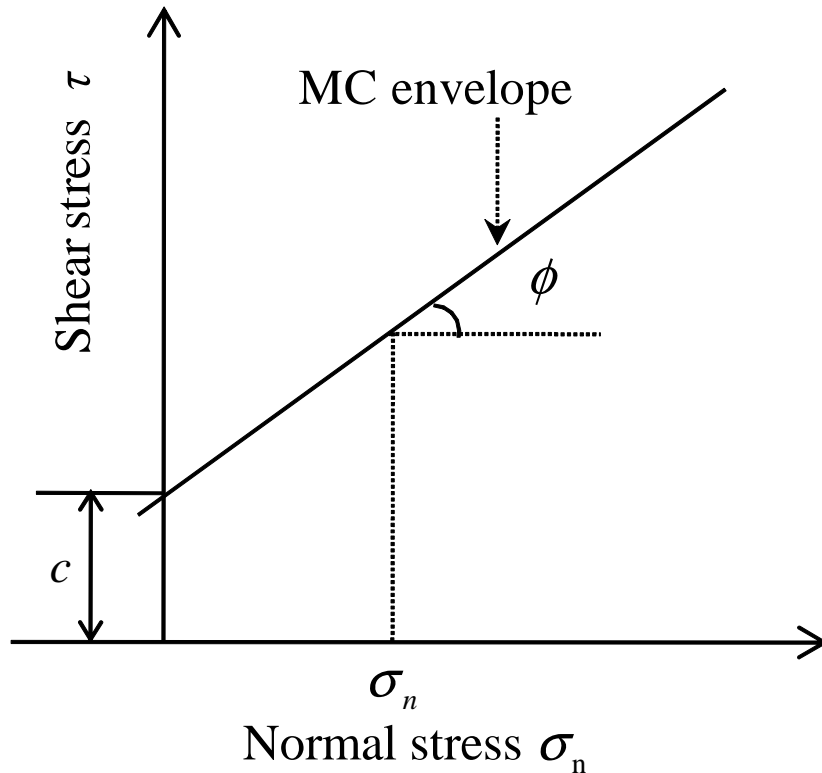


Fig. 2 The MC criterion showing shear strength defined by angle of friction ϕ and cohesion c

The Hoek-Brown (HB) criterion was originally proposed by Hoek and Brown [2]. Over the past 30 years the HB criterion has been widely adopted in rock engineering to estimate the strength of rock masses. If the HB criterion is used with LEM for assessing rock slope stability, it becomes necessary to determine the equivalent MC shear strength for a failure surface under a specified normal stress σ_n in a rock mass governed by the HB criterion. That means, slices (as shown in Fig. 1b) with different values of normal stresses σ_n have various c and ϕ values.

As Brown noted [3], deriving accurate analytical solutions for estimating the equivalent MC parameters at a given normal stress from the Generalized Hoek-Brown (GHB) criterion [4] has proven to be a challenging task.

In this research, an approximate analytical solution for estimating the rock mass shear strength from the GHB criterion [4] is proposed. The proposed approach is based on a symbolic regression (SR) analysis performed by genetic programming (GP).

Genetic programming [5] is a promising approach which attempts to find an explicit solution to explain the relations between the variables. GP is well suited to geotechnical problems and it is increasingly used by researchers in geotechnical engineering [6-9]. However, there is no evidence in the literature that GP based approaches are used to estimate the rock mass shear strength from the HB criterion.

In this paper, review of existing methods for the determination MC shear strength from the HB criterion is described in section 2. The GP approach is introduced in section 3. The GP modeling for the GHB criterion is described in section 4. Validation of the GP results is given in section 5.

2 Equivalent shear strength of the HB criterion

2.1 Introduction of the HB criterion

The non-linear Hoek-Brown (HB) criterion was initially proposed by Hoek and Brown [2] in 1980. The latest version is the Generalized Hoek-Brown (GHB) criterion presented by Hoek et al. [4] in 2002. The equations are expressed as follows:

$$\sigma_1 = \sigma_3 + \sigma_{ci} \left(\frac{m_b \sigma_3}{\sigma_{ci}} + s \right)^a \quad (1)$$

m_b , s and a are the Hoek-Brown input parameters that depend on the degree of fracturing of the rock mass [1-4] and can be estimated from the Geological Strength Index (GSI), given by :

$$m_b = m_i e^{\left(\frac{GSI-100}{28-14D}\right)} \quad (2)$$

$$s = e^{\left(\frac{GSI-100}{9-3D}\right)} \quad (3)$$

$$a = 0.5 + \frac{e^{\left(\frac{-GSI}{15}\right)} - e^{\left(\frac{-20}{3}\right)}}{6} \quad (4)$$

where, σ_1 is the maximum principal stresses, σ_3 is the minimum principal stresses, σ_{ci} is the uniaxial compressive strength of the intact rock, m_i is the Hoek-Brown constant for intact rock, D is the disturbance factor of the rock mass.

The GHB criterion Eq. 1 is expressed by the relationship between maximum and minimum principal stresses. However, it can also be expressed in terms of normal stress σ_n and shear stress τ on the failure plane by using Eqs. 5 and 6 which were proposed by Balmer [10].

$$\sigma_n = \sigma_3 + \frac{(\sigma_1 - \sigma_3)}{\partial\sigma_1/\partial\sigma_3 + 1} \quad (5)$$

$$\tau = (\sigma_n - \sigma_3) \sqrt{\partial\sigma_1/\partial\sigma_3} \quad (6)$$

Taking the derivative of σ_1 with the respect of σ_3 of Eq. 1 to get Eq. 7

$$\frac{\partial\sigma_1}{\partial\sigma_3} = 1 + am_b \left(\frac{m_b \sigma_3}{\sigma_{ci}} + s \right)^{a-1} \quad (7)$$

Substituting Eq. 7 into Eqs. 5 and 6 respectively, the GHB criterion can be expressed by the following equations

$$\sigma_n = \sigma_3 + \frac{\sigma_{ci} \left(\frac{m_b \sigma_3}{\sigma_{ci}} + s \right)^a}{2 + am_b \left(\frac{m_b \sigma_3}{\sigma_{ci}} + s \right)^{a-1}} \quad (8)$$

$$\tau = (\sigma_n - \sigma_3) \sqrt{1 + am_b \left(\frac{m_b}{\sigma_{ci}} \sigma_3 + s \right)^{a-1}} \quad (9)$$

Fig. 3 shows a graphical representation of the GHB criterion expressed by (a) maximum and minimum principal stresses (b) normal and shear stresses.

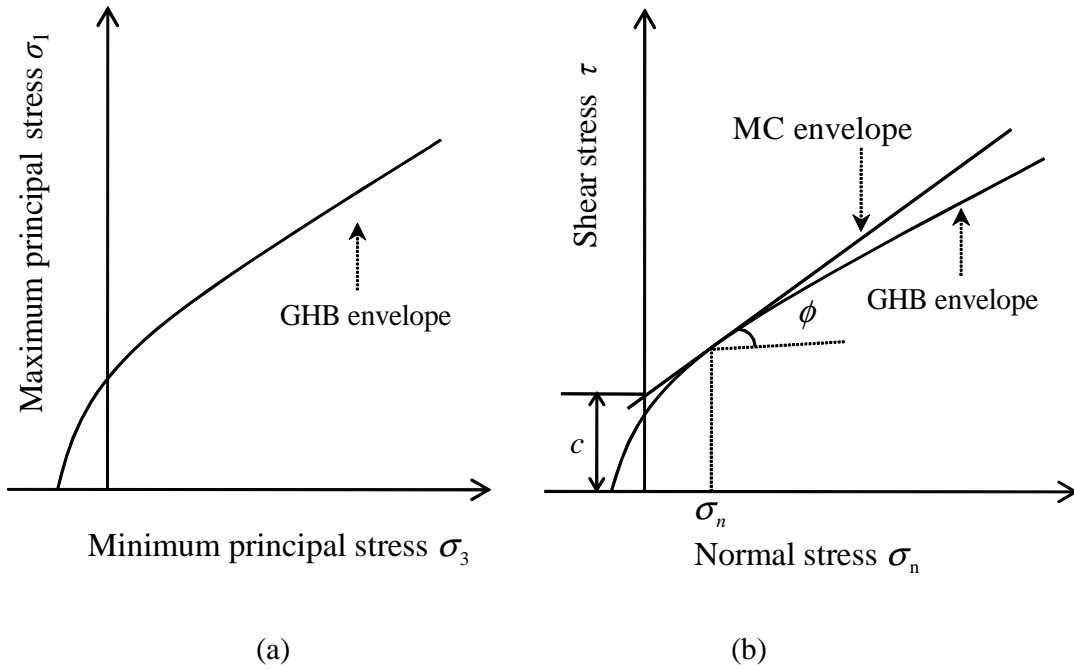


Fig. 3 (a) Maximum and minimum principal stresses for the GHB criterion, (b) Normal and shear stresses for the GHB criterion [27]

The instantaneous MC shear strength parameters can be estimated by locating the tangent of the GHB envelope under a given value of normal stress σ_n , as shown in Fig. 3b. The slope of the tangent to the GHB failure envelope gives instantaneous angle of friction ϕ and the intercept with the shear stress axis gives instantaneous cohesion c .

2.2 Methods for estimating shear strength from the HB criterion

The numerical method of determining instantaneous shear strength parameters from the original HB criterion [2] for slope stability analysis was initially proposed by Priest and Brown [11].

After that, a great number of attempts were made to estimate the MC shear strength from the original HB and GHB criteria [1-4, 12-27]. Comprehensive review of the literature and derivation of analytical and numerical solutions for estimating the MC shear strength from the HB criterion can be found in the paper by Carranza-Torres [1]. In this paper, the numerical methods proposed by Kumar [17] Eqs. (10) to (12) and Carranza-Torres [1] Eqs. (15) and (16) will be briefly introduced since these two methods will be used to propose the new approximate analytical solution in the following section.

One of the general numerical methods for the determination of the MC shear strength from the HB criterion was proposed by Kumar [17]. Equations are expressed as follows:

$$\frac{2}{m_b a} \left(m_b \frac{\sigma_n}{\sigma_{ci}} + s \right)^{(1-a)} = \frac{(1 - \sin \phi)}{\sin \phi} \left(1 + \frac{\sin \phi}{a} \right)^{(1-a)} \quad (10)$$

$$\tau = \frac{\sigma_{ci} \cos \phi}{2 \left(1 + \frac{\sin \phi}{a} \right)^a} \left(m_b \frac{\sigma_n}{\sigma_{ci}} + s \right)^a \quad (11)$$

$$c = \tau - \sigma_n \tan \phi \quad (12)$$

Rewriting Eqs. (8) and (10) the angle of friction ϕ can also be expressed by the following equations [27].

$$\phi = \arcsin \left(1 - \frac{2}{2 + am_b \left(\frac{\sigma_3}{\sigma_{ci}} m_b + s \right)^{a-1}} \right) \quad (13)$$

$$\frac{\sigma_3}{\sigma_{ci}} = \frac{\sigma_n}{\sigma_{ci}} - \frac{\left(\frac{m_b \sigma_3}{\sigma_{ci}} + s \right)^a}{2 + am_b \left(\frac{m_b \sigma_3}{\sigma_{ci}} + s \right)^{a-1}} \quad (14)$$

In Eqs. (10) to (14), m_b , s , a , σ_{ci} and σ_n are the input parameters. Deriving a precise closed form solution of shear stress τ expressed by m_b , s , a , σ_{ci} and σ_n is not feasible mathematically. In order to calculate τ value, firstly Eq. 14 is solved iteratively to calculate the intermediate parameter σ_3/σ_{ci} value. Having obtained σ_3/σ_{ci} , the angle of friction ϕ can be calculated from Eq. 13, and finally shear stress τ can be directly calculated from Eq. 11 [27].

Carranza-Torres [1] proposed a generic form of Balmer's equations [10] to calculate the rock mass shear strength from the GHB criterion. The equations are expressed as follows:

$$\sigma_n = \sigma_3 + \frac{\sigma_{ci}}{2} \left(m_b \frac{\sigma_3}{\sigma_{ci}} + s \right)^a \left[1 - \frac{am_b \left(m_b \frac{\sigma_3}{\sigma_{ci}} + s \right)^{a-1}}{2 + am_b \left(m_b \frac{\sigma_3}{\sigma_{ci}} + s \right)^{a-1}} \right] \quad (15)$$

$$\tau = \sigma_{ci} \left(m_b \frac{\sigma_3}{\sigma_{ci}} + s \right)^a \frac{\sqrt{1 + am_b \left(m_b \frac{\sigma_3}{\sigma_{ci}} + s \right)^{a-1}}}{2 + am_b \left(m_b \frac{\sigma_3}{\sigma_{ci}} + s \right)^{a-1}} \quad (16)$$

In order to calculate τ , for the given values of the input parameters m_b , s , a , σ_{ci} and σ_n , Eq. 15 is solved iteratively to calculate the σ_3 value. Having obtained σ_3 , Eq. 16 can be used to calculate shear stress τ , which were implemented with the software 'Slide'[28] and 'RocLab'[29]. In this research, the numerical method suggested by Carranza-Torres [1] will be used for testing the reliability of the proposed approximate analytical solution in the section 5.

As Brown [3] noted, due to the complexity of the mathematical derivation, an explicit closed form solution providing the MC shear strength from the GHB criterion is a challenging task.

A widely used analytical solution in rock slope engineering was presented by Hoek et al. [4]. This solution gives a convenient way for calculating the average MC parameters from the GHB criterion. However, it does not provide a direct method for estimating instantaneous MC shear

strength parameters [22]. Until now, in the general case of $a \neq 0.5$ no accurate analytical solution is available to calculate instantaneous MC shear strength of rock masses from the GHB criterion. In the special case when $a=0.5$ and $GSI=100$ the analytical solution derived by Bray and reported by Hoek [12] yield the accurate MC shear strength, however, this analytical solution cannot generate satisfactory shear strength of rock masses with low GSI values [27]. An alternative approximate analytical solution was proposed by Shen et al. [27], which produces quite satisfactory shear strength of highly fractured rock masses where $GSI < 40$.

In this paper, an approximate analytical solution which provides the shear strength of rock masses fairly good for the whole range GSI values was proposed as an extension to the work by Shen et al. [27]. The proposed approach is based on a symbolic regression (SR) analysis performed by genetic programming (GP).

3 Overview of genetic programming

In this section, genetic programming (GP) will briefly be introduced; further information about GP can be found from Koza [5].

3.1 Basic concepts of GP

GP was originally proposed by Koza [5]. GP is an extension of genetic algorithm (GA) [30]. GP is a method for finding a solution to complex problems via evolutionary algorithms and is usually expressed as a tree structure that consists of terminals and functions. Fig.4 is a typical tree structure of the function of $x*y-\sin(z)$, which contains terminals (x, y, z), and functions ($-$, $*$ and \sin).

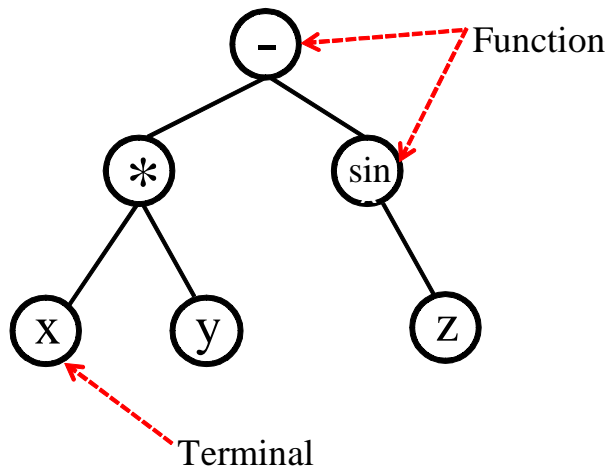


Fig. 4 A typical tree structure of the function of $x*y-\sin(z)$

3.2 How GP works

The general flow chart of a GP paradigm is given in Fig. 5.

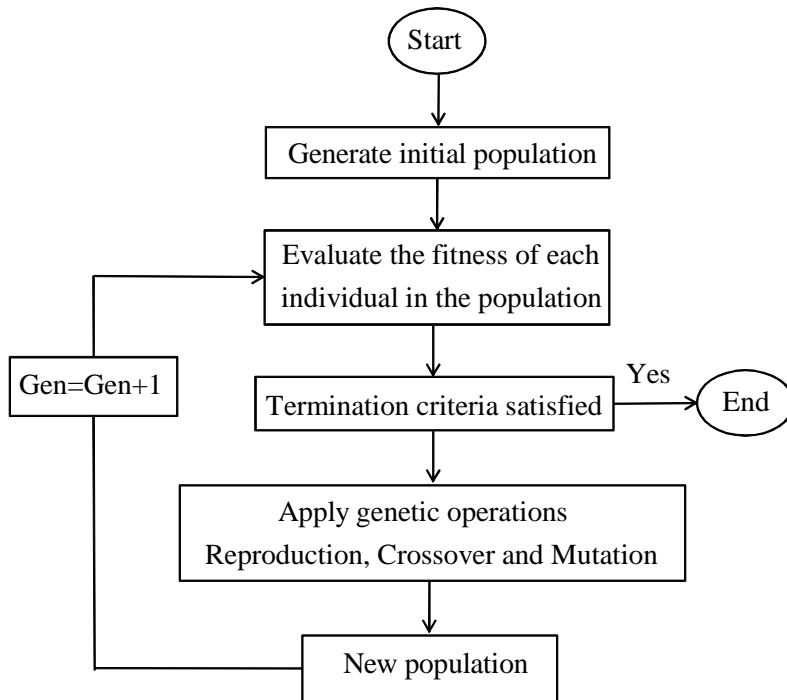


Fig. 5 A basic flow chart for GP

As with GA, in GP the individuals in the initial population are randomly generated. Various methods are available to generate the initial population, such as the full method, grow method and ramped half-and-half method [31]. Then, the fitness of each individual is calculated. The fitness function used in this study is the sum of the absolute difference of the accurate numerical data with predicted GP results (see Eq. 17). Lower fitness value indicates that the individual has the better structure.

$$fitness = \sum_{i=1}^N |y_i - y'_i| \quad (17)$$

where N is the number of individuals, y_i and y'_i are the accurate numerical and GP predicted values, respectively. Using fitness value as a guide, a number of individuals are chosen randomly from the population using appropriate selection methods (such as tournament and roulette wheel selections) [5, 9]. The “best” parents have more opportunity to create “better” offspring. After that, genetic operators (such as crossover and mutation) in GP are adopted to generate the next generation. The most commonly used form of crossover operation is tree crossover [6]. Random crossover nodes are chosen in each parent tree. Then it creates the offspring by swapping the respective subtree at the crossover node, as illustrated in Fig.6.

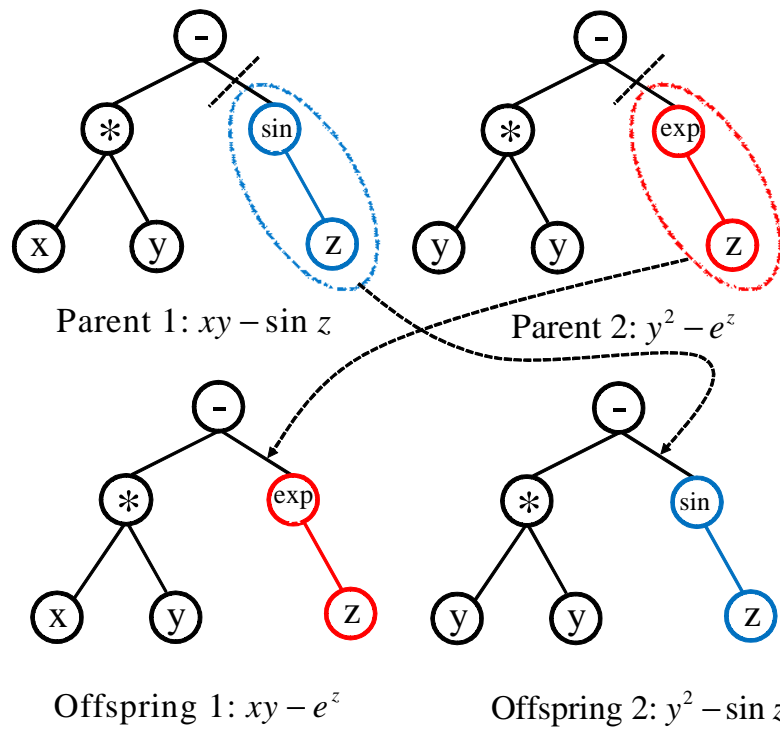


Fig. 6 Crossover operation in genetic programming

One of the usually adopted mutation operators is point mutation. A random node is selected from the parent tree and is substituted with a newly generated random node having a terminal or a function. Fig.7 illustrates a typical mutation operation in GP.

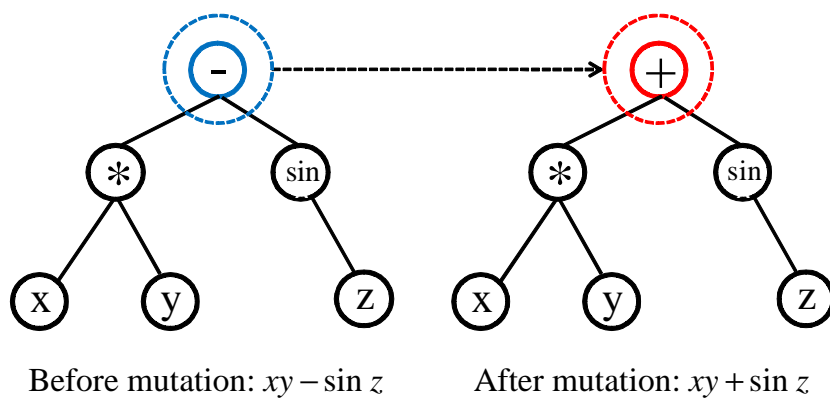


Fig. 7 Mutation operation in genetic programming

The choice of crossover and mutation operation is probabilistic. Often the crossover rate is more than 90 percent. However, mutation plays a minor role in GP and, therefore, the mutation rate is quite low, typically being in the region of one percent. It can even be disregarded in most cases [5]. The GP will run until the termination criterion is satisfied, such as maximum generation. Ultimately, the best individual with the lowest fitness will be found. Related GP parameters for the training models in this research are summarized in Table 1.

Table 1 Parameters used in GP analysis

Parameters	Values
Terminals	x_1, x_2, x_3 and x_4
Functions	$+, -, *, /, power, log, exp, sqrt$
Fitness function type	Sum of absolute difference (SAD)
Selection method	Tournament
Population size	200
Maximum tree depth	17
Maximum generation	200
Recombination probability	Dynamic
Mutation probability	Dynamic

4 GP modelling for the GHB criterion

GP is composed of functions and terminals appropriate to the characteristics of the problem. If the functions and terminals selected are not appropriate for the problem, the desired solution cannot be achieved [9]. Therefore, in order to overcome the limitation of GP and achieve

satisfactory results, it is crucial to have a deep understanding of the problem to choose the appropriate GP model.

In this research, there are two GP models available for finding a function for τ expressed by input parameters m_b , s , a and σ_n/σ_{ci} . The first model is based on Eq. 14, which builds up a function for intermediate parameter σ_3/σ_{ci} expressed by m_b , s , a and σ_n/σ_{ci} . Having derived the approximate analytical solution of σ_3/σ_{ci} , then the angle of friction ϕ can be calculated from Eq. 13, and finally using Eq. 11 the closed form solution for calculating shear stress τ can be achieved. The second model is based on Eq. 10, which directly builds up a function for ϕ in terms of input parameters m_b , s , a and σ_n/σ_{ci} . Having obtained ϕ , then τ can be calculated from Eq. 11. Both GP models were tested in this research. After 100 computer runs with the same calculation parameters, it was found that the first model yields better results than the second model.

The first model tries to find an analytical solution for intermediate parameter σ_3/σ_{ci} . The main structure of Eq. 13 for calculating ϕ was preserved, which ensures that the results are as accurate as possible. However, the second model ignores the original relationship between ϕ and the input parameters in Eq. 10. Therefore, Eq. 10 yields relatively worse results when compared with the first model.

GPLAB, a Matlab GP software package developed by Silva [31], was adopted to work out a relatively precise analytical solution for the GP model based on Eq. 14. Terminals used to drive a function for σ_3/σ_{ci} consist of x_1 , x_2 , x_3 and x_4 which correspond to m_b , s , a and σ_n/σ_{ci} respectively.

The process of generating data for GP analysis is as follows:

1. Selection of input parameters

The values of input parameters GSI, m_i , D and σ_3/σ_{ci} for generating the training data are shown in Table 2. The selection σ_3/σ_{ci} is based on Hoek and Brown's [16] suggestion that the values of σ_3/σ_{ci} should be in the range of $0 < \sigma_3/\sigma_{ci} < 0.25$ in rock mass slopes. The selection of GSI, m_i and D is based on 'Roclab' [29].

Table 2 Range of input parameters

Input parameters	Minimum	Maximum
GSI	1	100
m_i	1	35
D	0	1
σ_3/σ_{ci}	0	0.25

2. Calculation of the Hoek-Brown parameters

For the given values of the GSI, m_i and D , the parameters m_b , s and a can be estimated by using Eqs. (2) to (4), respectively.

3. Calculation of σ_n/σ_{ci} and shear stress τ

For the given values of the m_b , s , a and σ_3/σ_{ci} , the values of σ_n/σ_{ci} can be estimated from Eq. 14.

The instantaneous ϕ can be calculated from Eq. (13), and shear stress can be calculated from Eq. 11.

The strategy outlined above was coded into 'Matlab'. The program generated 500 random sets of data for the GP training operation. Table 3 indicates 500 random sets of data employed for the GP training analysis. Also, 2451 sets of testing data were generated based on Eqs. 15 and 16 for testing the performance of the proposed approximate analytical solution.

Table 3 Data of HB criterion for GP analysis

Input parameters					Calculated HB parameters			Output parameters		
No	σ_3/σ_{ci}	GSI	m_i	D	m_b Eq. 2	s Eq. 3	a Eq. 4	σ_n/σ_{ci} Eq. 14	ϕ Eq. 13	τ/σ_{ci} Eq. 11
1	0.034	12	27	0.4	0.469	1.01E-05	0.575	0.060	26.0	0.042
2	0.053	65	25	1.0	2.241	3.25E-03	0.502	0.120	38.0	0.137
-	-	-	-	-	-	-	-	-	-	-
500	0.053	33	16	0.0	1.388	5.26E-04	0.518	0.110	33.9	0.107

In this research, the GP solutions were compared with numerical results [1]. According to Eq. 18, the smaller the absolute average relative error percentage (AAREP) is, the better the function. The best function with a tree structure was converted into a corresponding mathematical formula.

$$AAREP = \frac{\sum_{i=1}^N \left| \frac{x_i - x'_i}{x_i} \right|}{N} \quad (18)$$

where N is the number of training sets, x_i and x'_i are the results from numerical and GP solutions, respectively.

5 Validation of the GP results

200 alternative expressions were generated by GP. Given lower AAREP value and the simplicity of the function generated, Eq. 19 was selected as the winning function.

$$\frac{\sigma_3}{\sigma_{ci}} = \frac{a \frac{\sigma_n}{\sigma_{ci}}}{\sqrt{a(1 + \sqrt{m_b})} - \frac{\sigma_n}{\sigma_{ci}}} \quad (19)$$

Substituting Eq. 19 in to Eq. 13, the angle of friction ϕ can be calculated as follows:

$$P = 2 + am_b \left(m_b \frac{\sigma_3}{\sigma_{ci}} + s \right)^{a-1} \quad (20)$$

$$\phi = \arcsin \left(1 - \frac{2}{P} \right) \quad (21)$$

Finally, with the help of Eq. 11 the shear stress τ can be expressed as follows:

$$\tau = \sigma_{ci} \frac{\sqrt{P-1}}{P} \frac{\left(m_b \frac{\sigma_n}{\sigma_{ci}} + s \right)^a}{\left(\frac{Pa + P - 2}{aP} \right)^a} \quad (22)$$

where P is the intermediate parameter. The proposed Eq. 22 differs from the original GHB criterion which is expressed by the major and minor principal stresses. Eq. 22 is an alternative form of the GHB criterion expressed in terms of normal and shear stresses. So that it can be directly used for estimating the instantaneous shear stress of each slice under a specified normal stress in the limit equilibrium method for the rock slope stability analysis.

Carranza-Torres [1] numerical method was used for generating 2451 random sets of testing data to verify the reliability of the proposed approximate analytical solution. The performance of Eq. 22 is shown in Fig. 8. The solid line in the figures represents a perfect estimation. Data located under the solid line represents over estimation, and located above the solid line represents under estimation. The results show that there is close agreement between the proposed approximate analytical solution and the numerical solution. The AAREP of shear stress τ is only 0.97%. The maximum discrepancy of τ is 7.97% as shown in Fig. 8. The discrepancy of 84.21% sets of data is less than 2% as shown in Fig. 9. The comparison results show that the proposed approximate analytical solution gives very good shear stresses results.

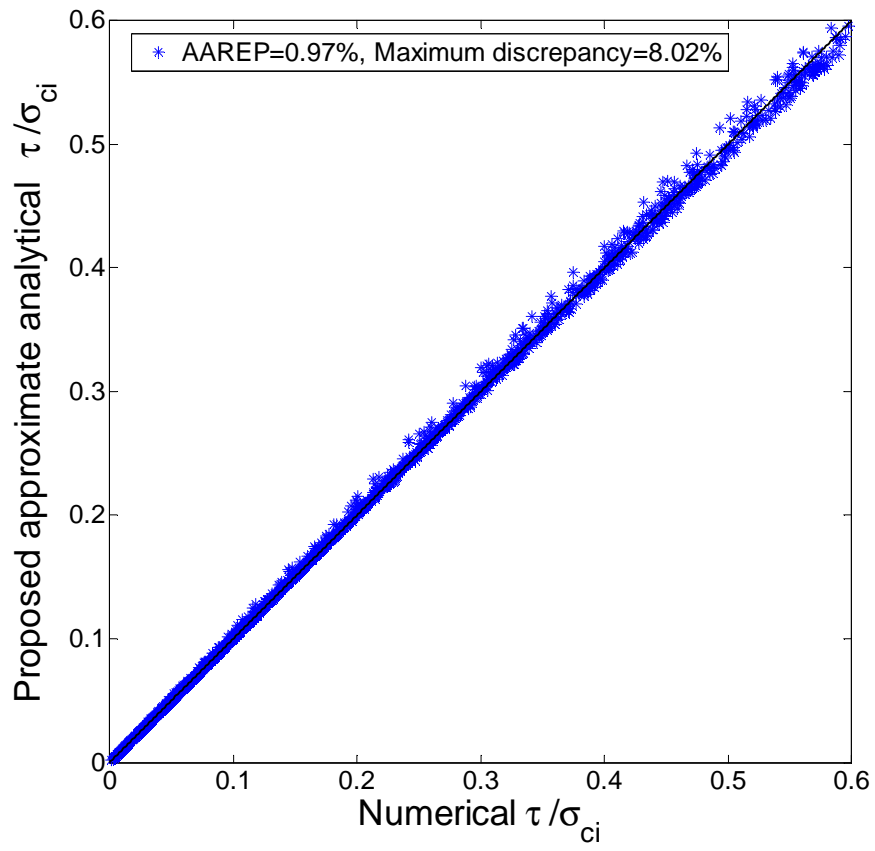


Fig. 8 Numerical versus GP value of τ/σ_{ci}

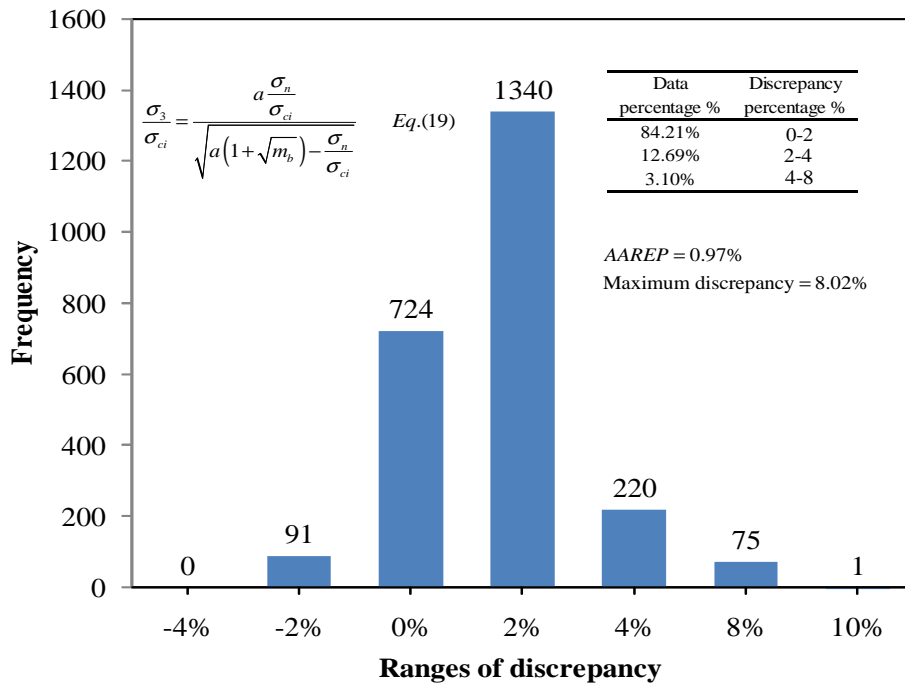


Fig. 9 Discrepancy analysis of the proposed analytical solution

Fig. 10 shows the alternative expression which has the lowest AAREP. The value of AAREP=0.72% is slightly lower than Eq. 19 with AAREP=0.97% and the maximum discrepancy is 7.19% which is quite close to Eq. 19 with 7.97%, however, the structure of the expression is much more complex than Eq. 19. Therefore, finally, Eq. 19 was selected as the winning function.

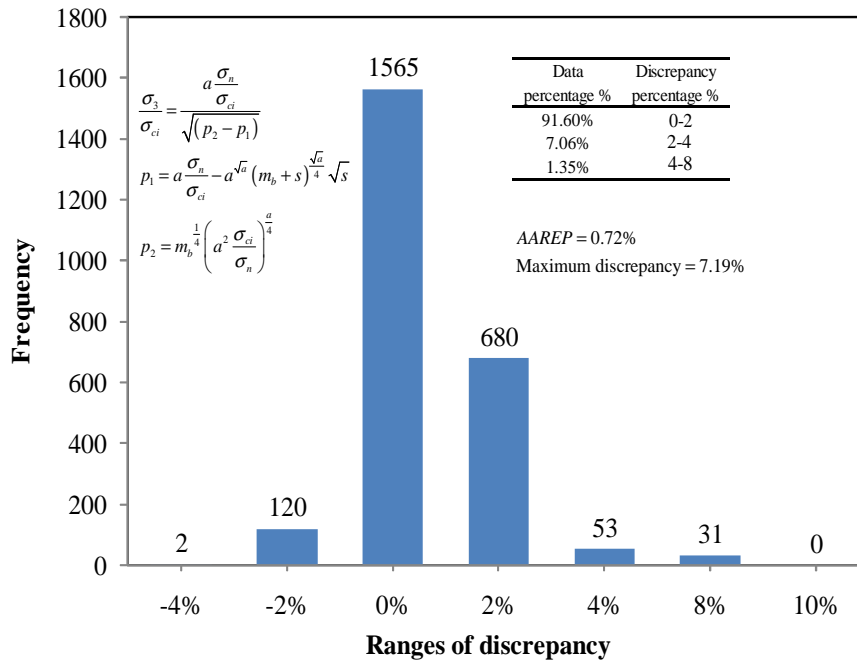


Fig. 10 Discrepancy analysis of the analytical solution which has the lowest value of AAREP

The data from Priest [22] was used to verify the reliability of the proposed Eq. 22. The following material parameters were used to generate data set $\sigma_{ci} = 30000 \text{ kPa}$, $m_i = 16$, $\text{GSI} = 15$, $\sigma_n = 800 \text{ kPa}$, $D = 0.7$. The Hoek-Brown parameters m_b , s and a were calculated using Eqs. 2 to 4 respectively. The value of shear stress τ calculated from Eq. 22 is 476.09 kPa . It is slightly different from the Priest numerical results with τ is 472.38 kPa . The discrepancy was found to be only 0.78% . Table 4 illustrates shear stresses τ from the proposed approximate analytical and numerical solutions over a range of σ_n . The resulting shear and normal stresses were plotted in Fig. 11. In all cases, there was found to be a close agreement between the proximate analytical and numerical solutions with $\text{AAREP} = 1.0\%$.

Table 4 Shear stresses obtained from numerical and GP analytical solutions over a range of normal stresses

		Shear stress, τ (kPa)		Discrepancy (%)
σ_n/σ_{ci}	σ_n (kPa)	GP analytical	Numerical	
Uniaxial compressive strength, σ_{ci} (kPa)				30000
Hoek-Brown constant for intact rock, m_i				16
Geological strength Index, GSI				15
Normal stress, σ_n (kPa)				30-20430
Disturbance factor, D				0.7
σ_n/σ_{ci}	σ_n (kPa)	GP analytical	Numerical	Discrepancy (%)
1.00E-03	30	48.92	45.62	7.23
2.10E-02	630	405.79	401.31	1.12
4.10E-02	1230	633.07	631.19	0.30
6.10E-02	1830	821.15	821.36	-0.03
8.10E-02	2430	986.97	988.71	-0.18
1.01E-01	3030	1137.80	1140.60	-0.25
1.21E-01	3630	1277.50	1280.90	-0.27
1.41E-01	4230	1408.70	1412.30	-0.25
1.61E-01	4830	1532.90	1536.40	-0.23
1.81E-01	5430	1651.20	1654.40	-0.19
2.01E-01	6030	1764.70	1767.30	-0.15
2.21E-01	6630	1873.90	1875.60	-0.09
2.41E-01	7230	1979.50	1980.00	-0.03
2.61E-01	7830	2081.70	2080.90	0.04
2.81E-01	8430	2181.10	2178.70	0.11
3.01E-01	9030	2277.80	2273.60	0.18
3.21E-01	9630	2372.20	2366.00	0.26
3.41E-01	10230	2464.50	2456.00	0.35
3.61E-01	10830	2554.90	2543.80	0.44
3.81E-01	11430	2643.40	2629.70	0.52
4.01E-01	12030	2730.40	2713.70	0.62
4.21E-01	12630	2815.90	2795.90	0.72
4.41E-01	13230	2900.10	2876.60	0.82
4.61E-01	13830	2983.10	2955.70	0.93
4.81E-01	14430	3064.90	3033.40	1.04
5.01E-01	15030	3145.80	3109.80	1.16
5.21E-01	15630	3225.80	3184.80	1.29
5.41E-01	16230	3305.00	3258.70	1.42
5.61E-01	16830	3383.60	3331.50	1.56
5.81E-01	17430	3461.70	3403.20	1.72
6.01E-01	18030	3539.50	3473.80	1.89
6.21E-01	18630	3617.00	3543.40	2.08
6.41E-01	19230	3694.60	3612.20	2.28
6.61E-01	19830	3772.60	3680.00	2.52
6.81E-01	20430	3851.40	3746.90	2.79

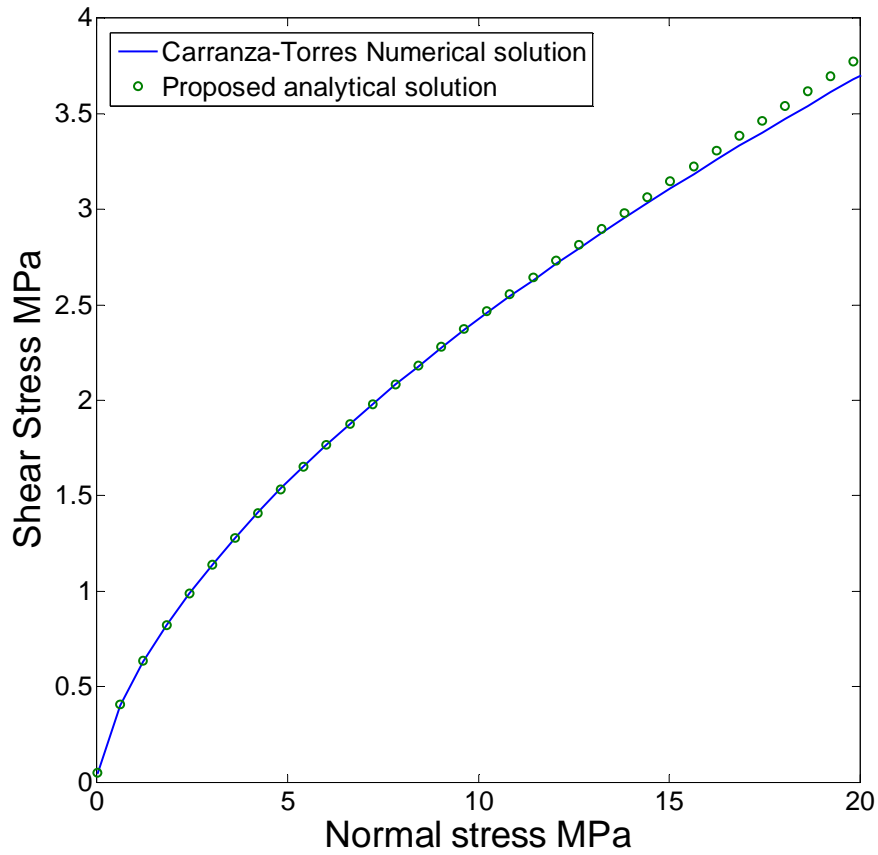


Fig. 11 Hoek-Brown shear strength envelope in shear stress/normal stress space

Fig. 12 illustrates the comparison of shear stress τ from the proposed analytical solution and Shen et al. solution [27] with that from numerical solution [1] for rock mass: $\sigma_{ci}=25000\text{kPa}$, $\sigma_n=5000\text{kPa}$, $m_i=15$, $D=0$ and the range of GSI from 0 to 100. The results show that there is a close agreement between the proposed analytical solution and the numerical solution for the whole range of GSI values. The AAREP of τ is found to be 0.63%. Compared with Shen et al. solution with AAREP=3.99%, the proposed solution produce better results.

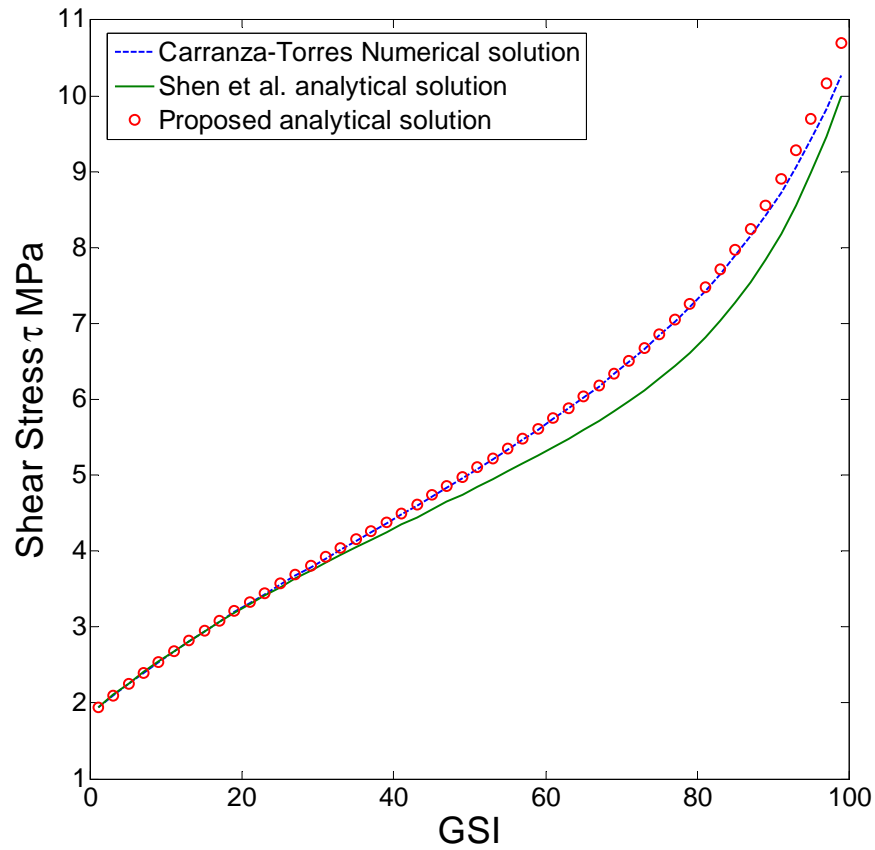


Fig. 12 Comparison of shear stress τ results

6 Conclusions

Existing numerical methods in conjunction with symbolic regression (SR) analysis performed by genetic programming (GP) have been used to derive analytical solutions for estimating the Mohr-Coulomb (MC) shear strength of rock masses from the non-linear Generalized Hoek-Brown (GHB) criterion.

The reported research used Eq. 14 to build a GP model as the basis for calculating the intermediate parameter σ_3/σ_{ci} expressed by input parameters m_b , s , a and σ_n/σ_{ci} . After obtaining analytical solution Eq. 19 for σ_3/σ_{ci} , closed form solution Eq. 22 has been derived for estimating shear stress τ .

The performance of the proposed approximate analytical solution has been tested against Carranza-Torres numerical solution using 2451 random sets of data. The results show that there is a close agreement between the proposed approximate analytical and numerical solutions. Shear stress τ calculated from the proposed approximate analytical solution exhibits only 0.97 % average absolute discrepancy from numerical solutions as shown Fig. 8, and the discrepancy of 84.21% sets of data range is less than 2% as shown in Fig. 9. In a practical sense, this small difference is acceptable.

The proposed approximate analytical solutions is an alternative form of the GHB criterion, which can be implemented into both limit equilibrium method and shear strength reduction methods for analyzing rock mass slopes.

Acknowledgement

PhD Scholarship provided by China Scholarship Council (CSC) is gratefully acknowledged. The sections 1 and 2 of the manuscript were developed with Prof. Stephen Priest as co-author. Thus, many thanks go to Prof. Stephen Priest for his contribution. The authors also would like to express their gratitude to anonymous reviewers for their constructive comments on the paper.

References

- [1] Carranza-Torres C. Some comments on the application of the Hoek–Brown failure criterion for intact rock and rock masses to the solution of tunnel and slope problems. In: Barla G, Barla M, editors, MIR 2004 – X Conference on rock and engineering mechanics, Torino, Italy, Patron Editore, Bologna; 24–25 November 2004. p. 285–326. [Chapter 10].
- [2] Hoek E, Brown ET. Underground excavations in rock. London: Instn Min Metall; 1980. p. 527.

- [3] Brown ET. Estimating the mechanical properties of rock masses. In: Proceedings of the 1st southern hemisphere international rock mechanics symposium: SHIRMS 2008, Perth, Western Australia, vol. 1; 2008. p. 3–21.
- [4] Hoek E, Carranza-Torres C, Corkum B. Hoek–Brown failure criterion-2002 edition. In: Proceedings of the North American rock mechanics society meeting, Toronto; July 2002.
- [5] Koza JR. Genetic programming: on the programming of computers by means of natural selection. Cambridge, MA: MIT press; 1992. p. 819.
- [6] Johari A, Habibagahi G, Ghahramani A. Prediction of soil–water characteristic curve using genetic programming. *J Geotech Geoenviron Eng* 2006;132(5):661–5.
- [7] Javadi AA, Rezanian M, Nezhad MM. Evaluation of liquefaction induced lateral displacements using genetic programming. *Comput Geotech* 2006;33(4–5):222–33.
- [8] Cabalar AF, Cevik A. Genetic programming-based attenuation relationship: an application of recent earthquakes in turkey. *Comput Geosci* 2009;35(9):1884–96.
- [9] Karakus M. Function identification for the intrinsic strength and elastic properties of granitic rocks via genetic programming (GP). *Comput Geosci* 2011;37:1318–23.
- [10] Balmer G. A general analytical solution for Mohr’s envelope. *Am Soc Test Mater* 1952;52:1269–71.
- [11] Priest SD, Brown ET. Probabilistic stability analysis of variable rock slopes. *Trans Instn Min Metall* 1983;92:A1–A12.
- [12] Hoek E. Rankine lecture: strength of jointed rock masses. *Géotechnique* 1983;33:187–223.
- [13] Ucar R. Determination of the shear stress failure in rock masses. *ASCE J Geotech Eng Div* 1986;112(3):303–15.
- [14] Londe P. Discussion on the paper ‘determination of the shear stress failure in rock masses’, by R. Ucar (Paper 20431), March, 1986, vol. 112, no. 3. *J Geotech Eng Div* 1988;114(3):374–6.
- [15] Hoek E. Estimating Mohr–Coulomb friction and cohesion values from the Hoek–Brown failure criterion. *Int J Rock Mech Min Sci Geomech Abstr* 1990;27(3):227–9.

- [16] Hoek E, Brown ET. Practical estimates of rock mass strength. *Int J Rock Mech Min Sci* 1997;34(8):1165–86.
- [17] Kumar P. Shear failure envelope of Hoek–Brown criterion for rockmass. *Tunn Undergr Space Technol* 1998;13(4):453–8.
- [18] Serrano A, Olalla C, Gonzalez J. Ultimate bearing capacity of rock masses based on the modified Hoek–Brown criterion. *Int J Rock Mech Mining Sci* 2000;37:1013–8.
- [19] Sofianos AI, Halakatevakis N. Equivalent tunneling Mohr–Coulomb strength parameters for given Hoek–Brown ones. *Int J Rock Mech Min Sci* 2002;39(1):131–7.
- [20] Sofianos AI. Tunnelling Mohr–Coulomb strength parameters for rock masses satisfying the generalized Hoek–Brown failure criterion. *Int J Rock Mech Min Sci* 2003;40(3):435–40.
- [21] Carranza-Torres C. Elasto-plastic solution of tunnel problems using the generalized form of the Hoek–Brown failure criterion. *Int J Rock Mech Min Sci* 2004; 41(3):480–1 [In: Hudson JA, Feng X-T, editors. *Proceedings of the ISRM SINOROCK 2004 symposium*].
- [22] Priest SD. Determination of shear strength and three-dimensional yield strength for the Hoek–Brown criterion. *Rock Mech Rock Eng* 2005;38(4):299–327.
- [23] Sofianos AI, Nomikos PP. Equivalent Mohr–Coulomb and generalized Hoek–Brown strength parameters for supported axisymmetric tunnels in plastic or brittle rock. *Int J Rock Mech Min Sci* 2006;43:683–704.
- [24] Jimenez R, Serrano A, Olalla C. Linearization of the Hoek and Brown rock failure criterion for tunnelling in elasto-plastic rock masses. *Int J Rock Mech Min Sci* 2008;45:1153–63.
- [25] Yang XL, Yin JH. Slope equivalent Mohr–Coulomb strength parameters for rock masses satisfying the Hoek–Brown criterion. *Rock Mech Rock Eng* 2010;43:505–11.
- [26] Fu W, Liao Y. Non-linear shear strength reduction technique in slope stability calculation. *Comput Geotech* 2010;37:288–98.
- [27] Shen J, Priest SD, Karakus M. Determination of Mohr–Coulomb shear strength parameters form generalized Hoek–Brown criterion for slope stability analysis. *Rock Mech Rock Eng* 2012;45:123–9.
- [28] Rocscience, Slide, Rocscience. <<http://www.rocscience.com>>, Toronto.

[29] Rocscience, Roclab. <<http://www.rocscience.com>>, Toronto.

[30] Holland JH. Adaptation in natural and artificial systems. Ann Arbor: The University of Michigan Press; 1975.

[31] Silva S. A genetic programming toolbox for MATLAB: Version 3, 2007. <<http://www.switch.dl.sourceforge.net/sourceforge/gplab/>>.

Statement of Authorship of Journal paper 4

A Comparative Study for Empirical Equations in Estimating Deformation Modulus of Rock Masses

Jiayi Shen, Murat Karakus* & Chaoshui Xu

School of Civil, Environmental and Mining Engineering, The University of Adelaide

Adelaide, South Australia, 5005, Australia

Tunnelling and Underground Space Technology 2012, 32: 245-250.

By signing the Statement of Authorship, each author certifies that their stated contribution to the publication is accurate and that permission is granted for the publication to be included in the candidate's thesis.

Jiayi Shen

Performed the analysis and wrote the manuscript.

Signature:

Date: 27th May 2013

Dr. Murat Karakus

Supervised development of work, manuscript evaluation and acted as corresponding author.

Signature:

Date: 27th May 2013

Associate Prof. Chaoshui Xu

Supervised development of work and manuscript evaluation.

Signature:

Date: 27th May 2013

Chapter 4

A Comparative Study for Empirical Equations in Estimating Deformation Modulus of Rock Masses

Abstract

The deformation modulus of rock masses (E_m) is one of the significant parameters required to build numerical models for many rock engineering projects, such as open pit mining and tunnel excavations. In the past decades, a great number of empirical equations were proposed for the prediction of the rock mass deformation modulus. Existing empirical equations were in general proposed using statistical technique and the reliability of the prediction relies on the quantity and quality of the data used. In this paper, existing empirical equations using both the Rock Mass Rating (RMR) and the Geological Strength Index (GSI) are compared and their prediction performances are assessed using published high quality *in-situ* data. Simplified empirical equations are proposed by adopting Gaussian function to fit the *in-situ* data. The proposed equations take the RMR and the deformation modulus of intact rock (E_i) as input parameters. It has been demonstrated that the proposed equations fit well to the *in-situ* data compared with the existing equations.

1 Introduction

The deformation modulus (E_m) is the most representative parameter of the mechanical behavior of rock masses. It is widely used in numerical modeling, such as finite element modeling, of rock

engineering projects where the analysis of displacement and stress distribution are required to characterize the rock mass behavior.

Commonly used approaches to estimate E_m includes: laboratory tests, *in-situ* loading tests and prediction by empirical equations. However, laboratory tests on limited size rock samples containing discontinuities cannot measure reliably values of E_m due to the limitation of size of the testing equipment (Palmström 1996). *In-situ* tests can provide direct information on the deformability of rock masses, however, as Bieniawski (1973) noted, it is difficult to rely on one *in-situ* test alone as different results may be obtained even in a fairly uniform and good quality rock mass condition. Therefore, in order to obtain reliable results multi-tests are necessary which are expensive and time consuming.

Due mainly to the above mentioned difficulties encountered in laboratory and *in-situ* testing, the estimation of E_m values using empirical equations becomes a very attractive and commonly accepted approach among rock engineers.

In the past decades, a great number of empirical equations were proposed for the estimation of the isotropic rock mass deformation modulus using various rock mass classification systems, such as the Rock Mass Rating (RMR), the Geological Strength Index (GSI) (see Table 1), the Tunneling Quality Index (Q) (Barton 1987, 1996, 2002) and the Rock Mass Index (RMi) (Palmström 1996, Palmström and Singh 2001). Other authors proposed equations on the basis of parameters which define the quality of the rock masses, such as the Rock Mass Quality Designation (RQD) (Zhang and Einstein 2004) and the Weathering Degree (WD) (Gokceoglu et al. 2003, Kayabasi et al. 2003).

Existing empirical equations were in general derived using statistical methods, such as the regression analysis, and the reliability of estimation of these equations depends on the quantity

and quality of data used in the statistical analysis. As a consequence, large discrepancies in the predicted values using different empirical relations can be experienced which reduce the confidence in the predicted values. For example, for a rock mass with the following properties: GSI=70, the disturbance factor, $D=0$ and the intact rock deformation modulus, $E_i=50\text{GPa}$, the values of E_m calculated from the empirical equations proposed by Carvalho (2004), Sonmez et al. (2004) and Hoek and Diederichs (2006) (see Group 4 in Table 1) are 21.7 GPa, 25.6 GPa and 36.6 GPa, respectively. Clearly the reliability of the prediction of these empirical equations needs to be assessed.

In this research, existing empirical equations using the RMR and the GSI classification systems are evaluated. The prediction performance of these equations is tested by using high quality well publicized *in-situ* data from Bieniawski (1978), Serafim and Pereira (1983) and Stephens and Banks (1989). These data are from high quality tests and are commonly acknowledged as reliable data sources (Hoek and Diederichs 2006). New simplified empirical equations are proposed by adopting Gaussian function to fit these *in-situ* data. The proposed equations take the RMR classification system and the deformation modulus of intact rock (E_i) as input parameters. It has been demonstrated that the proposed equations fit well to the mentioned *in-situ* data compared with the existing equations.

In this paper, the strategy of evaluation of existing equations for predicting E_m is described in section 2. The performance of existing equations using the RMR and GSI classification systems is assessed in section 3. The proposed simplified empirical relationships between E_m and the RMR system are described in section 4.

2 The strategy of evaluation of existing empirical equations

2.1 Category

In this research, we focus only on the empirical equations which contain the RMR and GSI as input parameters. According to different input parameters, the existing empirical equations using the RMR and GSI classification systems can be divided into five groups (see Table 1).

Table 1 Empirical equations using RMR and GSI for predicting E_m

Input Parameters		Empirical Equations
Group 1 RMR	Bieniawski (1978)	$E_m = 2RMR - 100, RMR > 50$
	Serafim and Pereira (1983)	$E_m = 10^{(RMR-10)/40}$
	Mehrotra (1992)	$E_m = 10^{(RMR-20)/38}$
	Read et al. (1999)	$E_m = 0.1(RMR/10)^3$
Group 2 RMR and E_i	Nicholson and Bieniawski (1990)	$E_m = 0.01E_i \left(0.0028RMR^2 + 0.9e^{\frac{RMR}{22.83}} \right)$
	Mitri et al. (1994)	$E_m = E_i \left[0.5 \left(1 - \left(\cos \left(\pi RMR / 100 \right) \right) \right) \right]$
	Sonmez et al. (2006)	$E_m = E_i 10^{((RMR-100)(100-RMR))/(4000 \exp(-RMR/100))}$
Group 3 GSI and D	Hoek et al. (2002)	$E_m = (1 - 0.5D) 10^{\left(\frac{GSI-10}{40} \right)}, \sigma_{ci} > 100MPa$
	Hoek and Diederichs (2006)	$E_m (MPa) = 10^5 \left(\frac{1-0.5D}{1+e^{((75+25D-GSI)/11)}} \right)$
Group 4 GSI, D and E_i	Carvalho (2004)	$E_m = E_i (s)^{0.25}, s = \exp \left(\frac{GSI-100}{9-3D} \right)$
	Sonmez et al. (2004)	$E_m = E_i (s^a)^{0.4}, s = \exp \left(\frac{GSI-100}{9-3D} \right)$ $a = 0.5 + \frac{1}{6} \left(e^{-GSI/15} - e^{-20/3} \right)$
	Hoek and Diederichs (2006)	$E_m = E_i \left(0.02 + \frac{1-0.5D}{1+e^{((60+15D-GSI)/11)}} \right)$
Group 5 GSI, D and σ_{ci}	Hoek and Brown (1997)	$E_m = \sqrt{\frac{\sigma_{ci}}{100}} 10^{\left(\frac{GSI-10}{40} \right)}$
	Hoek et al. (2002)	$E_m = (1-0.5D) \sqrt{\frac{\sigma_{ci}}{100}} 10^{\left(\frac{GSI-10}{40} \right)}, \sigma_{ci} \leq 100MPa$
	Beiki et al. (2010)	$E_m = \tan \left(\sqrt{1.56 + (\ln(GSI))^2} \right) \sqrt[3]{\sigma_{ci}}$

2.2 Testing Data

In-situ data from Bieniawski (1978), Serafim and Pereira (1983) and Stephens and Banks (1989) are from high quality tests and are commonly acknowledged as reliable data sources (Hoek and Diederichs 2006). These data also were widely used by many researchers (Barton 1996; Palmström and Singh 2001; Sonmez et al. 2006; Hoek and Diederichs 2006) to assess the reliability of their proposed equations. Therefore, in this research, 43 of the 76 sets of these data were used for assessing the prediction performance of equations in Groups 1, 3 and 5. The other 33 sets of data which contain E_i as input parameter were used to test the prediction performance of equations in Groups 2 and 4.

These *in-situ* data, however, are quantified on the basis of the RMR classification system. In order to use these data to evaluate the reliability of the empirical equations using the GSI system, the relationship between RMR and GSI will have to be used to transform RMR to GSI. Hoek and Diederichs (2006) suggested GSI equal to RMR if the RMR data were obtained before 1990. Therefore, for the *in-situ* data which were collected before 1989, the relationship of RMR = GSI is used in this research.

2.3 Indicators to assess the prediction performance of empirical equations

The value of Root Mean Square Errors (RMSE) (Eq. 1) and R-square (R^2) (Eq. 2) are adopted in this research as indicators to assess the reliability of prediction by empirical equations:

$$RMSE = \sqrt{\frac{1}{N} \sum_{i=1}^N (E_m^i - E_m^{i'})^2} \quad (1)$$

$$R^2 = 1 - \frac{\sum_{i=1}^N (E_m^i - E_m^{i'})^2}{\sum_{i=1}^N (E_m^i - \bar{E}_m)^2} \quad (2)$$

where N is the number of testing data used, E_m^i and E_m^e are deformation modulus of rock masses obtained from the observed *in-situ* data and derived from the empirical equations respectively. $\overline{E_m}$ is the mean value of E_m .

RMSE as defined is effectively the standard deviation of the errors associated with the estimation if it is unbiased. Clearly, the smaller the RMSE, the more reliable the estimation. The value of R^2 generally ranges from 0 to 1. For exact prediction, i.e., estimation with no error, the value of R^2 will be one. On the other hand, R^2 trends to zero for poor estimations. It should be noted that R^2 can be negative if the quality of the estimation is extremely poor.

3 The evaluation of existing empirical equations

3.1 Relations between E_m and RMR

Various attempts have been made to develop empirical equations taking the RMR as the input parameter to estimate E_m . These equations can be divided into two groups according to input variables as shown in Table 1.

3.1.1 Group 1 Input parameter: RMR

The first empirical equation for predicting the rock mass deformation modulus using the RMR system was proposed by Bieniawski (1978), which was followed by other equations proposed by various researchers. The prediction performance of these equations is illustrated in Fig. 1.

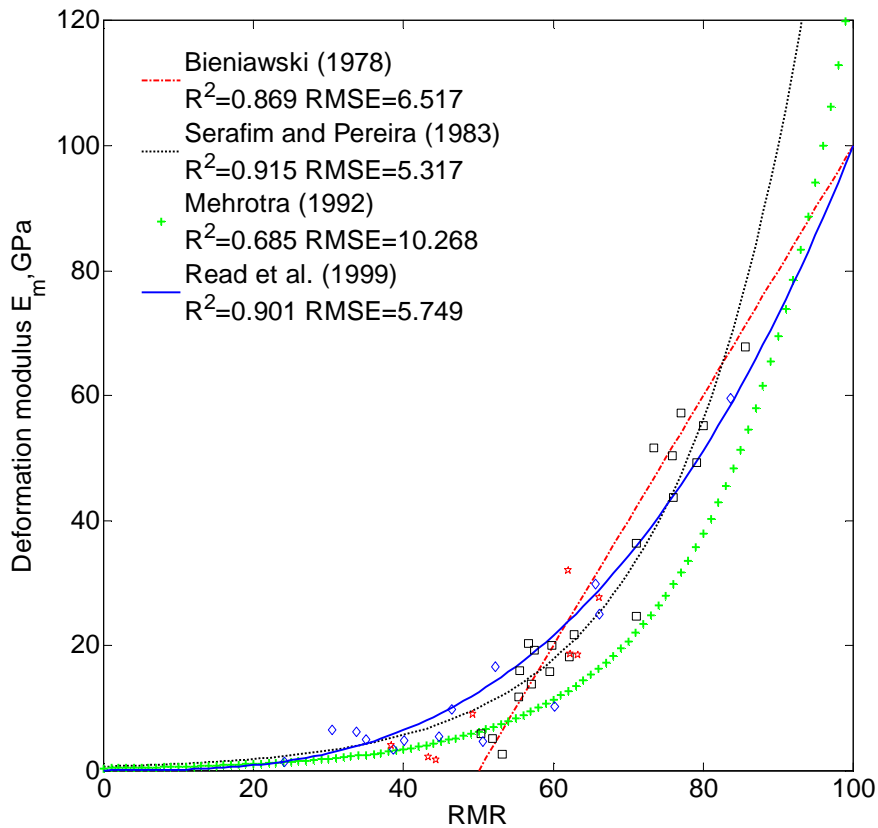


Fig. 1 Empirical equations in Group 1 for estimating E_m compared with *in-situ* data

Based on the assessment of R^2 and RMSE, the curve that best fits the *in-situ* data is the one proposed by Serafim and Pereira (1983) with the values of R^2 and RMSE equal to 0.915 and 5.317 respectively. The same equation, however, gives poor prediction for massive rock masses when RMR is approaching 100 where the predicted E_m value is unrealistically high. The third power function proposed by Read et al. (1999) ($R^2=0.901$, RMSE=5.749) overcomes the limitation of Serafim and Pereira's equation as it can give reasonable estimation of the value of E_m for massive rock masses. The equation proposed by Mehrotra (1992) generally produces E_m values lower than *in-situ* data when $RMR > 60$.

3.1.2 Group 2 Input parameter: RMR and E_i

One major limitation of the equations listed in Group 1 is that the deformation modulus of intact rock (E_i) is not considered. As pointed out by Sonmez et al. (2006), for high quality rock masses composed of softer intact rock, the value of deformation modulus of rock masses is mostly controlled by the properties of intact rock rather than by those of the discontinuities. To account for this situation, Nicholson and Bieniawski (1990), Mitri et al. (1994) and Sonmez et al. (2006) introduced E_i into their empirical equations for the estimation of E_m . Fig. 2 gives the prediction performance of these equations (Group 2).

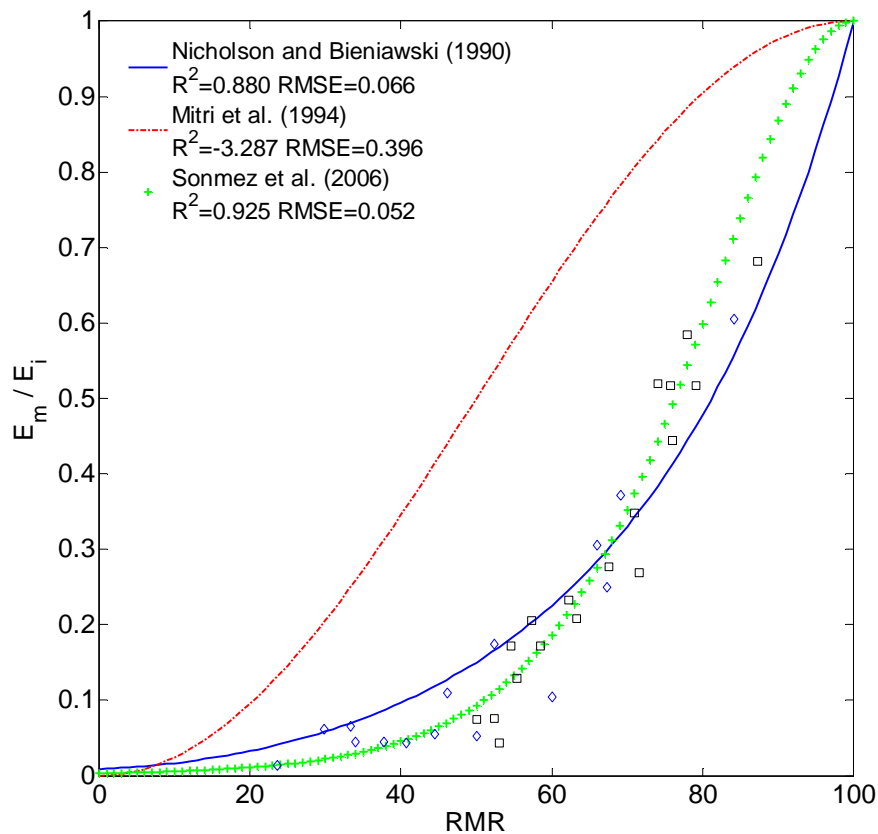


Fig. 2 Empirical equations in Group 2 for estimating E_m / E_i compared with *in-situ* data

The values of R^2 and RMSE in Fig. 2 demonstrate that the Sonmez et al.'s equation (2006) ($R^2=0.925$, $RMSE=0.052$) gives the best estimation within the group. The equation presented by

Nicholson and Bieniawski (1990) has $R^2=0.880$, $RMSE=0.066$, respectively. The performance of the Mitri et al.'s equation (1994) is the poorest as the estimated E_m values are significantly higher than observed data values across the whole range.

3.2 Relations between E_m and GSI

The empirical equations using the GSI classification system as the input parameter to estimate the rock mass deformation modulus can be divided into three groups according to the input variables as given in Table 1.

3.2.1 Group 3 Input parameter: GSI and D

In this group, the empirical equation proposed by Hoek and Brown (1997) was modified by Hoek et al. (2002) to take into account the effect of disturbance factor D . The limitation of the modified equation is that it is only applicable when the value of uniaxial compressive strength of the intact rock, σ_{ci} is greater than 100MPa. This limitation was later overcome by Hoek and Diederichs (2006). The prediction performance of the equations in Group 3 is shown in Fig. 3.

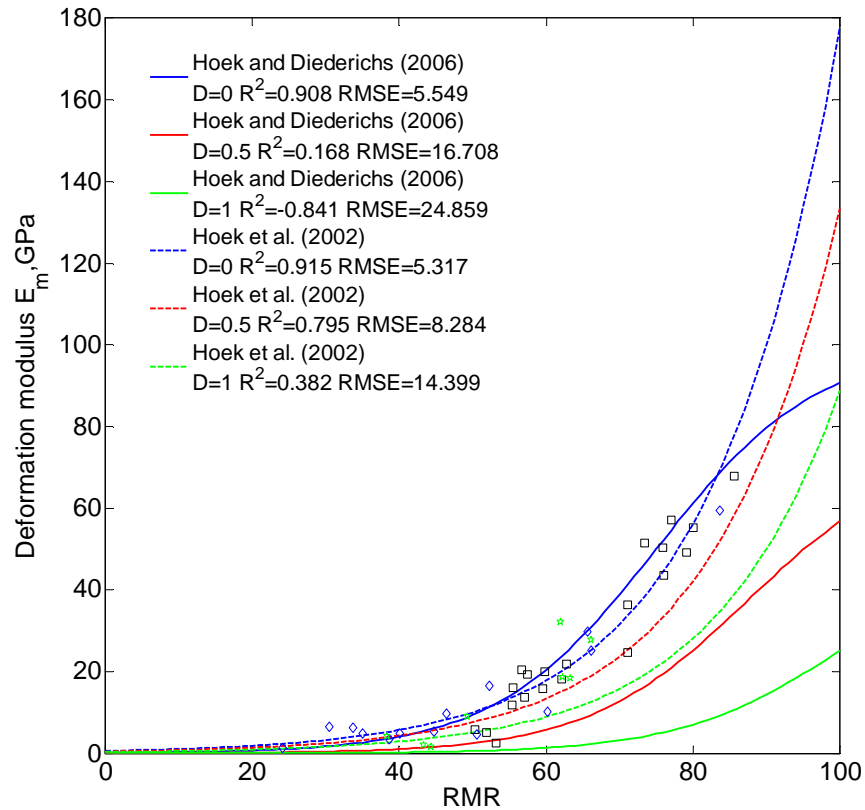


Fig. 3 Empirical equations in Group 3 for estimating E_m compared with *in-situ* data

Fig. 3 indicates that the value of D has a great influence on the value of E_m . The value of D , however, can vary in value from 0 for undisturbed *in-situ* rock masses to 1 for highly disturbed rock masses to reflect the effects of heavy blast damage as well as stress relief due to removal of the overburden. Hoek et al. (2002) proposed a descriptive guideline on how to choose an appropriate D value for a variety of different engineering practices.

The best fit equation in this group is the one proposed by Hoek et al. (2002) when $D=0$ (undisturbed conditions), which gives values of R^2 and RMSE at 0.915 and 5.317, respectively. The same equation, however, gives too high estimate for E_m when RMR is greater than 90. The sigmoid function proposed by Hoek and Diederichs (2006) has $R^2=0.908$ and RMSE=5.549, which can yield reasonable estimate for E_m even when RMR is greater than 90.

3.2.2 Group 4 Input parameter: GSI, D and E_i

Carvalho (2004), Sonmez et al. (2004) and Hoek and Diederichs (2006) proposed empirical equations taking GSI, D and E_i as input variables. The empirical equation proposed by Carvalho (2004) and Sonmez et al. (2004) rely on an approach which assumes the modulus ratio of the rock mass (E_m/σ_{cm}) is equal to that of the intact rock (E_i/σ_{ci}) when GSI=100. The equation by Hoek and Diederichs (2006) is proposed based on the *in-situ* data collected from areas in China and Taiwan. The prediction performance of these equations (Group 4) is shown in Fig. 4.

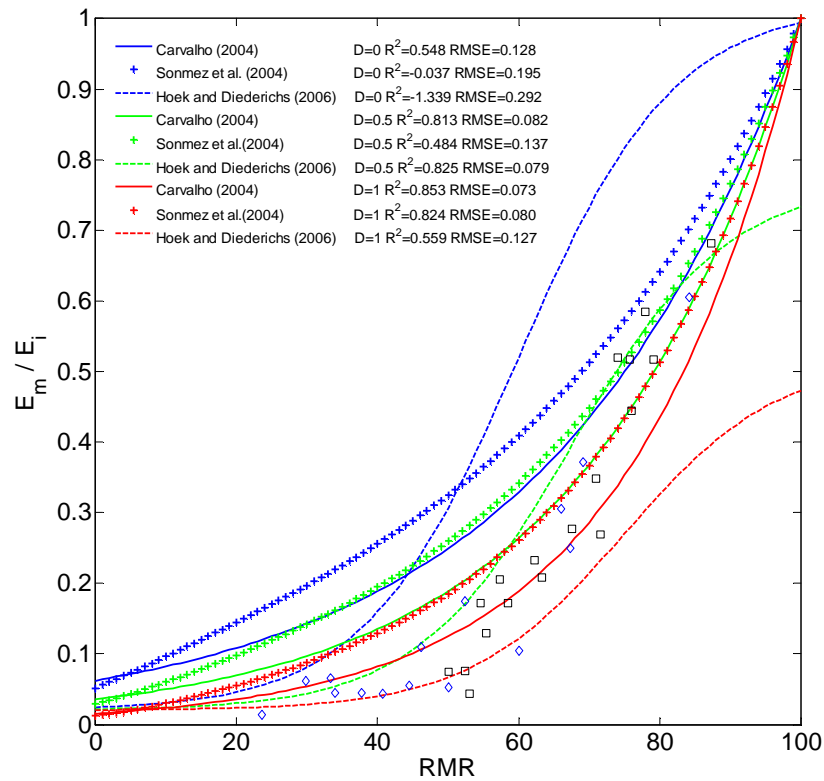


Fig. 4 Empirical equations in Group 4 for estimating E_m / E_i compared with *in-situ* data

From Fig. 4 it is clear that E_m values predicted from the equations proposed by Carvalho (2004) and Sonmez et al. (2004) are not dependent on the disturbance factor D when RMR=100, while the value of D has a great influence on E_m predicted from Hoek and Diederichs' proposed

(2006) equation. For $D=0$, the best fit equation is the one proposed by Carvalho (2004) ($R^2=0.548$, $RMSE=0.128$).

3.2.3 Group 5 Input parameter: GSI , D and σ_{ci}

The empirical equation proposed by Serafim and Pereira (1983) was modified by Hoek and Brown (1997) to incorporate the uniaxial compressive strength of the intact rock, σ_{ci} . Hoek et al. (2002) updated the Hoek and Brown's equation (1997) by considering a disturbance effect factor D in the rock mass for $\sigma_{ci} < 100\text{MPa}$. Beiki et al. (2010) adopted the genetic programming to determine E_m . Their proposed equation, however, has some limitations that the value of E_m becomes negative for case of $GSI < 20$ or $GSI > 90$. The performance of the equations in Group 5 is shown in Fig. 5

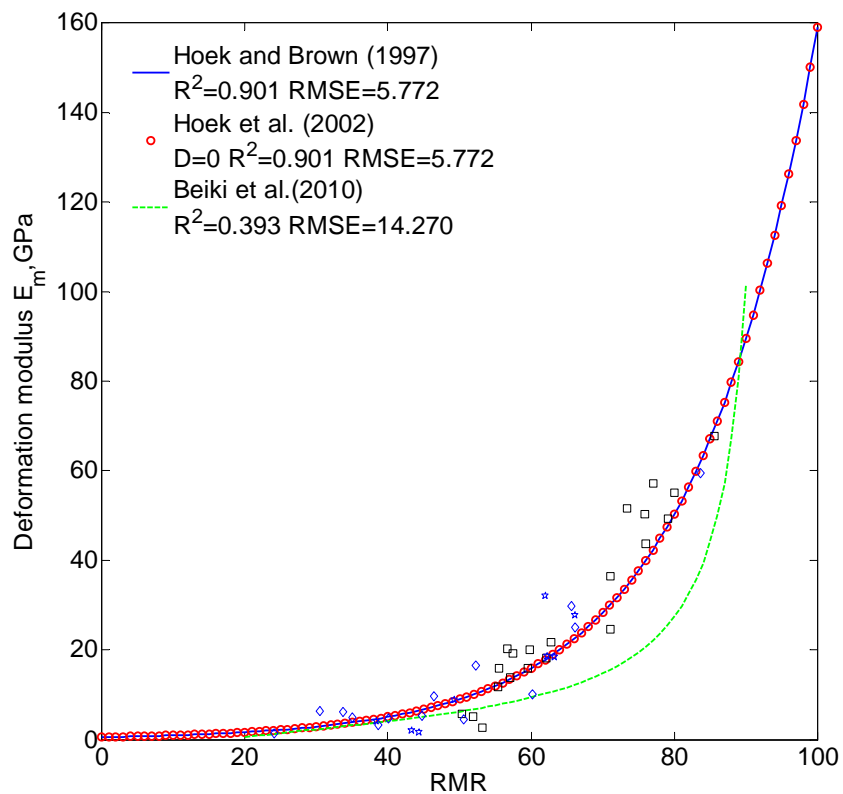


Fig. 5 Empirical equations in Group 5 for estimating E_m compared with *in-situ* data, $\sigma_{ci}=80\text{MPa}$

As seen from Fig. 5, Hoek et al.'s (2002) equation gives the same E_m values as Hoek and Brown's (1997) equation when D is assumed to be zero, and it gives the best fit to the data with $R^2=0.901$, $RMSE=5.772$, respectively. The equation proposed by Beiki et al. (2010) generally produces values of E_m lower than the measured data when GSI is greater than 55.

4 Proposed equations and their validations

Gaussian function (see the general form in Eq. 3) was used to fit empirical equations based on the *in-situ* data (Bieniawski 1978; Serafim and Pereira 1983; Stephens and Banks 1989).

$$y = ae^{-\left(\frac{x-b}{c}\right)^2} \quad (3)$$

where a , b and c are constants.

The proposed empirical equation is based on Gaussian function and use the RMR classification system as input parameters. The least square fitting based on the data used in this research gives the following equation:

$$E_m = 110e^{-\left(\frac{RMR-110}{37}\right)^2} \quad (4)$$

Fig. 6 demonstrates that the prediction performance of the proposed equation ($R^2=0.932$, $RMSE=4.772$) was improved compared to Read et al.'s (1999) equation and Hoek and Diederichs' (2006) equation which are considered to be the best fit equation for the RMR and GSI category in Groups 1 and 3, respectively.

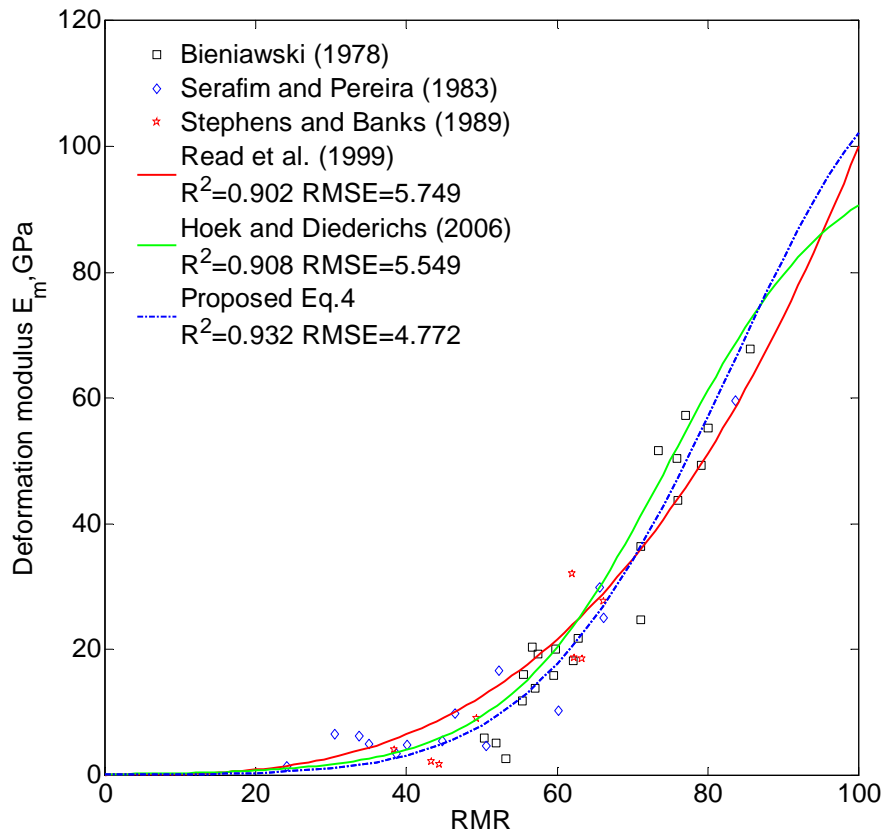


Fig. 6 Plot the Eq. 4 for the *in-situ* data

The comparison between the observed and estimated values calculated from the proposed Eq. 4 is shown in Fig. 7. The solid diagonal line in the figure represents a perfect prediction. The upper and lower dash lines represent the 10 GPa over-estimate and under-estimate of the true values respectively. Most of the predictions fall between these two lines, which suggests that the absolute error of Eq.4 is ± 10 GPa with a high level of confidence.

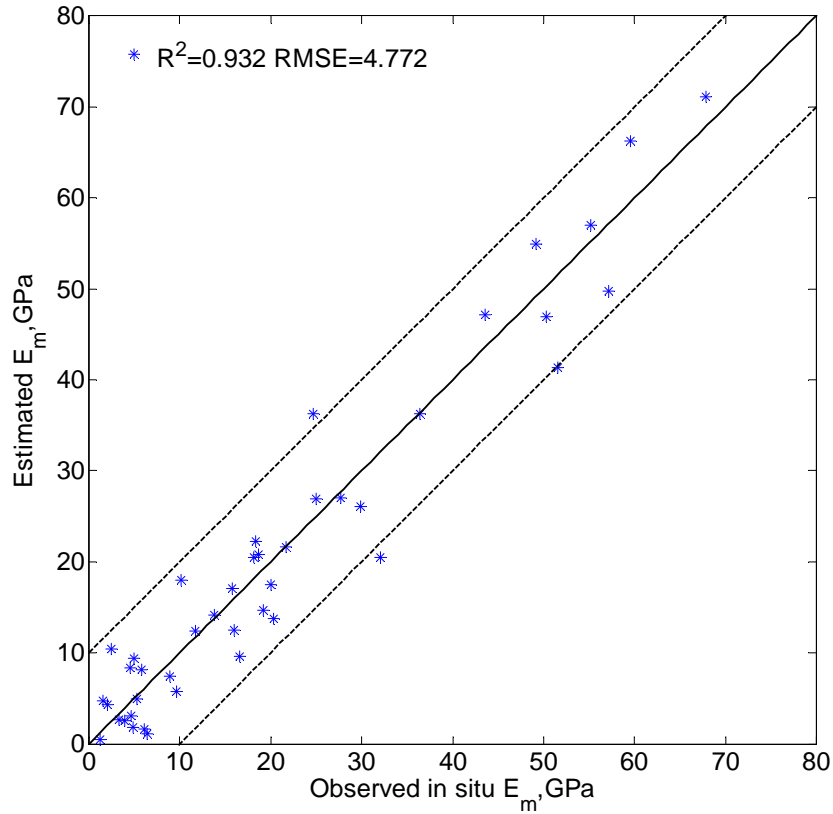


Fig. 7 Estimated E_m values from Eq. 4 versus *in-situ* data

To derive an equation which takes the RMR and E_i as input parameters Eq. 3 is adopted again to fit the data used in this research and the following best-fit equation is obtained:

$$E_m = 1.14E_i e^{-\left(\frac{RMR-116}{41}\right)^2} \quad (5)$$

The comparison of the prediction performances between Eq. 5 and the existing equations is shown in Fig. 8. As discussed in section 2, Sonmez et al.'s (2006) equation and Carvalho's (2004) equation perform the best among the existing equations for the RMR and GSI category in Groups 2 and 4, respectively. They are, however, over-performed by Eq. 5 which gives $R^2=0.936$ and RMSE=0.048.

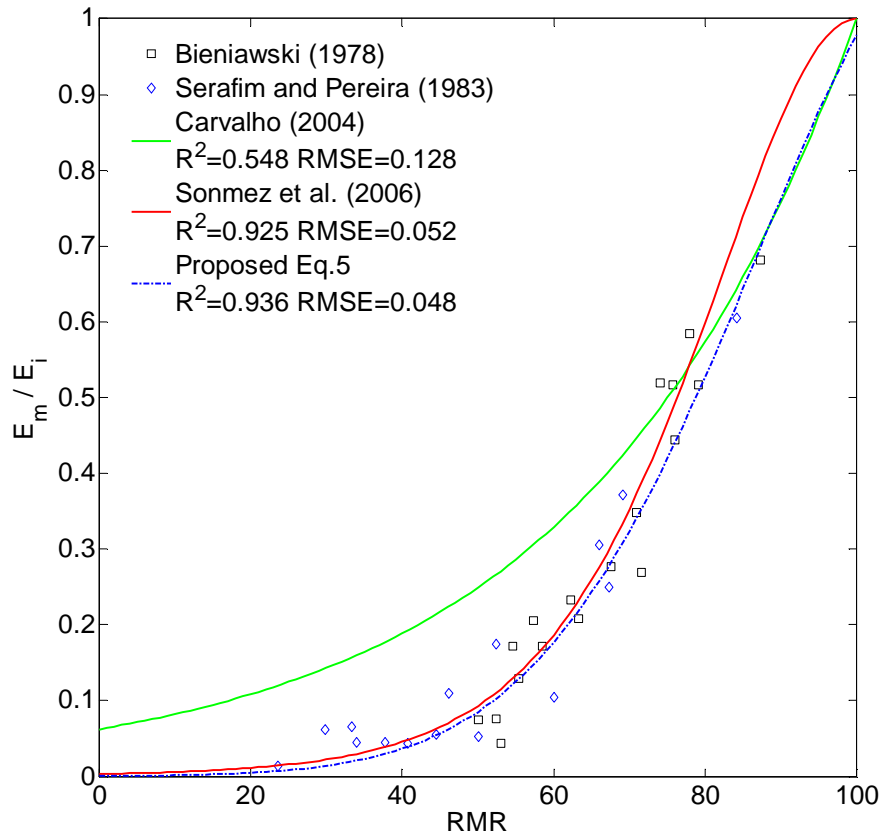


Fig. 8 Plot the Eq. 5 for the *in-situ* data

The comparison between the observed data and the estimated values calculated from Eq. 5 is given in Fig. 9, where the two dash lines represent error range of $\pm 0.1 E_m/E_i$. Most of the predictions from Eq. 5 fall between these two lines which suggests that accuracy of Eq. 5 is acceptable with the confidence interval of $\pm 0.1 E_m/E_i$.

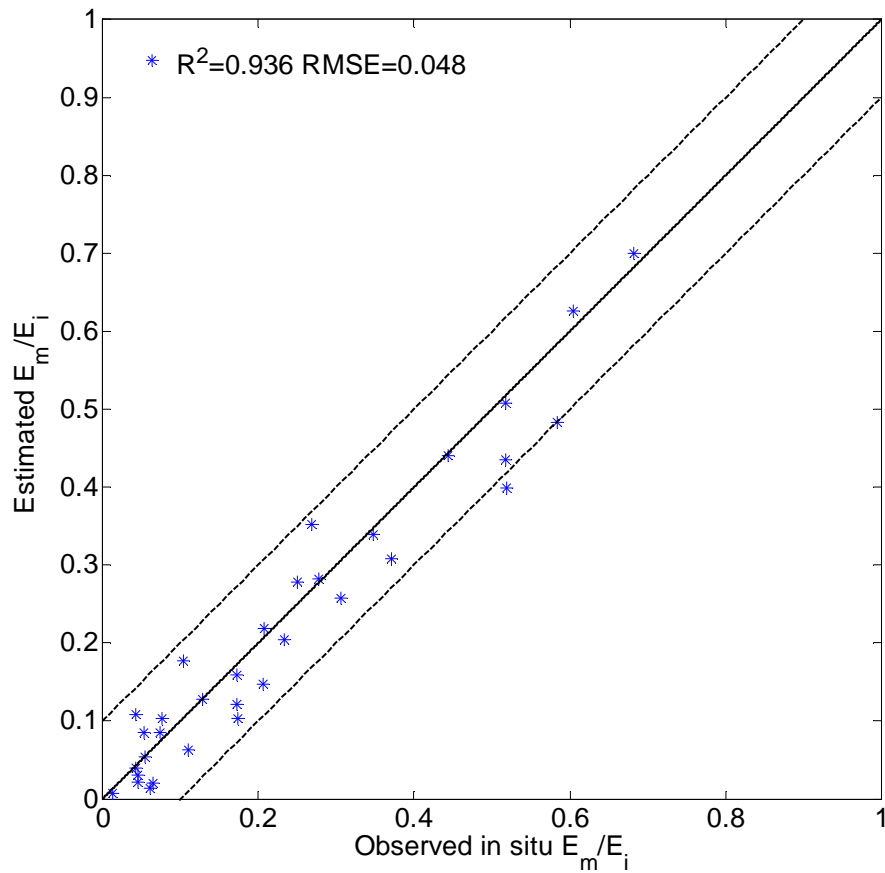


Fig. 9 Estimated E_m / E_i values from Eq. 5 versus *in-situ* data

As a further test of the prediction performance of Eqs. (4) and (5), their predicted values have been compared to measured field data reported in Hoek and Diederichs (2006). These data are generally regarded as the best collection of quality field data which can be used for any research. All of these GSI data are collected after 1989 and therefore the relationship of $RMR = GSI - 5$ is used to calculate RMR from GSI needed for the equations.

Scatter in the data in Fig. 10 represents inherent scatter in the values of GSI, rock mass properties E_m , and the effects of disturbance factor D due to blasting as well as stress relief.

Fig. 10 clearly demonstrates that the range of possible values of E_m is correctly predicted by Eq. 4, indicated by the envelope bounded by $D=0$ (upper bound). Fig. 11 illustrates that Eq. 5 gives a good prediction of the field data.

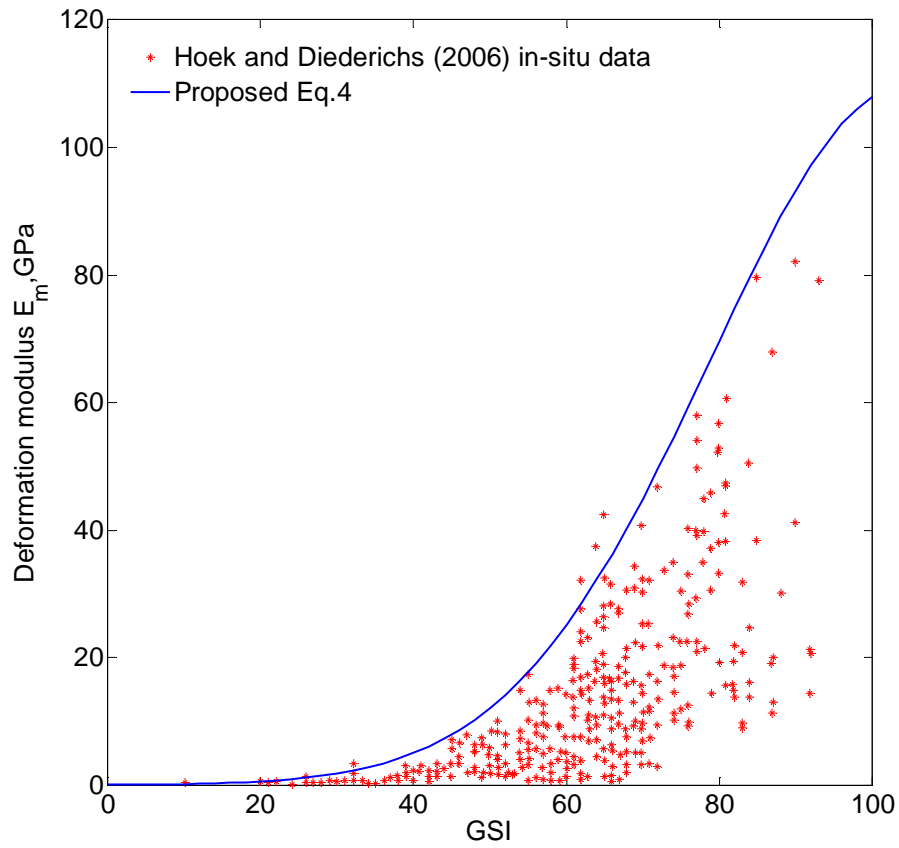


Fig. 10 E_m values estimated from Eq. 4 compared with Hoek and Diederichs (2006) *in-situ* data

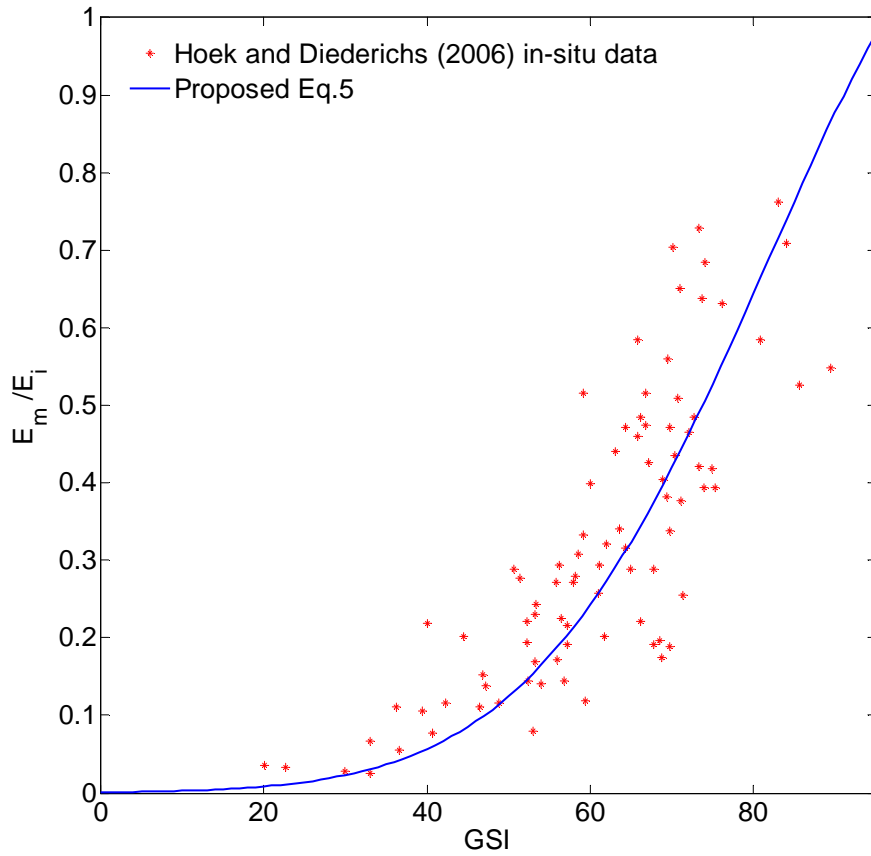


Fig. 11 E_m/E_i values estimated from Eq. 5 compared with Hoek and Diederichs (2006) *in-situ* data

5 Conclusions

In this paper, the most widely used empirical equations for the estimation of deformation modulus of rock masses based on the Rock Mass Rating (RMR) and the Geological Strength Index (GSI) classification systems have been reviewed. These equations were grouped according to the required input variables and their prediction performance were assessed using well acknowledged published *in-situ* data (Bieniawski 1978; Serafim and Pereira 1983; Stephens and Banks 1989).

Comparison analyses of existing equations show that in the category which does not involve the deformation modulus of intact rock (E_i) the equations proposed by Read et al. (1999) and Hoek and Diederichs (2006) give the best prediction for the RMR and GSI category respectively, as shown in Figs. 1 and 3. In the category where the deformation modulus of intact rock is considered, the equations proposed by Sonmez et al. (2006) and Carvalho (2004) performed the best for the RMR and GSI category respectively, as shown in Figs. 2 and 4.

Two simplified empirical equations have been proposed in this research using Gaussian function. The proposed empirical equations use the RMR classification system and the deformation modulus of intact rock (E_i) as input parameters. In absolute terms, it can be claimed with high level of confidence that the values of E_m predicted from Eq. 4 are accurate within ± 10 GPa, and the values of E_m predicted from Eq. 5 are accurate within a $\pm 0.1 E_m/E_i$.

As for all empirical relationships, the proposed empirical equations are open to further improvement as more *in-situ* data become available. At the time of writing, however, the proposed equations fit well to the in-situ data compared with existing equations based on the analyses presented in this paper (see Figs. 6 and 8).

Acknowledgement

PhD Scholarship provided by China Scholarship Council (CSC) is gratefully acknowledged. The authors also would like to express their gratitude to anonymous reviewers for their constructive comments on the paper.

References

Barton, N., 1987. Rock mass classification, tunnel reinforcement selection using the Q-system. In: Proceedings of the ASTM Symposium on Rock Classification Systems for Engineering Purposes. Cincinnati, Ohio.

- Barton, N., 1996. Estimating rock mass deformation modulus for excavation disturbed zone studies. In: International Conference on Deep Geological Disposal of Radioactive Waste, Winnipeg, EDZ workshop. Canadian Nuclear Society, pp. 133–144.
- Barton, N., 2002. Some new Q value correlations to assist in site characterization and tunnel design. *Int. J. Rock Mech. Min. Sci.* 39, 185–216.
- Beiki, M., Bashari, A., Majdi, A., 2010. Genetic programming approach for estimating the deformation modulus of rock mass using sensitivity analysis by neural network. *Int. J. Rock Mech. Min. Sci.* 47, 1091–1103.
- Bieniawski, Z.T., 1973. Engineering classification of rock masses. *Trans. S. African Inst. Civ. Eng.* 15 (12), 335–344.
- Bieniawski, Z.T., 1978. Determining rock mass deformability—experience from case histories. *Int. J. Rock Mech. Min. Sci. Geomech. Abstr.* 15, 237–247.
- Carvalho, J., 2004. Estimation of rock mass modulus (see paper by Hoek and Diederichs 2006).
- Gokceoglu, C., Sonmez, H., Kayabasi, A., 2003. Predicting the deformation moduli of rock masses. *Int. J. Rock Mech. Min. Sci.* 40, 701–710.
- Hoek, E., Brown, E.T., 1997. Practical estimates of rock mass strength. *Int. J. Rock Mech. Min. Sci.* 34 (8), 1165–1186.
- Hoek, E., Diederichs, M.S., 2006. Empirical estimation of rock mass modulus. *Int. J. Rock Mech. Min. Sci.* 43, 203–215.
- Hoek, E., Carranza-Torres, C., Corkum, B., 2002. Hoek-Brown failure criterion – 2002 Edition. In: Hammah, R., Bawden, W., Curran, J., Telesnicki, M. (Eds.), *Proceedings of NARMS-TAC 2002, Mining Innovation and Technology*, Toronto [downloadable for free at Hoek's corner, www.rocscience.com].
- Kayabasi, A., Gokceoglu, C., Ercanoglu, M., 2003. Estimating the deformation modulus of rock masses: a comparative study. *Int. J. Rock Mech. Min. Sci.* 40, 55–63.
- Mehrotra, V.K., 1992. Estimation of engineering parameters of rock mass. PhD thesis, Department of Civil Engineering, University of Roorkee, India.

- Mitri, H.S., Edrissi, R., Henning, J., 1994. Finite element modeling of cable bolted stopes in hard rock ground mines. In: Presented at the SME annual meeting, New Mexico, Albuquerque, pp. 94–116. Nicholson, G.A., Bieniawski, Z.T., 1990. A nonlinear deformation modulus based on rock mass classification. *Int. J. Min. Geol. Eng.* 8, 181–202.
- Palmström, A., 1996. Characterizing rock masses by R_{Mi} for use in practical rock engineering (Part 1: the development of the rock mass index (R_{Mi})). *Tunn. Undergr. Space Technol.* 11 (2), 175–188.
- Palmström, A., Singh, R., 2001. The deformation modulus of rock masses—comparisons between in situ tests and indirect estimates. *Tunn. Undergr. Space Technol.* 16 (3), 115–131.
- Read, S.A.L., Richards, L.R., Perrin, N.D., 1999. Applicability of the Hoek–Brown failure criterion to New Zealand greywacke rocks. In: Vouille, G., Berest, P. (Eds), *Proceedings of the ninth international congress on rock mechanics*, vol. 2, Paris, August 1999, pp. 655–660.
- Serafim, J.L., Pereira, J.P., 1983. Considerations on the geomechanical classification of Bieniawski. In: *Proceedings of the symposium on engineering geology and underground openings*. Portugal, Lisboa, pp. 1133–1144.
- Sonmez, H., Gokceoglu, C., Ulusay, R., 2004. Indirect determination of the modulus of deformation of rock masses based on the GSI system. *Int. J. Rock Mech. Min. Sci.* 41, 849–857.
- Sonmez, H., Gokceoglu, C., Nefeslioglu, H.A., Kayabasi, A., 2006. Estimation of rock modulus: for intact rocks with an artificial neural network and for rock masses with a new empirical equation. *Int. J. Rock Mech. Min. Sci.* 43, 224–235.
- Stephens, R.E., Banks, D.C., 1989. Moduli for deformation studies of the foundation and abutments of the Portugues Dam—Puerto Rico. In: *Rock mechanics as a guide for efficient utilization of natural resources: Proceedings of the 30th US symposium*, Morgantown. Balkema, Rotterdam, pp. 31–38.
- Zhang, L., Einstein, H.H., 2004. Using RQD to estimate the deformation modulus of rock masses. *Int. J. Rock Mech. Min. Sci.* 41, 337–341.

Statement of Authorship of Journal paper 5

Three-Dimensional Numerical Analysis for Rock Slope Stability Using Non-linear Shear Strength Reduction Method

Jiayi Shen & Murat Karakus*

School of Civil, Environmental and Mining Engineering, The University of Adelaide

Adelaide, South Australia, 5005, Australia

Canadian Geotechnical Journal

Submitted 22th May 2013

(Under review)

By signing the Statement of Authorship, each author certifies that their stated contribution to the publication is accurate and that permission is granted for the publication to be included in the candidate's thesis.

Jiayi Shen

Performed the analysis, wrote the manuscript.

Signature:

Date: 27th May 2013

Dr. Murat Karakus

Supervised development of work, manuscript evaluation and acted as corresponding author.

Signature:

Date: 27th May 2013

Chapter 5

Three-Dimensional Numerical Analysis for Rock Slope Stability Using Non-linear Shear Strength Reduction

Method

Abstract

Existing numerical modeling of three-dimensional (3D) slopes is mainly performed by the shear strength reduction (SSR) technique based on the linear Mohr-Coulomb (MC) criterion, whereas the non-linear failure criterion for rock slope stability is seldom used in slope modeling. However, it is known that rock mass strength is a non-linear stress function and that, therefore, the linear MC criterion does not agree with the rock mass failure envelope very well. In this current research, therefore, a non-linear SSR technique is proposed that can use the Hoek-Brown (HB) criterion to represent the non-linear behavior of a rock mass in FLAC^{3D} program to analyze 3D slope stability. Extensive case studies are carried out to investigate the influence of convergence criterion and boundary conditions on 3D slope modeling. Results show that the convergence criterion used in the 3D model plays an important role, not only in terms of the calculation of the factor of safety (FOS), but also in terms of the shape of the failure surface. The case studies also demonstrate that the value of the FOS for a given slope will be significantly influenced by the boundary condition when the slope angle is less than 50°.

1 Introduction

Rock slope stability is one of the major challenges of rock engineering projects, such as open pit mining. Rock slope failure can affect mining operations and result in costly losses in terms of time and productivity. Therefore, the evaluation of the stability of rock slopes is a critical component of open pit design and operation (Naghadehi et al. 2013).

In most of the geotechnical applications two-dimensional (2D) plain strain analysis are commonly used to simulate stability of earth structures (Basarir et al. 2005; Karakus et al. 2007; Kurakus 2007; Eid 2010; Tutluoglu et al. 2011). The majority of rock slope analyses in practical projects are still performed using 2D limit equilibrium or plane strain analysis because 2D analysis is relative simple and yields a conservative factor of safety (FOS) compared with three-dimensional (3D) analysis (Griffiths and Marquez 2007). However, it is known that 3D analysis provides the more realistic model because it can take into account the appropriate geometry and boundary conditions. Therefore, the development of 3D slope analysis has become a popular research topic in geotechnical engineering in recent years. A list of 3D slope stability papers published in the last seven years is shown in Table 1.

Table 1 3D slope stability analysis using different methods

Authors	Methods
Cheng and Yip (2007)	LEM
Griffiths and Marquez (2007)	SSR
Frazaneh et al. (2008)	LAM
Li et al. (2009)	LAM
Michalowski and Drescher (2009)	LAM
Wei et al. 2009	SSR/LEM
Li et al. (2010)	LAM
Michalowski (2010)	LAM
Detournay (2011)	SSR
Stianson et al. (2011)	SSR
Gharti et al. (2012)	SSR
Zheng (2012)	LEM
Nian et al. (2012)	SSR
Michalowski and Nadukuru (2013)	LAM
Nadukuru and Michalowski (2013)	LAM
Zhang et al. (2013)	SSR

Commonly used approaches for 3D slope stability analysis include: the limit equilibrium method (LEM), limit analysis method (LAM), and numerical modeling performed by shear strength reduction technique (SSR), such as the finite element method (FEM) and finite difference method (FDM). The 3D LEM model involves various assumptions about the internal

force distribution, and it is difficult to locate the critical failure surface, as is well documented in the literature (Griffiths and Marquez 2007; Wei et al. 2009; Zhang et al. 2013). The 3D LAM model has been used for slope with simple geometry. However, the construction of the 3D failure mechanism for LAM is not straightforward for complicated slope models, which leads to this method being seldom used for complex conditions (Wei et al. 2009).

Currently, 3D numerical modeling performed by the SSR technique is a very attractive and commonly accepted approach among geotechnical researchers and engineers because it not only can automatically locate the critical failure surface, but can also simulate the stress-strain behavior and give the progressive shear failure of the slope in complex geometry and loading conditions.

Although the SSR technique has the above merits, however, we still must take into account its limitations in order to use it for the analysis of 3D isotropic rock slopes, as follows: (1) the existing 3D SSR technique is mainly based on the linear Mohr-Coulomb (MC) criterion. It is known that rock strength is non-linear, and many researches (Priest 2005; Li et al. 2008; Jimenez 2008; Shen et al. 2012a) showed that the MC criterion generally can not represent rock mass behavior very well, especially for slope stability problems where the rock mass is in a state of low confining stresses that make the non-linearity more obvious; (2) the selection of appropriate convergence criterion is not easy for a 3D SSR model because the value of the FOS for a given slope can be considerably influenced by the convergence criterion; (3) boundary conditions play an important role in the distribution of internal stresses in the slope model and can affect the simulation results.

With the aim of better understanding the fundamental rock slope failure mechanisms and improving the accuracy of the rock slope stability results of 3D numerical models, in the current

research a new non-linear SSR technique is proposed to be used with the Hoek-Brown (HB) criterion, which can ideally represent the non-linear behavior of a rock mass, in FLAC^{3D} program in order to analyze 3D slope stability. Extensive case studies are carried out to investigate the influence of the convergence criterion and boundary conditions on the numerical results, which include rock mass shear strength, the shape of the failure surface, as well as the FOS values.

2 Instantaneous shear strength of the HB criterion

The non-linear HB criterion, initially proposed by Hoek and Brown (1980), has been widely used for predicting intact rock and rock mass strength in rock engineering for several decades. The latest version of the HB criterion presented by Hoek et al. (2002), is expressed as:

$$\sigma_1 = \sigma_3 + \sigma_{ci} \left(m_b \frac{\sigma_3}{\sigma_{ci}} + s \right)^a \quad (1)$$

where σ_1 and σ_3 are the maximum and minimum principal stresses, σ_{ci} is the uniaxial compressive strength (UCS) of the intact rock, m_b , s and a are the Hoek-Brown input parameters which can be estimated from the Geological Strength Index (GSI), disturbance factor D and intact rock constant m_i .

$$m_b = m_i e^{\left(\frac{GSI-100}{28-14D} \right)} \quad (2)$$

$$s = e^{\left(\frac{GSI-100}{9-3D} \right)} \quad (3)$$

$$a = 0.5 + \frac{e^{\left(\frac{-GSI}{15} \right)} - e^{\left(\frac{-20}{3} \right)}}{6} \quad (4)$$

In order to use the HB criterion in conjunction with SSR methods for calculating the FOS of rock slopes, methods are required to determine the instantaneous MC shear strength parameters of cohesion c and angle of friction ϕ from the HB criterion (Fu and Liao 2010). The HB criterion

(see Eq. 1) is expressed by the relationship between maximum and minimum principal stresses. However, it can also be expressed in terms of normal stress σ_n and shear stress τ on the failure plane as shown in Fig. 1. The instantaneous cohesion c and angle of friction ϕ can be calculated by locating the tangent of the HB envelope under a given value of normal stress σ_n , as illustrated in Fig. 1. The intercept with the τ axis gives the c value, and the slope of the tangent to the HB failure envelope yields the ϕ value.

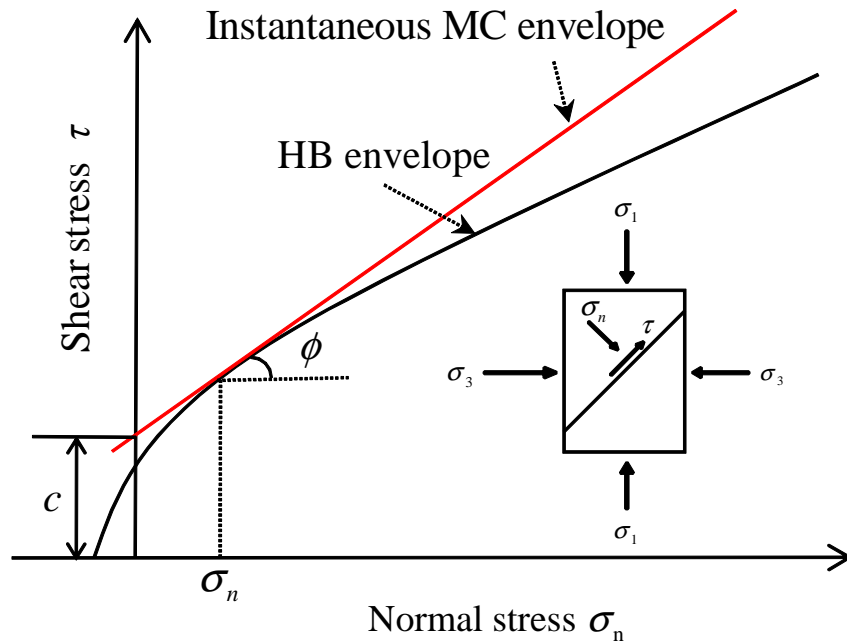


Fig. 1 Instantaneous MC envelope of the HB criterion in the normal and shear stress plane

Fig. 1 also illustrates the stress state of an element where the strength can be defined by the MC criterion. If the stress state (σ_1, σ_3) of an element is known, the corresponding instantaneous c and ϕ values can be calculated using Eqs. 5 to 8 proposed by Shen et al. (2012b).

$$\frac{\sigma_n}{\sigma_{ci}} = \frac{\sigma_3}{\sigma_{ci}} + \frac{\left(\frac{m_b \sigma_3}{\sigma_{ci}} + s\right)^a}{2 + am_b \left(\frac{m_b \sigma_3}{\sigma_{ci}} + s\right)^{a-1}} \quad (5)$$

$$\phi = \arcsin \left(1 - \frac{2}{2 + am_b \left(m_b \frac{\sigma_3}{\sigma_{ci}} + s \right)^{a-1}} \right) \quad (6)$$

$$\tau = \frac{\sigma_{ci} \cos \phi}{2 \left(1 + \frac{\sin \phi}{a} \right)^a} \left(m_b \frac{\sigma_n}{\sigma_{ci}} + s \right)^a \quad (7)$$

$$c = \tau - \sigma_n \tan \phi \quad (8)$$

The numerical slope model can be divided into numbers of elements using mesh techniques. When the slope is modeled under the loading condition, the stress states of the elements in the model will vary, which leads to the elements having different values of c and ϕ .

An example can be used to show the relationship between instantaneous c , ϕ and minimum principal stress σ_3 , as shown in Fig. 2. The following parameters were used for the calculation: $\sigma_{ci}=25$ MPa, $GSI=80$, $m_i=15$, $D=0.5$; the values of σ_3 range from 0 to 25 MPa. Fig. 2 illustrates that the values of instantaneous c increase and ϕ decrease with the increase of σ_3 values, which reflects the non-linear behavior of the HB criterion.

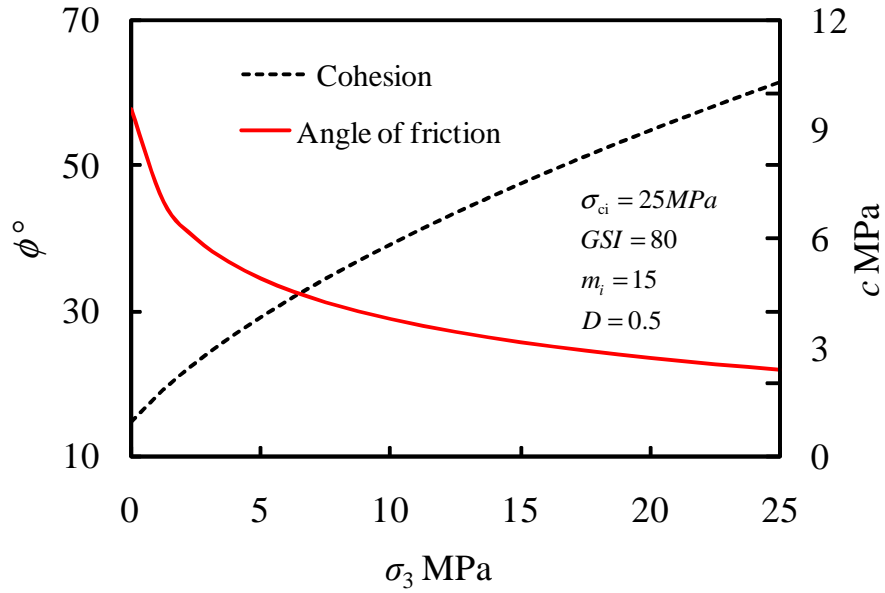


Fig. 2 The correlations between MC parameters and σ_3

3 Non-linear SSR method for the HB criterion

The calculation of the FOS using the SSR technique is based on reducing the MC shear strength parameters c and ϕ until the slope collapse, and then the value of the FOS can be defined as the ratio of the actual shear strength to the minimum shear strength of the rock or soil materials that is required to prevent failure (Duncan 1996). The reduced shear strength parameters c_f and ϕ_f are given by:

$$c_f = \frac{c}{RF} \quad (9)$$

$$\phi_f = \arctan \frac{\tan \phi}{RF} \quad (10)$$

where RF is a reduction factor, and the value of RF is equal to the FOS when slope failure occurs.

One of the most promising ways to use the HB criterion in conjunction with SSR techniques is to estimate the instantaneous MC shear strength parameters c and ϕ for elements in the slope. The details of the application of this non-linear SSR technique for 2D FEM slope analysis can be

found the paper by Fu and Liao (2010). Kumar's (1998) solution was used by Fu and Liao (2010) to calculate the instantaneous ϕ values, which requires Newton's iteration formula to calculate the ϕ values. It should be noted that Eqs. 5-8 are an alternative form of Kumar's (1998) solution. However, the equations offer the benefit of being able to calculate the instantaneous c and ϕ of an element from its' stress state (σ_1, σ_3) without the need of iteration analysis.

In the current research, the non-linear SSR strategy, together with Eqs. 5-8, was used to implement the HB criterion in FLAC^{3D} for 3D rock slope stability analysis. Fig. 3 is a flow chart showing the steps of implementing the HB criterion in the FLAC^{3D} slope model, as follows: Step 1: Build the slope model according to slope geometry, rock mass properties, loading and boundary conditions. Mesh techniques are used to generate the grid elements for a slope. Step 2: Carry out the elastic stress analysis to determine the stress state of each element in the slope model. Step 3: Use Eqs. 5 to 8 to calculate the cohesion c as well as the angle of friction ϕ for each element. Step 4: Reduce the c and ϕ values of all elements by a reduction factor RF. Step 5: Use the reduced c_f and ϕ_f for the elasto-plastic analysis using the MC constitutive model. Step 6: Repeat steps 2 to 5 when a new reduction factor RF is generated until slope failure. Finally, the value of the FOS of a given slope is equal to the reduction factor RF.

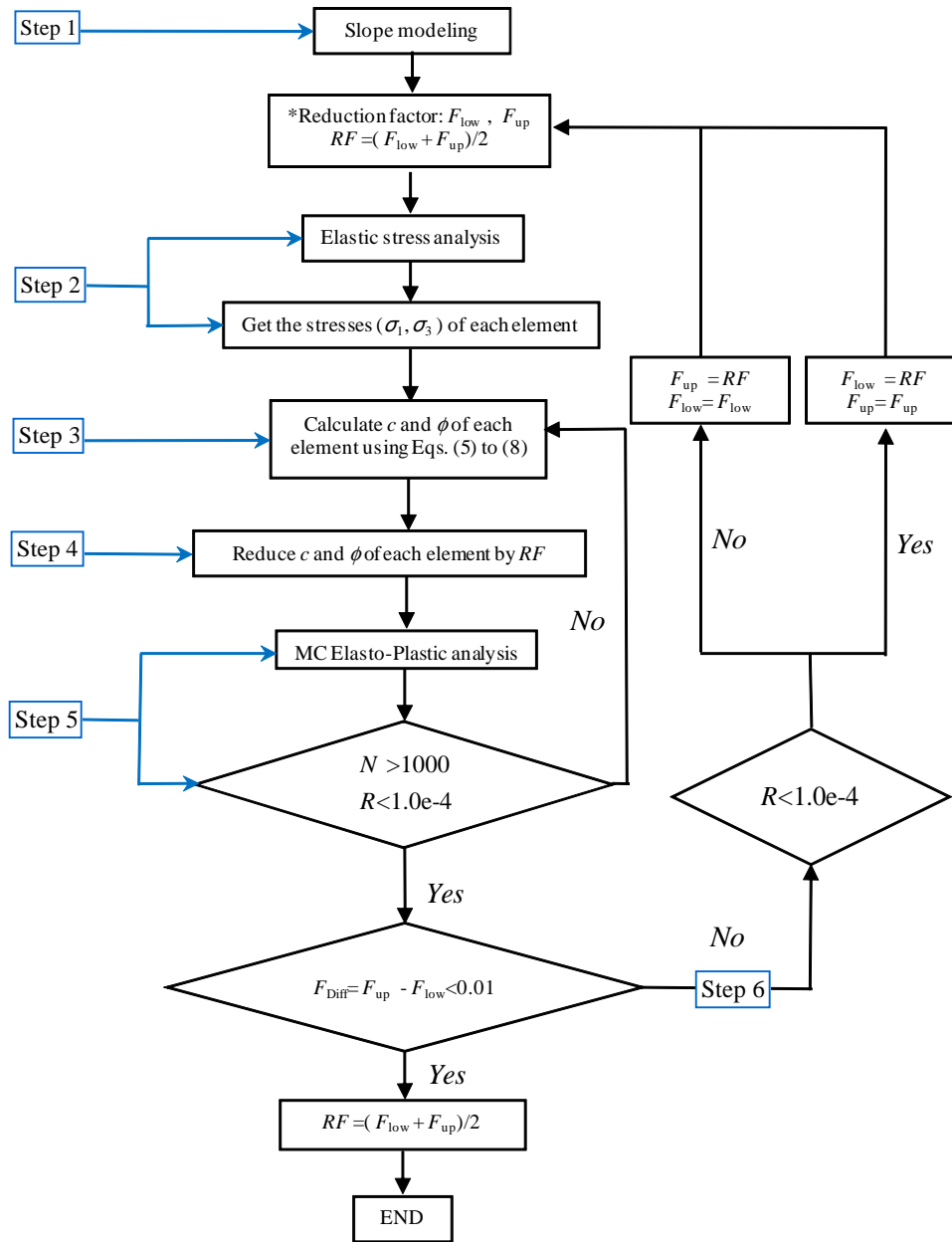


Fig. 3 Flow chart of the application of HB criterion into $FLAC^{3D}$ using non-linear SSR technique

* The values of RF can be adjusted using the bracketing approach proposed by Dawson et al. (1999). F_{low} and F_{up} are the lower and upper bracket values of FOS. F_{Diff} is the difference between upper and lower FOS values.

4 Convergence criterion in the 3D models

Research by Wei et al. (2009) demonstrated that the value of the factor of safety of the 3D SSR model can be significantly influenced by the selection of the convergence criterion. Therefore, it is necessary to carry out some trial and error analysis to select an appropriate convergence criterion for a slope model.

The convergence criterion in FLAC^{3D} is the nodal unbalanced force ratio R , and the user must specify a number of calculation steps N to bring the model to a state of equilibrium. An example of data from the paper by Hammah et al. (2005) can be used to check the influence of the convergence criterion on the 3D slope model. The example has the following slope geometry and rock mass properties: slope height $H=10\text{m}$, slope angle $\beta=45^\circ$, $\sigma_{ci}=30\text{MPa}$, $m_i=2$, $\text{GSI}=5$, $D=0$, unit weight $\gamma=25\text{ kN/m}^3$, Deformation modulus $E_m=5000\text{MPa}$ and Poisson's ratio $\nu=0.3$.

The model has 475 elements and the analyses were carried out using 1m unit width. The boundary conditions for the slope are: x -direction displacement at the front and back faces of the slope model are fixed; x , y and z direction displacement at the base face of the slope model are fixed; and y -direction displacement of the end faces of the slope model are fixed (see Fig. 4).

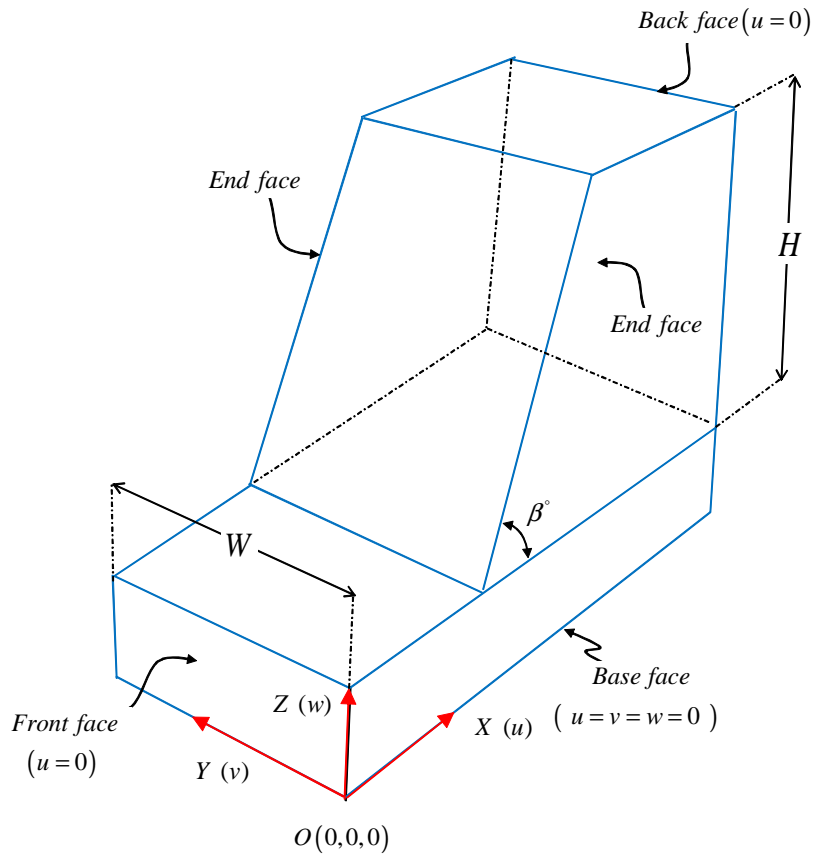
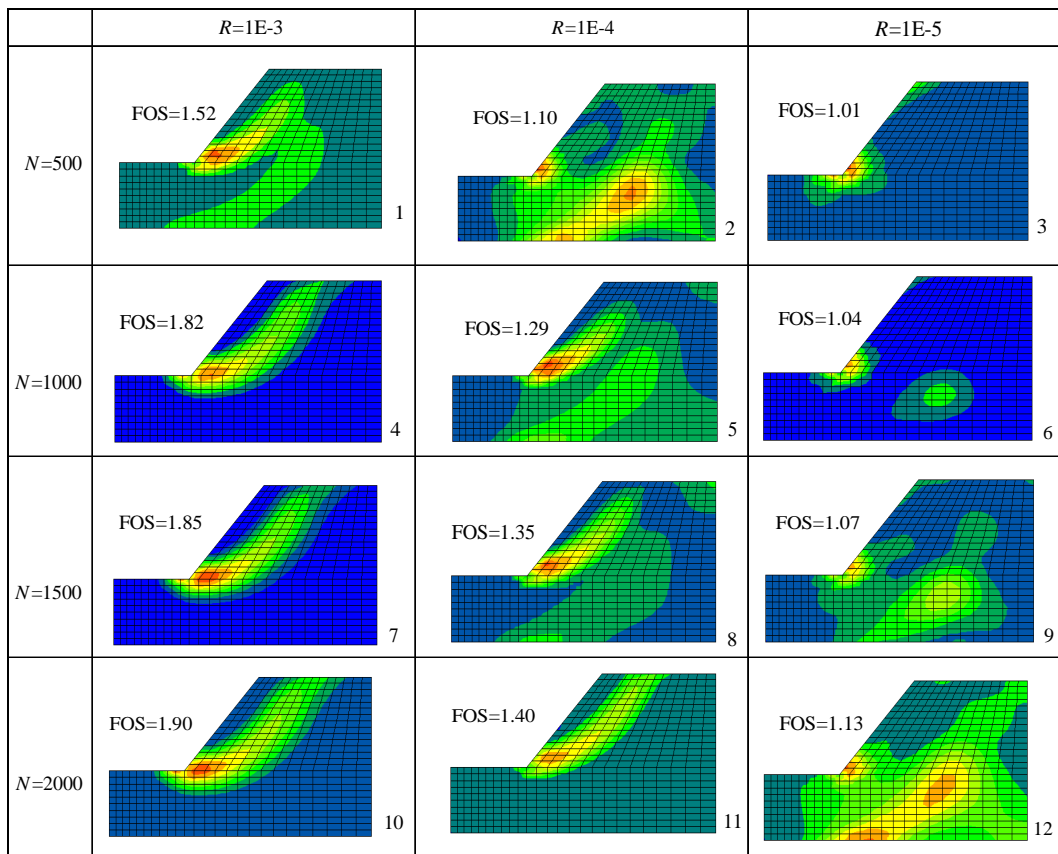


Fig. 4 Boundary conditions for a slope model

Table 2 compares the failure surfaces corresponding to the FOS values using various convergence criteria in the slope model. The results show that when the convergence criteria change, the values of the FOS vary from 1.01 to 1.90. The results indicate a clear trend for the FOS to increase with the increase of R . For example, when R values are increased from $1E-5$ to $1E-3$, $N=1000$, the values of the FOS increase from 1.04 to 1.82. Calculation step N only has a slight effect on the FOS when N is more than 1000. For example, when $R=1E-3$, the values of the FOS are equal to 1.82 for $N=1000$ and increase to 1.90 for $N=2000$.

Table 2 Comparison of failure surfaces corresponding to FOS values using different convergence criteria



We ran several case studies, finding similar results each time. As shown in Table 2, the slope model will produce the appropriate failure surface, and the FOS value tends to stabilize when the convergence criterion is $R=1E-4$ and the value of N is more than 1000.

The choice of the mesh techniques can also influence the FOS results in the SSR analysis. A comprehensive study of the influence of different mesh techniques and mesh elements on the calculation of the FOS using FLAC^{3D} models has been conducted by Zhang et al. (2013). Fig. 5 compares the different mesh sizes for the calculation of the FOS. The results show that when the

mesh size is more than 1400, the value of the FOS tends to equal 1.16, which is close to Hammah et al.'s (2005) result of a FOS of 1.15.

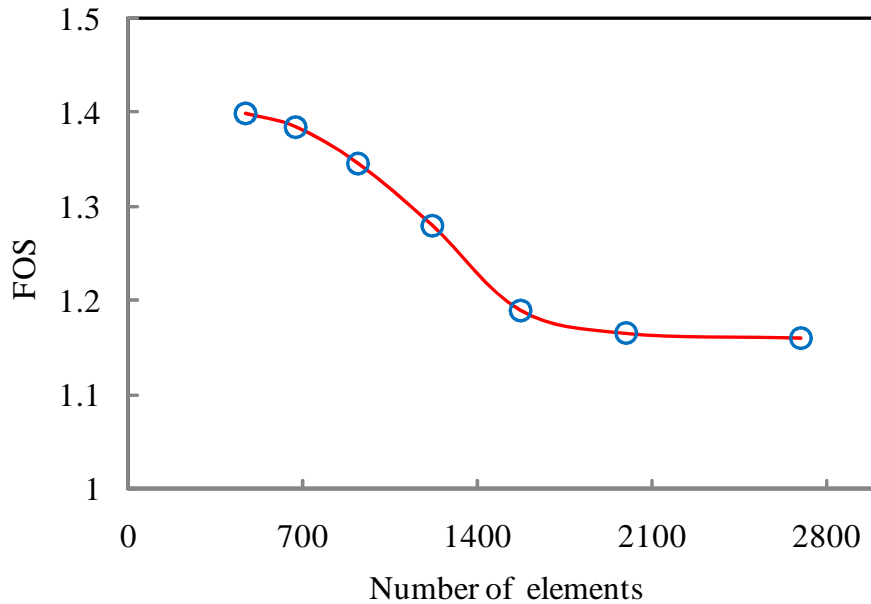


Fig. 5 Plot of FOS values versus mesh elements

5 Boundary conditions in 3D models

The choice of appropriate boundary conditions is important for 3D slope stability analysis as boundary conditions play an important role in the development of internal stresses in a slope, which will change the shape of failure surface corresponding to the value of the FOS.

The commonly used boundary conditions for a 3D slope model (see Fig. 4) are: fixing the x -direction displacement ($u=0$) at the front and back faces of slope model; fixing the x , y and z direction displacement ($v=u=w=0$) at the base of slope model. For the end faces, there are three types of boundary conditions as suggested by Chugh (2003). Condition 1: fixing the y -direction displacement ($v=0$), which represents contact with a rigid, smooth abutment that can provide a reacting thrust but no in-plane shear restraint; Condition 2: fixing the x , y direction displacement

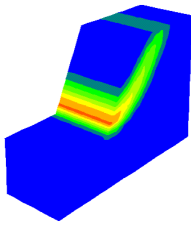
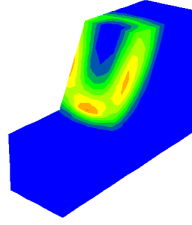
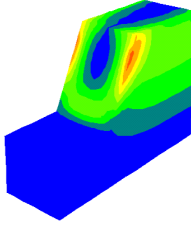
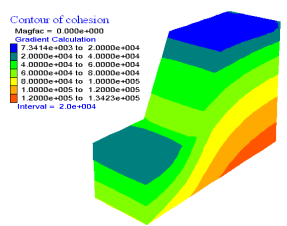
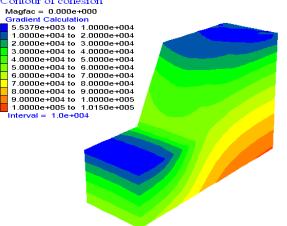
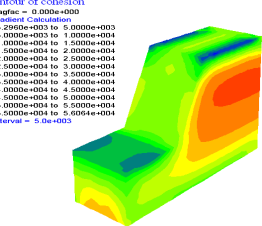
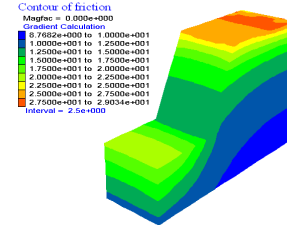
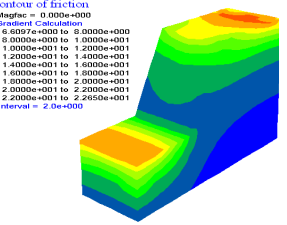
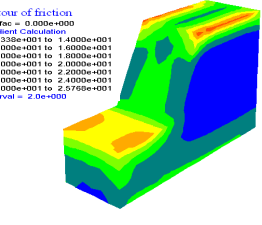
($u=v=0$), which represents a contact that provides side shear resistance; Condition 3: fixing the x , y , z direction displacement ($u=v=w=0$), which is used to characterize contacts with no movement.

An example (see Table 3) was used to analyze the influence of boundary conditions on slope stability. Table 4 compares the slope failure surfaces corresponding to the FOS values, as well as the contours of instantaneous cohesion and angle of friction in a given slope under different boundary conditions.

Table 3 Input parameters of a slope case

Input parameters	Values
H , m	20
β , °	60
γ , kN/m ³	27
σ_{ci} , MPa	5
GSI	40
m_i	12
D	0.7

Table 4 Comparison of failure surfaces, contours of c and ϕ and FOS of a slope model under various boundary conditions

Boundary condition used at the end faces of the 3D models			
	Condition 1 (Fix y)	Condition 2 (Fix x, y)	Condition 3 (Fix x, y, z)
Failure surface			
Contour of Cohesion			
Contour of angle of friction			
FOS	1.883	2.502	2.057
f_B		$f_{B,x,y}=1.329$	$f_{B,x,y,z}=1.092$

The contours of the instantaneous c and ϕ shown in Table 4 are calculated using Eqs. 5 to 8 together with the final stress states of each element when the slope failures, which can be used to illustrate the failure mechanics performed by the non-linear SSR technique. For boundary conditions 1 and 2, where the z -direction displacement of the end faces is not fixed, the slope surfaces have relatively higher ϕ values and lower c values compared with the values at the bottom of the slope. This disparity is a result of the fact that the stress state of the elements at the bottom of the slope is greater than the stress state of the elements near the slope surface; and the

values of instantaneous c increase and ϕ decrease with the increase of σ_3 values as shown in Fig.

2.

For boundary condition 3, where x,y, z -direction displacement of the end faces is fully fixed, the contours of c and ϕ are obviously different from those of conditions 1 and 2. This can be explained by the fact that the stress state in the slope under boundary condition 3 is different from the stress state in the slope under boundary conditions 1 and 2. Therefore, the values of instantaneous c and ϕ will change, which leads to the change of the shape of the failure surface, as well as the FOS values.

The value of the FOS for boundary condition 1 is equal to 1.883, which is lower than the FOS for boundary conditions 2 and 3, where the FOS is equal to 2.502 and 2.057, respectively. In order to investigate the possible correlation of the FOS under different boundary conditions, we proposed a boundary weighting factor, f_B , as shown in Table 4, which represents the ratio of the FOS from boundary conditions 2 and 3 to boundary condition 1. In this case, $f_{B,xy}=2.502/1.883=1.329$ and $f_{B,xyz}=2.057/1.883=1.092$.

Table 5 compares the FOS values under different boundary conditions for the slope (see Table 3), with the slope angle β varying from 30° to 90° . The correlations between f_B and β in Table 5 are plotted in Fig. 6. The figure demonstrates that the boundary weighting factor f_B decreases as the slope angle increases when $\beta < 50^\circ$. However, f_B tends to reach stable values ($f_{B,xy}=1.4$ and $f_{B,xyz}=1.1$) when $\beta > 50^\circ$.

Table 5 The results of FOS and f_B of the slope with different slope angle

Slope angle β°	Boundary condition used at end faces of slope model			Boundary weighting factor, f_B	
	FOS_y	FOS_{xy}	FOS_{xyz}	$f_{B,xy}$	$f_{B,xyz}$
30	2.11	3.75	3.42	1.78	1.62
45	2.06	2.97	2.52	1.44	1.22
60	1.88	2.50	2.06	1.33	1.09
75	1.57	2.11	1.73	1.34	1.10
90	1.29	1.69	1.43	1.31	1.11

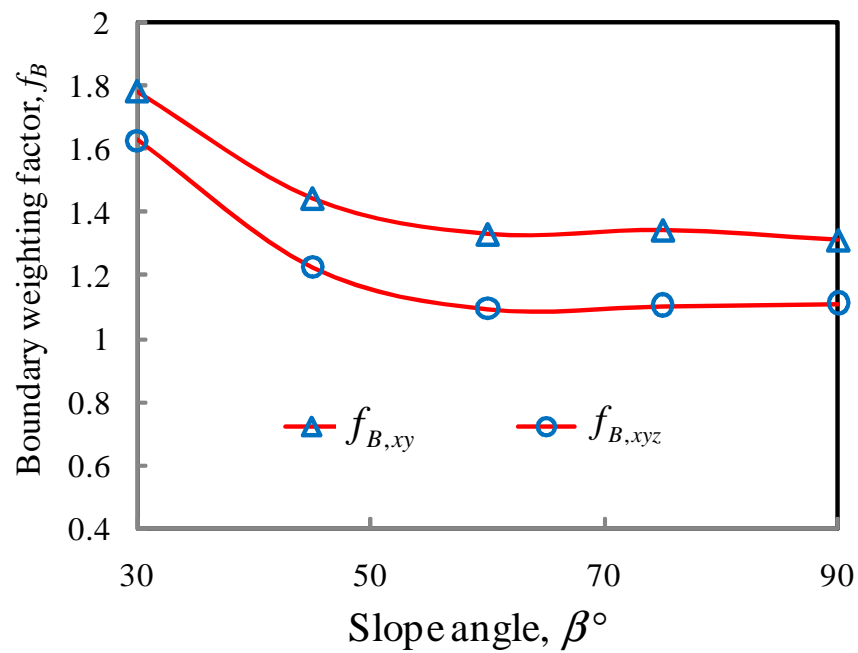


Fig. 6 The correlations between f_B and β under different boundary conditions for a slope case

Results presented in Fig. 6 and Table 5, however, provide only one example for a specific rock property and slope height. To further check the correlation between f_B and β , we conducted a comprehensive study using 21 real cases collected from Douglas (2002) and Taheri and Tani (2010), with various slope geometries and rock mass properties as indicated in Table 6.

Our analysis of the database showed that there is a strong correlation between f_B and β as shown in Fig. 7. Most of the data lie along the lines which have a trend of decreasing f_B with the increase of β when $\beta < 50^\circ$. When $\beta > 50^\circ$, f_B tends to achieve constant values. The results that were presented demonstrate that the effects of boundary conditions on the values of the FOS are more obvious for a slope with a low angle than a steep slope. The values of $f_{B,xy}$ and $f_{B,xyz}$ will go up to 1.7 and 1.5 when the slope angle is less than 35° . On the other hand, when the slope angle is more than 50° , the values of $f_{B,xy}$ and $f_{B,xyz}$ tend to equal 1.4 and 1.1, respectively.

Table 6 The results of FOS and f_B of real slope cases

Cases	H (m)	β (°)	γ (kN/m ³)	σ_{ci} (MPa)	GSI	m_i^a	D^b	FOS_y	FOS_{xy}	FOS_{xyz}	$f_{B,xy}$	$f_{B,xyz}$
1	184	55	27	153	47	9	0.9	2.67	3.67	3.04	1.38	1.14
2	140	34	26	50	28	8	0.7	1.52	2.52	2.27	1.66	1.49
3	220	45	27	65	44	17	0.8	2.48	3.54	2.97	1.43	1.20
4	135	65	27	172	58	9	0.9	4.16	5.70	4.92	1.37	1.18
5	70	50	27	29	41	7	0.8	1.83	2.59	2.19	1.42	1.20
6	110	45	26.5	50	25	10	0.7	1.60	2.28	1.96	1.43	1.23
7	270	45	27	109	39	18	0.9	2.21	3.18	2.68	1.44	1.21
8	170	55	30	104	48	7	0.7	2.63	3.63	3.01	1.38	1.15
9	60	60	27	65	44	13	1	2.53	3.44	2.80	1.36	1.11
10	35	67	27	109	28	12	1	1.93	2.61	2.14	1.35	1.11
11	63	35	27	109	28	12	1	2.04	3.15	2.78	1.55	1.37
12	70	49	27	3	49	24	1	1.20	1.72	1.46	1.44	1.22
13	58	50	27	5	55	22	1	1.80	2.53	2.12	1.41	1.18
14	60	48	27	5	54	22	1	1.75	2.48	2.11	1.42	1.20
15	60	52	27	5	56	22	1	1.83	2.50	2.09	1.37	1.14
16	40	71	27	50	33	14	1	1.70	2.29	1.87	1.35	1.10
17	110	50	27	50	25	14	1	1.05	1.48	1.26	1.40	1.20
18	41	50	27	3	46	24	1	1.34	1.90	1.62	1.42	1.21
19	41	55	27	3	49	24	1	1.42	1.96	1.64	1.38	1.16
20	46	55	27	3	50	24	1	1.40	1.93	1.62	1.38	1.16
21	57	49	27	3	48	24	1	1.26	1.81	1.55	1.44	1.23
22 ^c	57	37	27	3	48	24	1	1.36	2.13	1.88	1.56	1.38
23 ^c	57	40	27	3	48	24	1	1.33	2.03	1.79	1.52	1.34
24 ^c	57	42	27	3	48	24	1	1.32	1.97	1.72	1.49	1.30

^a The values of m_i are estimated based on the information of uniaxial compressive strength for general rock type (Shen and Karakus 2013)

^b By considering the excavation methods for cases 9 and 10 were poor and the cases 11- 21 were obtained from open pit mines (the excavation method was assumed to be production blasting), therefore, according to the guidelines by Hoek et al. (2002), D was assumed to be 1 for all cases.

^c Cases 22- 24 are additional cases which have the same rock mass properties as case 21 except slope angle.

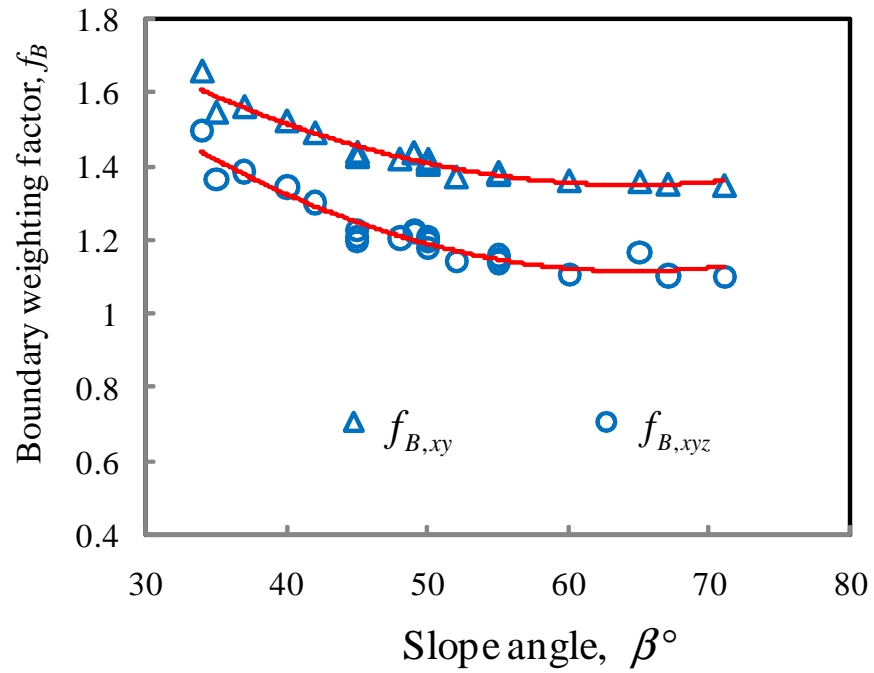


Fig. 7 The correlations between f_B and β under different boundary conditions for open pit cases

The possible connections between f_B and other parameters (H , σ_{ci} , GSI and m_i) were also investigated as shown in Fig. 8. No strong relationship was observed between f_B and these parameters.

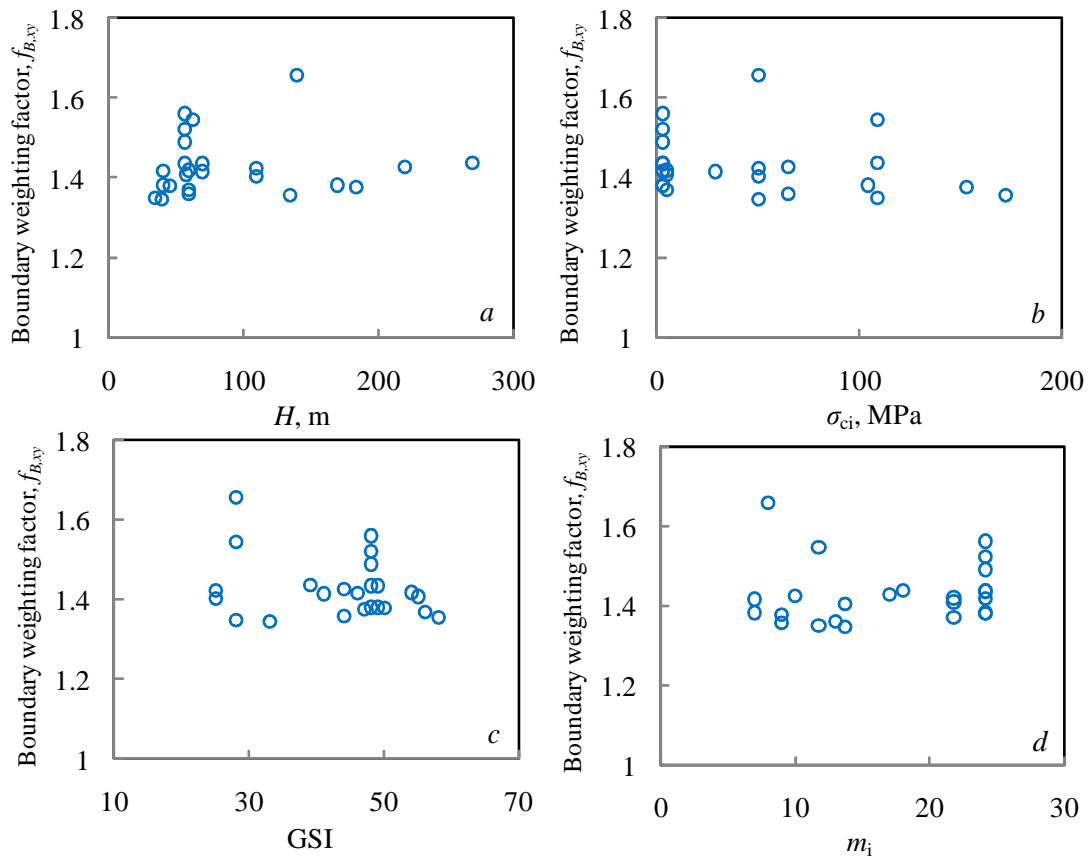


Fig. 8 The correlations between $f_{B,xy}$ and H , σ_{ci} , GSI, m_i

6 Conclusions

A new non-linear SSR method has been proposed to analyse the stability of 3D rock slopes satisfying the HB failure criterion. This method is based on estimating the instantaneous MC shear strength parameter c and ϕ values from the HB criterion for elements in a FLAC^{3D} model.

The reliability of the proposed 3D slope model has been tested using an example from Hammah et al. (2005). The value of the FOS calculated by the proposed slope model (fine mesh) is equal to 1.16, which is close to Hammah et al.'s results with FOS=1.15. However, it was found that the convergence criterion used in the model plays an important role not only in the calculation of the FOS, but also in locating the failure surface as shown in Table 2.

Then, the proposed 3D slope model has been used to analyse the influence of the boundary condition on the calculation of the FOS using 21 real open pit cases with various slope geometries and rock mass properties as indicated in Table 6. We have proposed a boundary weighting factor, f_B , to investigate the possible correlation of the FOS under different boundary conditions.

Our analysis demonstrates that there is a strong correlation between f_B and slope angle β as shown in Fig. 7. The value of f_B will decrease with the increase of the slope angle when β is less than 50° . However, f_B tends to reach stable values ($f_{B,xy}=1.4$ and $f_{B,xyz}=1.1$) when $\beta > 50^\circ$. Therefore, great care should be taken to select appropriate boundary conditions when the researchers perform 3D numerical analysis of slope with low slope angle.

Acknowledgement

Scholarship supports provided by China Scholarship Council (CSC) is gratefully acknowledged. Many thanks go to Mrs Barbara Brougham for editing the manuscript.

References

- Basarir, H., Ozsan, H., and Karakus, M. 2005. Analysis of support requirements for a shallow diversion tunnel at Guledar dam site, Turkey. *Engineering Geology*, 81(2):131-145.
- Cheng, Y.M., and Yip, C.J. 2007. Three-dimensional asymmetrical slope stability analysis extension of bishop's, janbu's, and Morgenstern-price's techniques. *Journal of Geotechnical and Geoenvironmental Engineering*, 133(12):1544-1555.
- Chugh, A.K. 2003. On the boundary conditions in slope stability analysis. *International Journal for Numerical and Analytical Methods in Geomechanics*, 27:905-926.
- Dawson, E.M., Roth, W.H., and Drescher, A. 1999. Slope stability analysis by strength reduction. *Géotechnique*, 49(6):835-840.
- Detournay, C., Hart, R., and Varona, P. 2011 Factor of safety measure for Hoek-Brown material. *Continuum and Distinct Element Numerical Modeling in Geomechanics -2011-Sainsbury*, Hart, Detournay & Nelson (eds.) Paper: 13-07.
- Duncan, J. 1996. State of the Art: Limit equilibrium and finite-element analysis of slopes. *Journal of Geotechnical and Geoenvironmental Engineering*, 122(7):577-596.
- Douglas, K.J. 2002. The shear strength of rock masses. Ph.D. Thesis, University of New South Wales, Australia.
- Eid, H.T. 2010 Two-and three-dimensional analyses of translational slides in soils with nonlinear failure envelopes. *Canadian Geotechnical Journal*, 47(4):388-399.
- Farzaneh, O., Askari, F., and Ganjian, N. 2008. Three-dimensional stability analysis of convex slopes in plan view. *Journal of Geotechnical and Geoenvironmental Engineering*, 134(8): 1192-1200.
- FLAC^{3D} - Fast Lagrangian Analysis of Continua, Ver. 4.0 User's Manual. Minneapolis: Itasca.
- Fu, W., and Liao, Y. 2010. Non-linear shear strength reduction technique in slope stability calculation. *Computers and Geotechnics*, 37:288-298.

- Gharti, H.N., Komatitsch, D., Oye, V., Martin, R., and Tromp, J. 2012. Application of an elastoplastic spectral-element method to 3D slope stability analysis. *International Journal for Numerical Methods in Engineering*, 91(1):1-26.
- Griffiths, D.V., and Marquez, R.M. 2007. Three-dimensional slope stability analysis by elastoplastic finite elements. *Géotechnique*, 57(6):537-546.
- Hoek, E., and Brown, E.T. 1980. *Underground excavations in rock*. Instn Min Metall, London.
- Hoek, E., Carranza-Torres, C., and Corkum, B. 2002. Hoek-Brown failure criterion - 2002 Edition. In R. Hammah, W. Bawden, J. Curran, and M. Telesnicki (Eds.), *Proceedings of NARMS-TAC 2002, Mining Innovation and Technology*. Toronto available from www.rocscience.com. [assessed 20 September 2011]
- Hammah, R.E., Yacoub, T.E., Corkum, B.C., and Curran, J.H. 2005. The shear strength reduction method for the generalized Hoek-Brown criterion. *ARMA/USRMS 05-810*.
- Jimenez, R., Serrano, A., and Olalla, C. 2008. Linearization of the Hoek and Brown rock failure criterion for tunnelling in elasto-plastic rock masses. *International Journal of Rock Mechanics and Mining sciences*, 45:1153-1163.
- Karakus, M. 2007. Appraising the methods accounting for 3D tunnelling effects in 2D plane strain FE analysis. *Tunnelling and Underground Space Technology*, 22(1):47-56.
- Karakus, M., Ozsan, A., and Basarir, H. 2007. Finite element analysis for the twin metro tunnel constructed in Ankara Clay, Turkey. *Bulletin of Engineering Geology and the Environment*, 66 (1):71-79.
- Kumar, P. 1998. Shear failure envelope of Hoek-Brown criterion for rockmass. *Tunnelling and Underground Space Technology*, 13(4):453-458.
- Li, A.J., Merifield, R.S., and Lyamin, A.V. 2008. Stability charts for rock slopes based on the Hoek-Brown failure criterion. *International Journal of Rock Mechanics and Mining sciences*, 45(5):689-700.
- Li, A.J., Merifield, R.S., and Lyamin, A.V. 2009. Limit analysis solutions for three dimensional undrained slopes. *Computers and Geotechnics*, 36(8):1330-1351.

- Li, A.J., Merifield, R.S., and Lyamin, A.V. 2010. Three-dimensional stability charts for slopes based on limit analysis methods. *Canadian Geotechnical Journal*, 47(12):1316-1334.
- Michalowski, R.L., and Drescher, A. 2009. Three-dimensional stability of slopes and excavations. *Géotechnique*, 59(10):839-850.
- Michalowski, R.L. 2010. Limit analysis and stability charts for 3D slope failures. *Journal of Geotechnical and Geoenvironmental Engineering*, 136(4):583-593.
- Michalowski, R.L., and Nadukuru, S.S. 2013. Three-dimensional limit analysis of slopes with pore pressure. *Journal of Geotechnical and Geoenvironmental Engineering*, (DOI: 10.1061/(ASCE)GT.1943-5606.0000867).
- Nadukuru, S.S., and Michalowski, R.L. 2013. Three-dimensional displacement analysis of slopes subjected to seismic loads. *Canadian Geotechnical Journal*, (DOI: 10.1139/cgj-2012-0223).
- Naghadehi, M., Jimenez, R., KhaloKakaie, R., and Jalali, S. 2013. A new open-pit mine slope instability index defined using the improved rock engineering systems approach. *International Journal of Rock Mechanics and Mining Sciences*, 61:1-14.
- Nian, T.K., Huang, R.Q., Wan, S.S., and Chen, G.Q. 2012. Three-dimensional strength-reduction finite element analysis of slopes: Geometric effects. *Canadian Geotechnical Journal*, 49(5):574-588.
- Priest, S. D. 2005. Determination of shear strength and three-dimensional yield strength for the Hoek-Brown criterion *Rock Mechanics and Rock Engineering*, 38(4):299-327.
- Stianson, J.R., Fredlund, D.G., and Chan, D. 2011. Three-dimensional slope stability based on stresses from a stress-deformation analysis. *Canadian Geotechnical Journal*, 48 (6):891-904.
- Shen, J., Karakus, M., and Xu, C. 2012a. Direct expressions for linearization of shear strength envelopes given by the Generalized Hoek-Brown criterion using genetic programming. *Computers and Geotechnics*, 44:139-146.
- Shen, J., Priest, S.D., and Karakus, M. 2012b. Determination of Mohr-Coulomb shear strength parameters from Generalized Hoek-Brown criterion for slope stability analysis. *Rock Mechanics and Rock Engineering*, 45:123-129.

- Shen, J., and Karakus, M. 2013. A simplified method for estimating the Hoek-Brown constant for intact rocks. *Journal of Geotechnical and Geoenvironmental Engineering*. (Under review)
- Taheri, A., and Tani, K. 2010. Assessment of the stability of rock slopes by the slope stability rating classification system. *Rock Mechanics and Rock Engineering*, 43:321-333.
- Tutluoglu, L., Ferid, I., and Karpuz, C. 2011. Two and three dimensional analysis of a slope failure in a lignite mine. *Computers and Geosciences*, 37 (2):232-240.
- Wei, W.B., Cheng, Y.M., and Li, L. 2009. Three-dimensional slope failure analysis by the strength reduction and limit equilibrium methods. *Computers and Geotechnics*, 36(1-2):70-80.
- Zhang, Y., Chen, G., Zheng, L., Li, Y., and Zhuang, X. 2013. Effects of geometries on three-dimensional slope stability. *Canadian Geotechnical Journal*, 10.1139/cgj-2012-0279
- Zheng, H. 2012. A three-dimensional rigorous method for stability analysis of landslides. *Engineering Geology*, 145-146:30-40.

Statement of Authorship of Journal paper 6

Chart-Based Slope Stability Assessment Using the Generalized Hoek-Brown Criterion

Jiayi Shen, Murat Karakus* & Chaoshui Xu

*School of Civil, Environmental and Mining Engineering, The University of Adelaide
Adelaide, South Australia, 5005, Australia*

International Journal of Rock Mechanics and Mining sciences

Submitted 13th October 2012; Submitted Revised form 4th April 2013

(Under review)

By signing the Statement of Authorship, each author certifies that their stated contribution to the publication is accurate and that permission is granted for the publication to be included in the candidate's thesis.

Jiayi Shen

Performed the analysis and wrote the manuscript.

Signature:

Date: 27th May 2013

Dr. Murat Karakus

Supervised development of work, manuscript evaluation and acted as corresponding author.

Signature:

Date: 27th May 2013

Associate Prof. Chaoshui Xu

Supervised development of work and manuscript evaluation.

Signature:

Date: 27th May 2013

Chapter 6

Chart-Based Slope Stability Assessment Using the Generalized Hoek-Brown Criterion

Abstract

Slope stability charts are used extensively in practical application to meet the need of quick assessment of rock slope design. However, rock slope stability charts based on the Generalized Hoek-Brown (GHB) criterion, which is one of the most widely adopted failure criteria to estimate rock mass strength in rock engineering, are considerably limited. This paper presents new stability charts for the analysis of rock mass slopes satisfying the GHB criterion. Firstly, charts for calculating the factor of safety (FOS) of a slope for a specified slope angle $\beta = 45^\circ$ are proposed. Secondly, a disturbance weighting factor f_D is introduced to illustrate the effect of disturbance factor D upon the stability of rock slopes. Thirdly, a slope angle weighting factor f_β is proposed to show the influence of slope angle β on slope stability. Combined with stability charts based on $\beta = 45^\circ$, the weighting factors f_D and f_β allow the calculation of the FOS of a slope assigned various slope angle under different blasting damage and stress relief conditions. The reliability of the proposed charts is tested against numerical solutions. The results show that FOS from the proposed charts exhibits only 3.1 % average discrepancy from numerical solutions using 1680 sets of data. The proposed charts are simple and straightforward to use and can be adopted as useful tools for the preliminary rock slope stability analysis.

1 Introduction

Determining the stability of rock mass slopes is an important task in many areas of civil and mining engineering, such as open pit excavation and large dam construction. Most slope stability analysis is based on seeking the factor of safety (FOS), which is a traditional measure of the safety margin of a given slope [1]. Having the merit of quick assessment of preliminary slope design, stability charts have been extensively used to estimate the stability of a slope in practical applications. The most common charts widely used in slope engineering is the Taylor's stability charts [2], which require the Mohr-Coulomb (MC) shear strength parameters cohesion c and angle of friction ϕ to estimate the FOS of a slope. However, rock mass strength is a non-linear stress function, therefore, the linear MC criterion generally do not agree with the rock mass failure envelope [3- 6], especially for slope stability problems where the rock mass is in a state of low confining stresses that make the nonlinearity more obvious.

Currently, the Hoek-Brown (HB) [7] criterion is one of the most broadly adopted failure criteria to estimate rock mass strength in rock engineering. Over the past 30 years the HB criterion has been applied successfully to a wide range of intact and fractured rock types. The latest version is the Generalized Hoek-Brown (GHB) criterion presented by Hoek et al. [8]. The equations are expressed as follows:

$$\sigma_1 = \sigma_3 + \sigma_{ci} \left(\frac{m_b \sigma_3}{\sigma_{ci}} + s \right)^a \quad (1)$$

m_b , s and a are the Hoek-Brown input parameters that depend on the degree of fracturing of the rock mass and can be estimated from the Geological Strength Index (GSI), given by:

$$m_b = m_i e^{\left(\frac{GSI-100}{28-14D} \right)} \quad (2)$$

$$s = e^{\left(\frac{GSI-100}{9-3D} \right)} \quad (3)$$

$$a = 0.5 + \frac{e^{\left(\frac{-GSI}{15}\right)} - e^{\left(\frac{-20}{3}\right)}}{6} \quad (4)$$

where, σ_1 is the maximum principal stresses, σ_3 is the minimum principal stresses, σ_{ci} is the uniaxial compressive strength of the intact rock, m_i is the Hoek-Brown constant of the intact rock, and D is the disturbance factor of the rock mass. The input parameters of the GHB criterion can be achieved directly from mineralogical assessment, uniaxial compressive testing of rock materials, and measurement of discontinuities characteristic of rock masses [9]. Therefore, a great advance in the field of rock slope stability assessment could be achieved if suitable stability charts could be developed to estimate the FOS directly from the GHB criterion.

Development of rock slope stability charts based on the GHB criterion, however, is a challenging task since there are at least six input parameters (GSI , m_i , σ_{ci} , γ , β , H) involved to calculate the FOS for a given dry slope with $D = 0$, where, γ is the unit weight of the rock mass, β is the slope angle, and H is the slope height. Based on our literature review, charts for the estimation of FOS directly from the GHB criterion is still a under research area and very few charts are available in the literature.

In the current research, we propose new charts which can be used to estimate the FOS of a slope directly from the Hoek-Brown parameters (GSI , m_i and D), slope geometry (β and H) and rock mass properties (σ_{ci} and γ). The proposed charts are straightforward to use and can be adopted as useful tools for the preliminary rock slope stability assessment.

In this paper, the existing rock slope stability charts related to the HB criterion are briefly reviewed in section 2. The proposed stability charts are presented in section 3. Charts application to slope cases is presented in section 4.

2 Review of existing rock slope stability charts based on the HB criterion

Since Taylor [2] proposed a set of stability charts for soil slopes, chart solutions have been presented by many researchers [1, 10-21] and are still widely used as design tools in slope engineering. At present, rock slope stability charts, such as Hoek and Bray's [11], often need to use the equivalent MC shear strength parameters cohesion c and angle of friction ϕ , which can be estimated from software *RocData* [22] as shown in Fig. 1. The equivalent fitting MC envelope is a straight line. The slope of the tangent to the MC envelope gives the value of ϕ , and the intercept with the shear stress axis gives the value of c . However, this conversion has been found to yield inconsistent estimates of the FOS of a slope, with a discrepancy between the HB and equivalent MC envelopes of up to 64% [13].

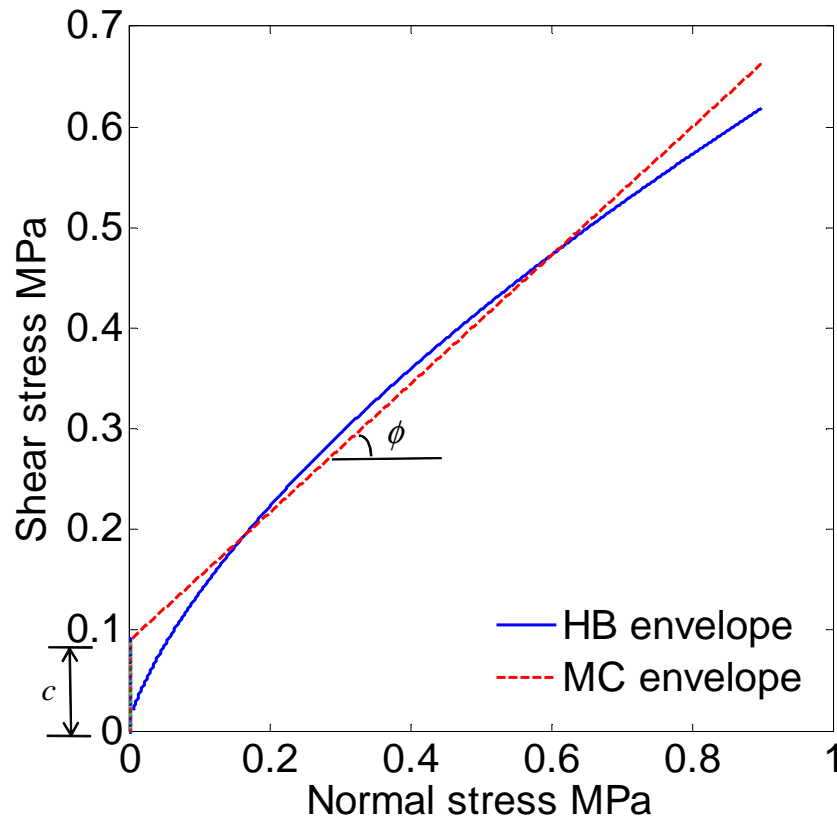


Fig. 1 Relationship between HB and equivalent MC envelopes

Until now, the slope stability charts by Carranza-Torres [12] and Li et al. [13-15] have been among the few charts that can be used to estimate the FOS directly from the HB criterion. Carranza-Torres [12] proposed a solution for estimating the shear strength of rock masses from the HB criterion, which was incorporated in the Bishop simplified method [23] for the analysis of rock slope stability. Carranza-Torres [12] revealed that when the Hoek-Brown parameter $a = 0.5$, the FOS of a given slope only depends on the three independent variables, $\overline{\gamma H}$, s/m_b^2 and β .

$$\overline{\gamma H} = \frac{\gamma H}{\sigma_{ci} m_b} + \frac{s}{m_b^2} \quad (5)$$

In order to estimate the FOS of a slope with a given geometry (β and H), rock mass properties (γ and σ_{ci}) and Hoek-Brown parameters (GSI, m_i and D), firstly, the values of m_b and s can be

calculated using Eqs. (2) and (3), respectively. Thereafter, the values of the dimensionless parameters $\overline{\gamma H}$ and s/m_b^2 can be calculated. Finally, the FOS can be directly estimated from the chart as shown in Fig. 2.

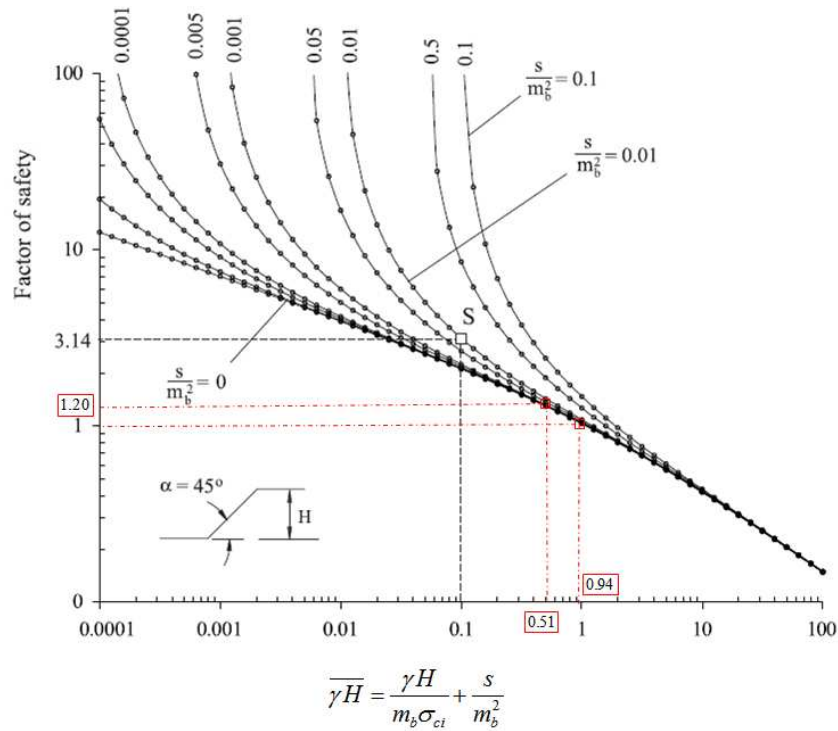


Fig. 2 Slope stability chart ($\beta=45^\circ$, $a=0.5$) [12]

While Carranza-Torres [12] proposed a chart is based on $a=0.5$ with only a single slope angle, $\beta = 45^\circ$, the current research proposed a slope angle weighting factor f_β to illustrate the influence of slope angle β on slope stability, to be discussed in section 3. Combined with the Fig. 2 based on $\beta = 45^\circ$, the slope angle weighting factor chart (as shown in Fig. 11) can be used for estimating the FOS of a slope assigned various angles.

Stability charts for estimating rock mass slopes directly from the Hoek-Brown parameters GSI, m_i and D were originally proposed by Li et al. [13] using limit analysis (LA). Li et al.'s [13] charts are based on the assumption $D = 0$, which means that the rock slope is undisturbed.

Similar stability charts utilizing $D = 0.7$ and $D = 1.0$ were also proposed by Li et al. [14] in order to examine the effects of these rates of disturbance on rock slope stability. Seismic stability charts were also proposed by Li et al. [15] to account for seismic effects on rock slope stability. The current research, however, focuses on static slope stability analysis, and seismic charts were not discussed in detail here.

Fig. 3 shows typical stability charts with a slope angle of $\beta = 45^\circ$. N is the non-dimensional stability number, defined as:

$$N = \frac{\sigma_{ci}}{\gamma H FOS_{LA}} \quad (6)$$

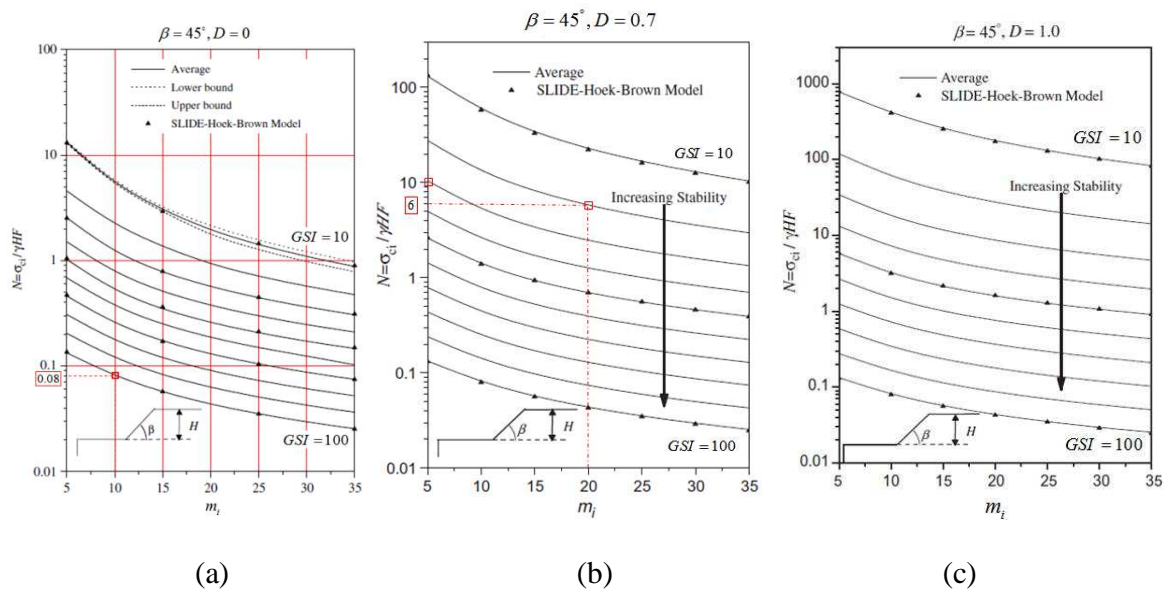


Fig. 3 (a) Slope stability chart with $D=0$ [13], (b) Slope stability chart with $D=0.7$ [14], (c) Slope stability chart with $D=1.0$ [14]

Because the upper and lower boundary results bracket a narrow range of N within $\pm 9\%$ or better, Li et al. [13, 14] adopted the average value limit solution to generate the charts in order to keep their calculations simple. The use of these charts is quite easy. Firstly, the stability number N can be calculated using the values of GSI and m_i from an appropriate chart according to a

specified D value ($D = 0, 0.7$ and 1) as shown in Fig. 3. Having obtained the value of N , Eq. 6 can be used to calculate the FOS_{LA} .

As noted by Li et al. [24], the definition of factor of safety for Eq. 6 is different from that of FOS obtained from the limit equilibrium method (LEM) which was defined as a function of resisting force f_R divided by driving force f_D , $FOS_{LEM} = f_R / f_D$. Therefore, the values of FOS_{LA} obtained from Eq. 6 are generally not equal to FOS_{LEM} . Such variations can be illustrated using four examples in Table 1.

Table 1 Comparison of the factor of safety estimated from different stability charts

Input parameters	Example 1[12]	Example 2[14]	Example 3	Example 4
σ_{ci} , MPa	0.75	10	13.5	5.4
GSI	100	30	30	20
m_i	10	8	5	20
D	0	1	0.7	0.7
γ , kN/m ³	25	23	27	27
H , m	27	50	50	25
β , °	45	60	45	45
Calculated parameters				
m_b	10	0.054	0.107	0.247
s	1	8.57E-06	3.93E-05	9.22E-06
a	0.5	0.522	0.522	0.544
s/m_b^2	0.0100	0.0030	0.0034	0.0002
$\bar{\gamma}H$	0.10	2.13	0.94	0.51
$\sigma_{ci}/(\bar{\gamma}H)$	1.11	8.70	10	8
N	0.08	50	10	6
Factor of safety				
Carranza-Torres				
Chart (LEM)	3.14	0.44*	1.00	1.20
Li et al. Chart (LA)	13.89	0.17	1.00	1.33

* FOS of example 2 is calculated from Fig. 2 together with Fig. 11.

Considering that the LEM is still the most widely used methods for slope stability analysis, we proposed an alternative stability chart based on the LEM. The proposed charts are able to estimate the FOS of a slope directly from the Hoek-Brown parameters (GSI , m_i and D), slope geometry (β and H) and rock mass properties (σ_{ci} and γ).

3 Proposed stability charts for rock mass slopes

The work outlined here required hundreds of runs on a microcomputer, analyzing the stability of various slopes having different geometries and rock mass properties. The slope models were analyzed using *Slide 6.0* [25]. Details of the slope model settings are shown in Table 2.

Table 2 Slope modeling setting in *Slide 6.0*

Modeling setting summary	
Analysis method	Bishop simplified
Number of slides	25
Search method	Auto grid search
Rock strength type	Generalized Hoek-Brown
Ground water	None
Failure surface type	Circular toe failure
Disturbance factor	0-1

The competency factor, the ratio of the uniaxial compressive strength σ_{ci} to the pressure of the overburden γH of tunnels, proposed by Muirwood [26] was used in current study. For rock slope application, γH can represent the vertical stress of the rock slope, in this paper, $\sigma_{ci} / (\gamma H)$ was termed the strength ratio (SR) of a rock slope. We interested the stability number N proposed by Li et al. [13], which contains SR as shown Eq. 6. The use of SR is a significant innovation for the

rock slope stability analysis because when the values of the input parameters GSI, m_i , D and β are determined, the FOS is related only to the SR of that slope.

In this section, the derivation of the theoretical relationship between the SR and FOS of a given slope slip surface will be explained in detail. In the next stage, based on the relationship between the SR and FOS, charts for calculating the FOS_{45°} when $\beta = 45^\circ$, $D=0$ are proposed. A disturbance weighting factor f_D is then introduced to illustrate the effect of disturbance D upon the stability of rock mass slopes. Finally, a slope angle weighting factor f_β is proposed to illustrate the influence of the slope angle β on slope stability. Combined with stability charts based on $\beta = 45^\circ$, the weighting factors f_β and f_D allow for the calculation of the FOS of slopes exhibiting various angle under different blast damage and stress relief conditions. Also, some slope examples are presented to illustrate the use of the proposed charts.

3.1 Theoretical relationship between SR and FOS

Combined with a generic form of Balmer's equations [12], the GHB criterion was input into *Slide 6.0* in order to calculate the instantaneous shear stress τ of each slice of a failure surface under a specified normal stress σ_n . The generic form of Balmer's equations are expressed as follows:

$$\frac{\sigma_n}{\sigma_{ci}} = \frac{\sigma_3}{\sigma_{ci}} + \frac{1}{2} \left(m_b \frac{\sigma_3}{\sigma_{ci}} + s \right)^a \left[1 - \frac{am_b \left(m_b \frac{\sigma_3}{\sigma_{ci}} + s \right)^{a-1}}{2 + am_b \left(m_b \frac{\sigma_3}{\sigma_{ci}} + s \right)^{a-1}} \right] \quad (7)$$

$$\frac{\tau}{\sigma_{ci}} = \left(m_b \frac{\sigma_3}{\sigma_{ci}} + s \right)^a \frac{\sqrt{1 + am_b \left(m_b \frac{\sigma_3}{\sigma_{ci}} + s \right)^{a-1}}}{2 + am_b \left(m_b \frac{\sigma_3}{\sigma_{ci}} + s \right)^{a-1}} \quad (8)$$

For a generic case $a \neq 0.5$, in order to calculate shear stress τ , for the given values of the input parameters m_b , s , a , σ_{ci} and σ_n , Eq. 7 is solved iteratively to calculate the σ_3 value [27]. Having obtained σ_3 , Eq. 8 can be used to calculate shear stress τ , therefore, σ_3/σ_{ci} can be expressed as follows:

$$\frac{\sigma_3}{\sigma_{ci}} = f_1 \left(\frac{\sigma_n}{\sigma_{ci}}, m_b, s, a \right) \quad (9)$$

Also, τ/σ_{ci} can be expressed as follows:

$$\frac{\tau}{\sigma_{ci}} = f_2 \left(\frac{\sigma_n}{\sigma_{ci}}, m_b, s, a \right) \quad (10)$$

The FOS can be defined as a function of resisting force f_R divided by driving force f_D as shown in Fig. 4a. The forces of f_R and f_D can also be expressed in terms of τ and σ_n acting on the base of an arbitrary slice i as shown in Fig. 4b. Resisting shear stress τ_R^i of the rock mass is governed by Eq. 10, and driving shear stress τ_D^i will depend on the weight of the slice γh^i as indicated in Fig. 4b.

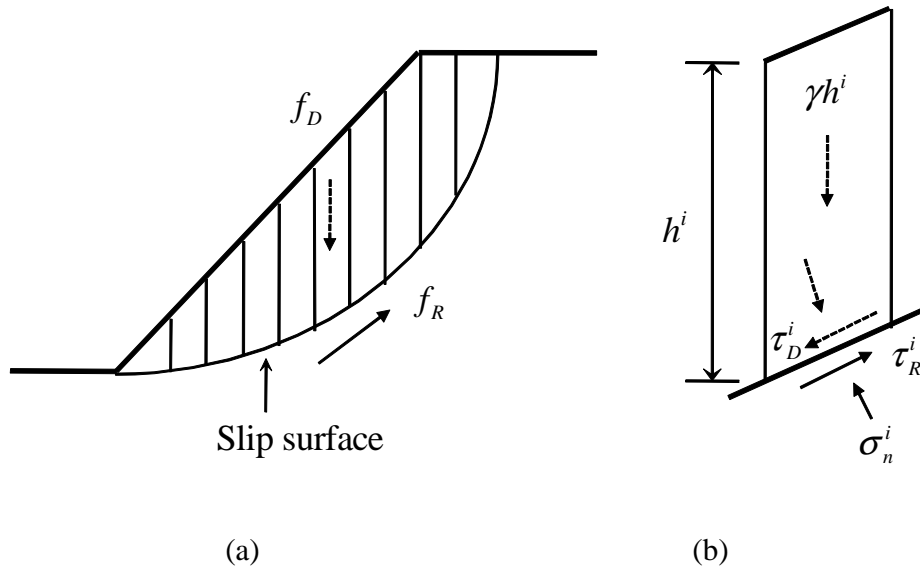


Fig. 4 (a) The basic of method of slices, (b) Stresses acting on a given slice

Therefore, with the help of Eq. 10, the FOS can be expressed as follows:

$$FOS = f_3 \left(\frac{\tau}{\gamma h} \right) = f_3 \left[\frac{\sigma_{ci}}{\gamma h} f_2 \left(\frac{\sigma_n}{\sigma_{ci}}, m_b, s, a \right) \right] \quad (11)$$

The value of σ_n of arbitrary slice depends on the weight of slice γh , which in turn depends on the characteristic stress γH and slope angle β [12]. Eq. 11, therefore, can be transformed into Eq. 12.

$$FOS = f_5 \left[\frac{\sigma_{ci}}{\gamma H} f_4 \left(\frac{\gamma H}{\sigma_{ci}}, m_b, s, a, \beta \right) \right] \quad (12)$$

The parameters m_b , s and a in Eq. 12 can be calculated from Eqs. 2 to 4, respectively. Finally, the FOS can be expressed as Eq. 13

$$FOS = f_6 \left(\frac{\sigma_{ci}}{\gamma H}, GSI, m_i, D, \beta \right) = f_6 (SR, GSI, m_i, D, \beta) \quad (13)$$

Eq. 13 illustrates the fact that when the values of GSI, m_i and D are given in a homogeneous slope, along with the slope angle β , the FOS of a slip surface for a particular method of slices is uniquely related to the dimensionless parameter SR regardless of the magnitude of individual parameters σ_{ci} , γ and H .

Table 3 shows three different groups of σ_{ci} , γ and H associated with the same SR value for a slope that has the same values of GSI, m_i , D and β . The values of FOS were calculated using four limit equilibrium methods in *Slide 6.0* [25], with finite element method (FEM) conducted using the program *Phase² 8.0* [28].

Table 3 Comparison of the FOS of a given slope with the same value of SR

Input parameters	Group 1 [13]	Group 2	Group 3
GSI	30	30	30
m_i	8	8	8
D	0	0	0
$\beta, ^\circ$	60	60	60
σ_{ci} , MPa	20	25	250
γ , kN/m ³	23	28.75	23.96
H , m	25	25	300
$\sigma_{ci}/(\gamma H)$	34.783	34.783	34.783
Factor of safety			
Bishop simplified	2.026	2.026	2.026
Janbu simplified	1.934	1.934	1.934
Spencer	2.032	2.032	2.032
Morgenstern-Price	2.027	2.027	2.027
<i>Phase² 8.0</i> (FEM)	2.000	2.040	2.030

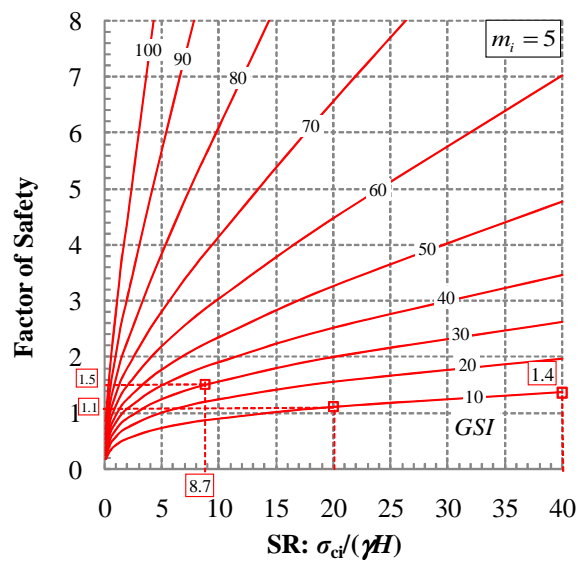
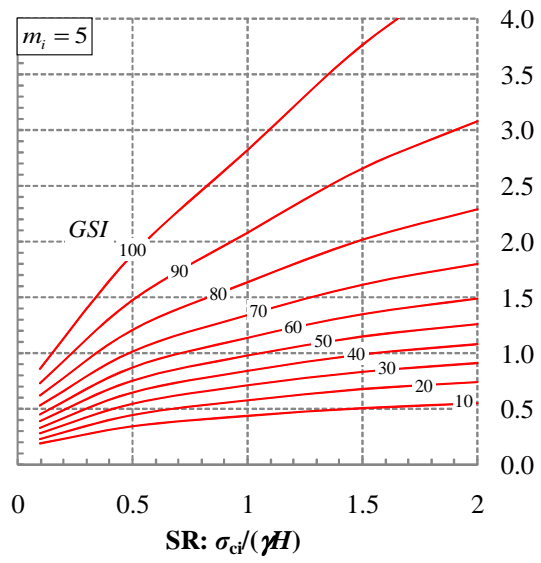
The results show that FOS values for all three groups are exactly the same. Results of the comparison of the FOS calculated for the three groups over a range of GSI and m_i are shown in Table 4. Again, the results reveal that the FOS of a slope depends only on the magnitude of SR when the values of β , GSI, m_i and D are the same. Based on the relationship between the SR and FOS, the number of independent parameters for calculating the FOS can be reduced to four (SR, GSI, m_i and β) when $D = 0$. In the next stage, we will propose the rock slope stability charts based on the SR, GSI and m_i for slopes with $\beta = 45^\circ$, $D = 0$.

Table 4 Comparison of the FOS of a given rock slope with various Hoek-Brown parameters.

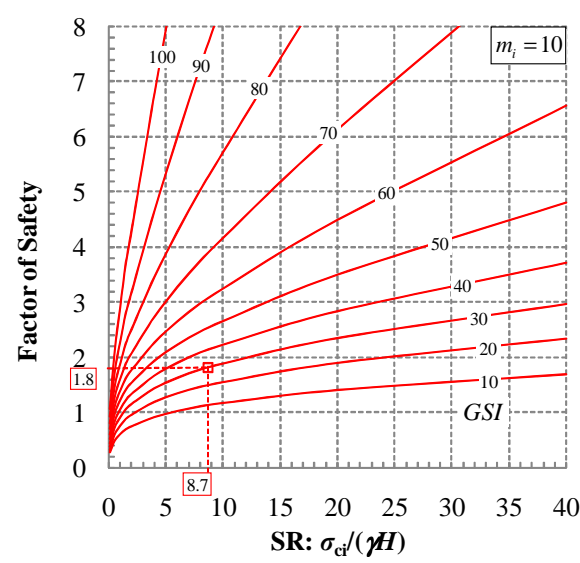
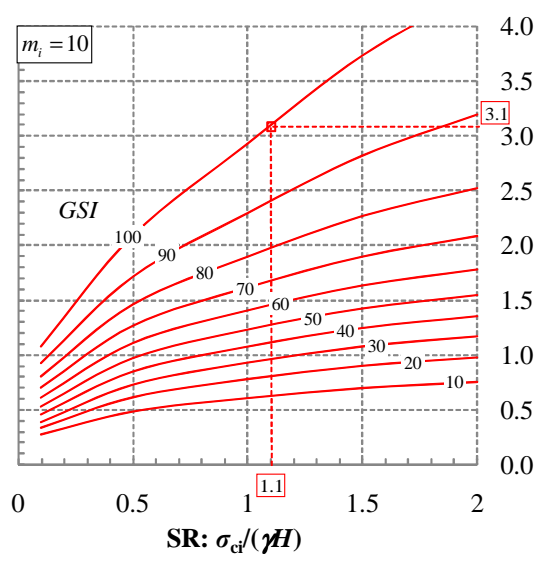
Hoek-Brown parameters		Group 1	Group 2	Group 3
GSI	m_i	FOS	FOS	FOS
10	5	0.958	0.958	0.958
10	15	1.326	1.326	1.326
10	25	1.547	1.547	1.548
10	35	1.705	1.705	1.706
40	5	2.532	2.532	2.532
40	15	2.819	2.819	2.819
40	25	3.043	3.043	3.043
40	35	3.227	3.227	3.227
100	5	46.854	46.854	46.856
100	15	30.840	30.840	30.842
100	25	25.540	25.540	25.542
100	35	22.753	22.753	22.755

3.2 Slope stability charts based on slope angle $\beta = 45^\circ$

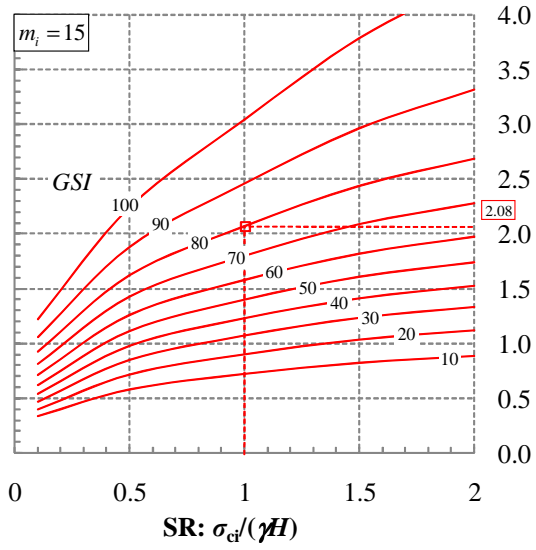
The examination of 54 slope case histories [20] from Iran and Australia shows that the average slope angle is 46.3° . Therefore, firstly, the proposed stability charts for the current study were based on the GHB criterion from a range of SR, GSI and m_i , but with a specified slope angle $\beta = 45^\circ$ and $D = 0$ as shown in Fig. 5.



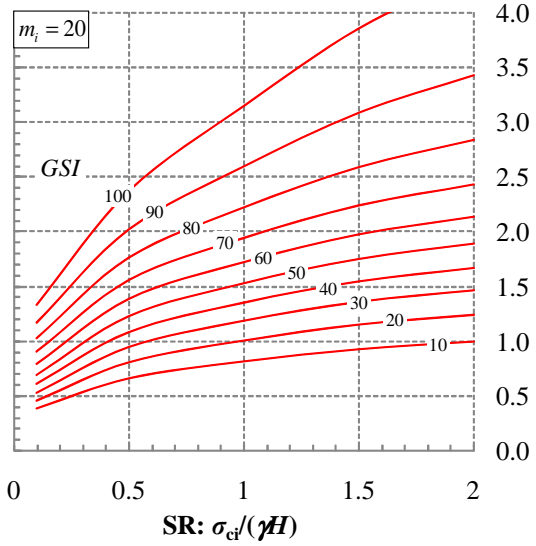
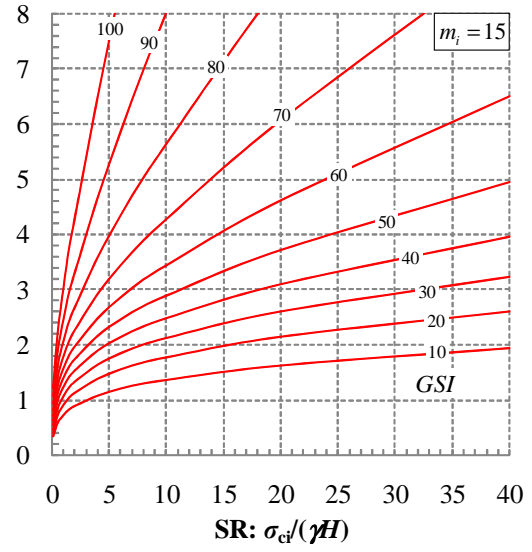
(a)



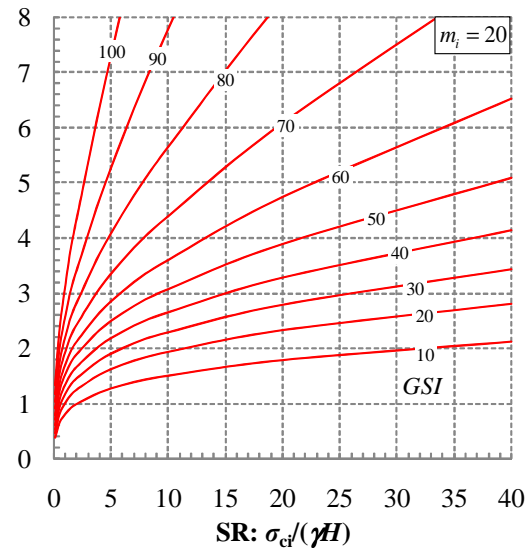
(b)

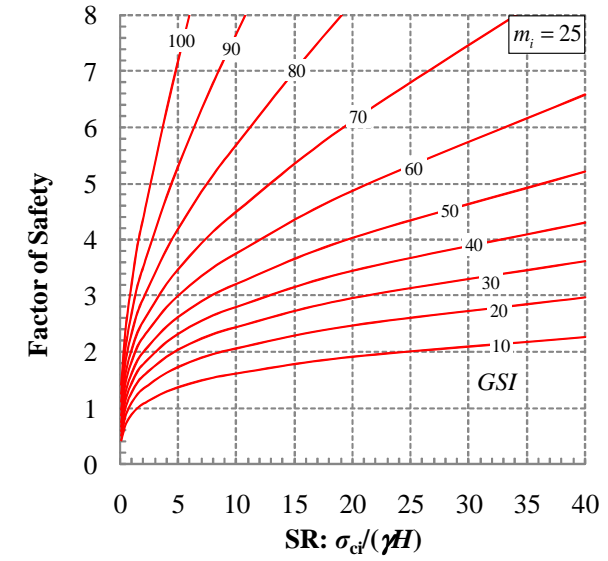
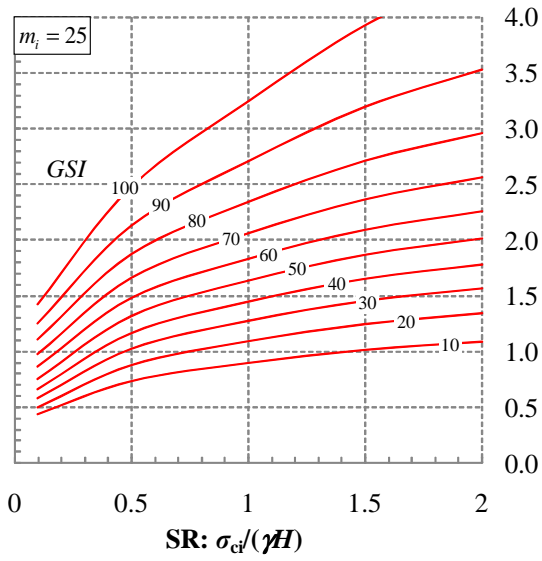


(c)

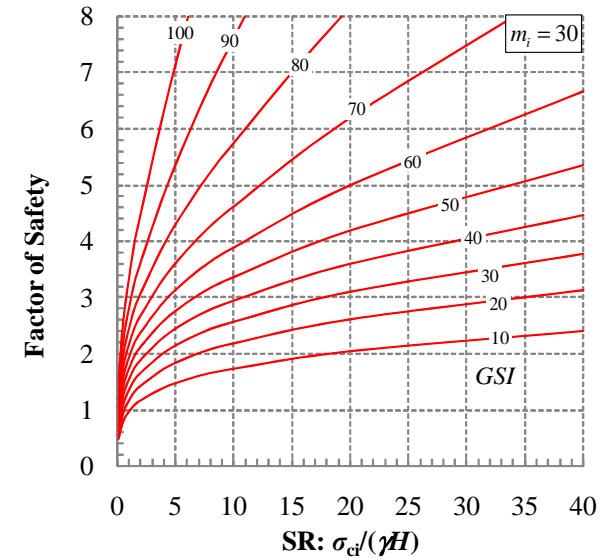
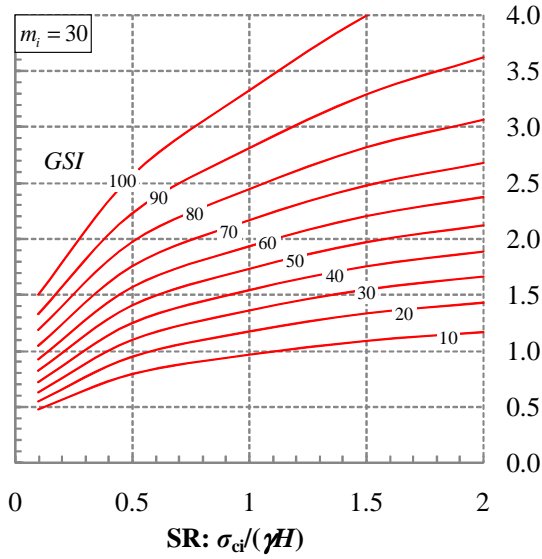


(d)

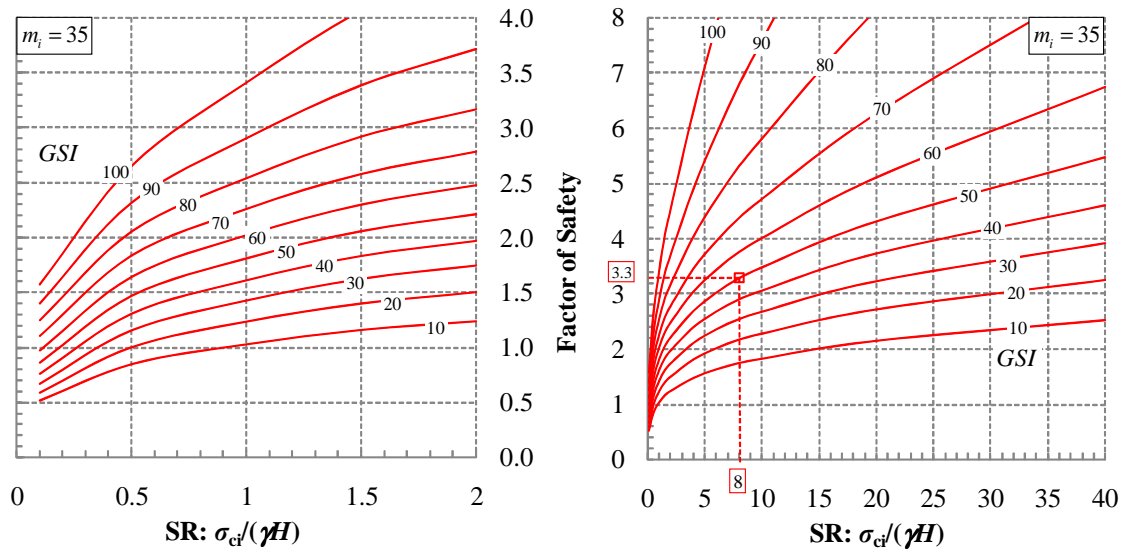




(e)



(f)



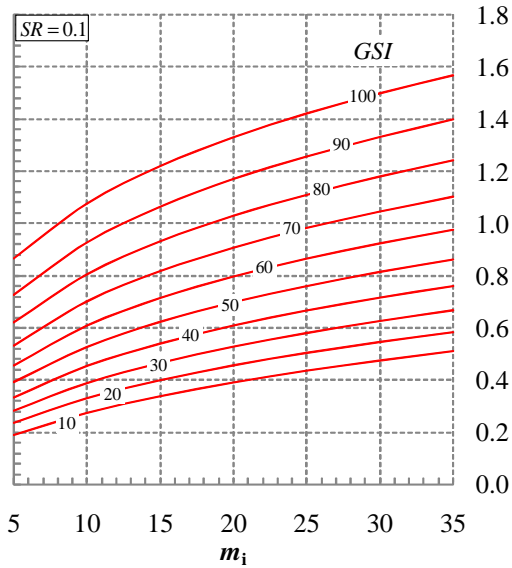
(g)

Fig. 5 Proposed stability charts for rock mass slope, $\beta=45^\circ$, $D=0$ ($5 \leq m_i \leq 35$)

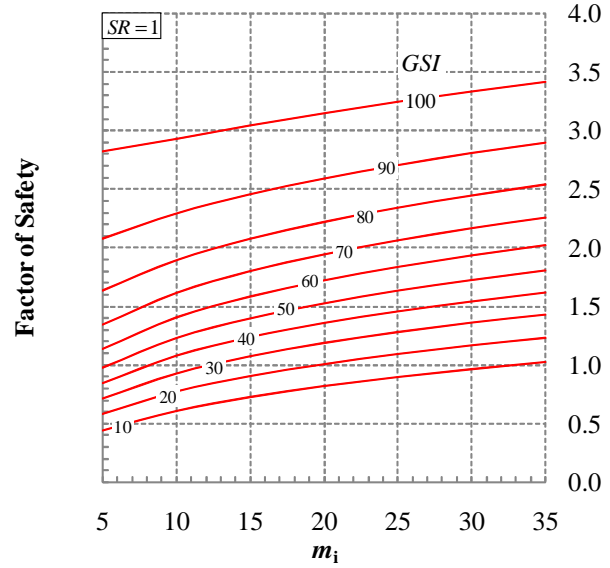
Fig. 5 indicates that there is a clear trend of the increase of FOS with the increase of GSI and SR. For example, increasing GSI values from 10 to 100 when SR=1, the values of FOS increase from 0.45 to 2.80 as shown in Fig. 5a. It is also found that SR has a considerable effect on the FOS, especially, under the state of high GSI values. For example, when GSI=90, the values of FOS are equal to 3.1 for SR=2 and increase to 5.7 for SR=5 in Fig. 5a. On the other hand, under the state of low GSI values, there is a moderate increase of FOS with the increase of SR. For instance, when GSI=10, the value of FOS is equal to 1 for SR=15, and FOS increase to 1.4 for SR=40 as shown in Fig. 5a.

Alternative form of stability charts are shown in Fig. 6. We can see that, overall, the FOS increase with the increase of m_i values. However, at the state of high GSI and SR values, the FOS decrease with the increase of m_i values as shown in Fig. 6 (c) and (d). This phenomenon can be explained by Fig. 7 [29], which illustrates the relationship between the Mohr-Coulomb shear strength parameters and Hoek-Brown parameters GSI and m_i values. It is clear that the values of

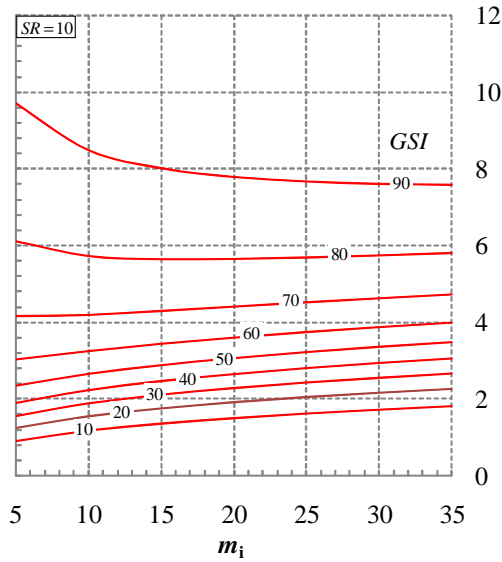
cohesion decrease with the increase of m_i values when $60 < GSI < 90$. Therefore, the resisting shear strength will decrease, which leads to the decrease of FOS, when m_i values increase in these specified cases.



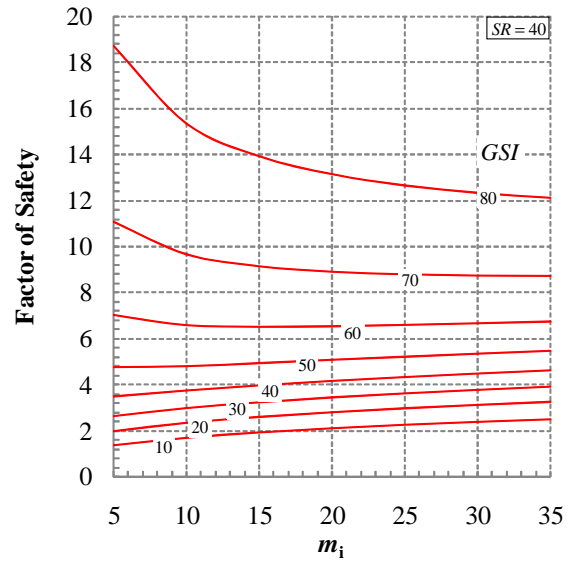
(a)



(b)



(c)



(d)

Fig. 6 Proposed stability charts for rock mass slope, $\beta=45^\circ$, $D=0$ (SR=0.1, 1, 10, 40)

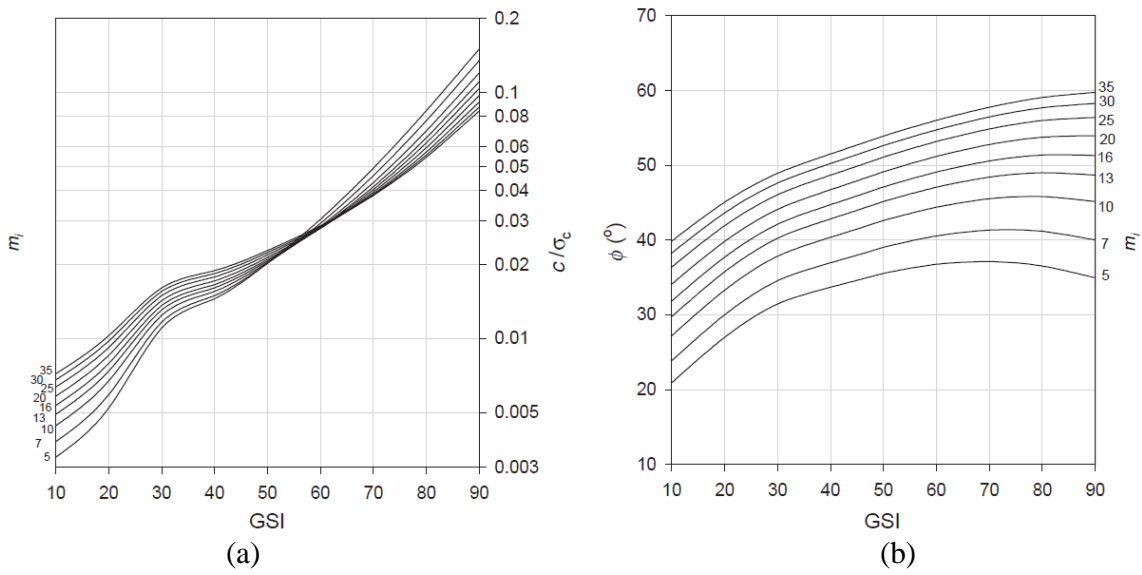


Fig. 7 (a) Relationship between c/σ_{ci} and GSI for different m_i values [29], (b) Relationship between ϕ and GSI for different m_i values [29]

Fig. 8 is an alternative form of Fig. 6a using the stability number N proposed by Li et al. [13]. It should be noted that the values of N obtained from Fig. 8 are different from Fig. 3a, as the FOS calculated from limit equilibrium method are generally not equal to those from limit analysis [24].

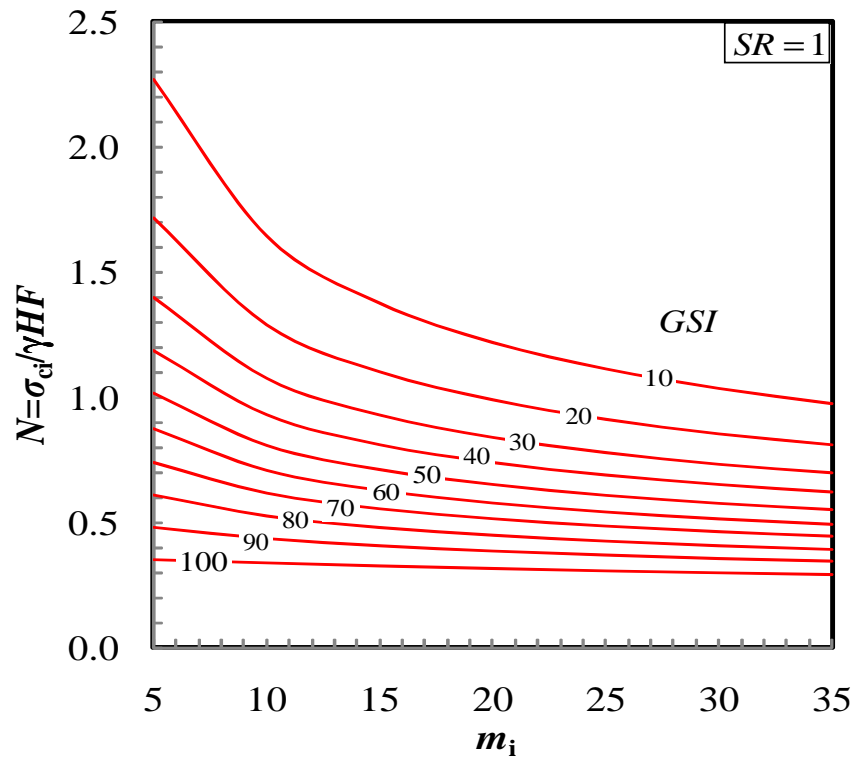


Fig. 8 Alternative form of Fig. 6b using the stability number N

3.3 The disturbance weighting factor f_D

Practical experience in the design of large open pit slopes has demonstrated that the estimation of rock mass properties from the HB criterion are too optimistic when $D = 0$ because of the realities of rock mass disturbance. Therefore, Hoek et al. [8] introduced the disturbance factor D , which can vary from zero for undisturbed in situ rock masses to one for highly disturbed rock masses, to consider the effects of heavy blast damage as well as stress relief result in disturbance of the rock mass.

It is not easy to determine the exact value of D as various factors can influence the degree of disturbance in the rock mass. Hoek et al. [8], Hoek and Diederichs [30] and Hoek [31], therefore, presented a number of slope cases to illustrate how to choose an appropriate D value for practical application. In civil engineering, small scale rock slope blasting results in modest rock mass

damage, $D=1.0$ and 0.7 were recommended under poor blasting and good blasting, respectively. For folded sedimentary rocks in a carefully excavated road cutting, $D = 0.3$ is suggested since the disturbance is relatively shallow. In mining engineering, large scale open pit mine slopes suffer significant disturbance under heavy production blasting, and $D = 1.0$ is the suggested value. For softer rocks under mechanical excavation, D is assumed to equal to 0.7 . However, these guidelines are based on a limited number of case histories, and it can be argued that they should be extended and modified by considering more cases obtained from practical applications [32].

Thus, in order to understand the real influence of D upon the stability of rock mass slopes, it is critical that researchers and engineers perform studies of a range of D values rather rely on the results from a single D analysis. As noted by Hoek and Diederichs [30], the sensitivity analysis of a design is probably more significant in judging the acceptability of the design than a single calculated FOS.

The current study, therefore, proposes a disturbance weighting factor f_D to use in refining the influence of D upon the stability of rock mass slopes. The first step in proving the importance of factor f_D in determining the influence of D in calculating the FOS is to assume a disturbance factor D from 0 to 1, using the same values of GSI, m_i , SR and β as those found in the slope models in section 3.2 with $D = 0$. Fig. 9 illustrates the relationship between D and f_D for a slope with SR = 10 and $\beta = 45^\circ$. It is found that the minimum value of $m_i = 5$ and the maximum value of $m_i = 35$ generates a narrow range of f_D , which indicates that the value of m_i has an insignificant influence upon the estimation of f_D . For example, for a slope with GSI = 10, SR = 10, $\beta = 45^\circ$, $D = 0.7$, increasing m_i from 5 to 35 only results in an increase in f_D from 0.42 to 0.48.

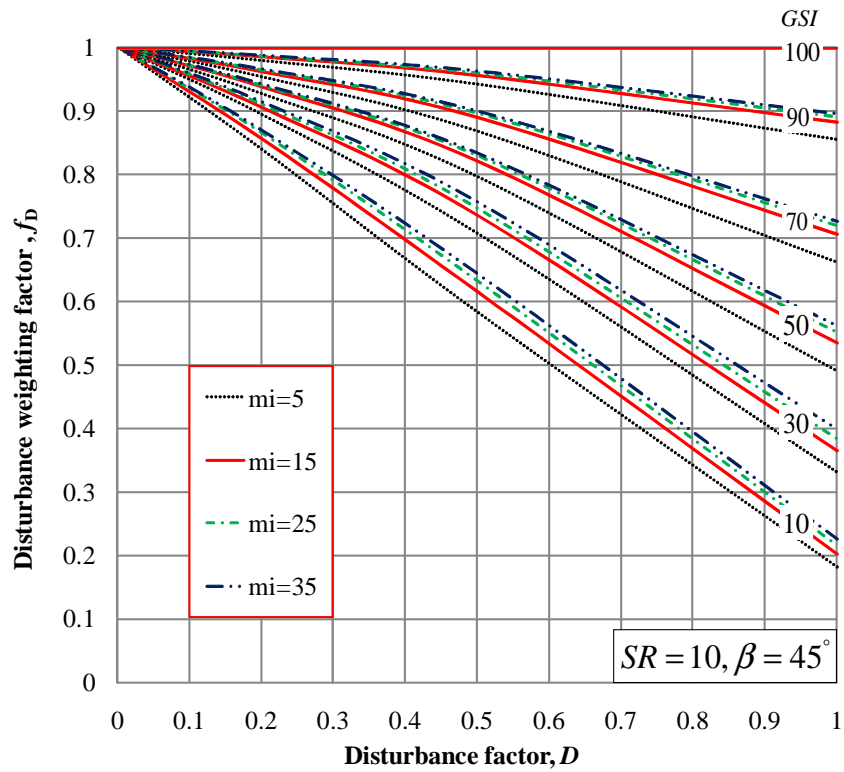
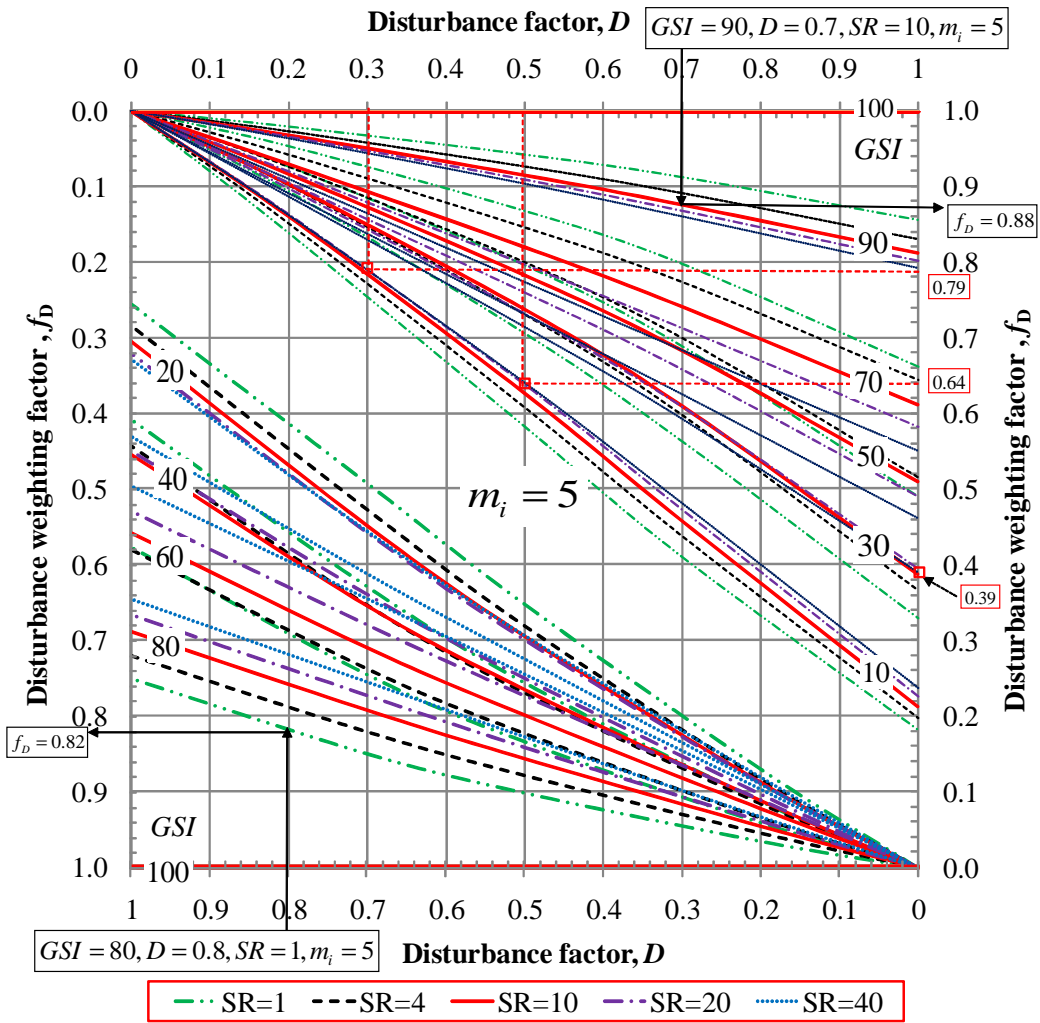
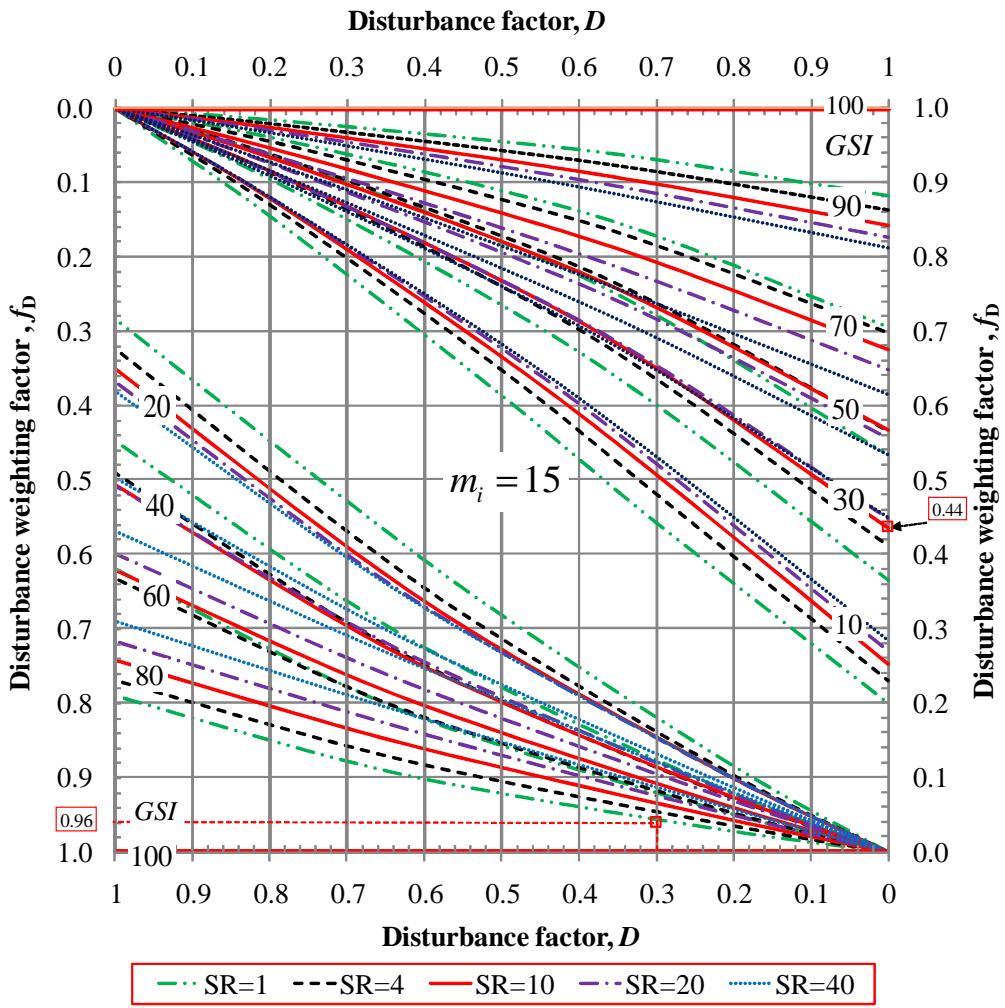


Fig. 9 Chart for estimating disturbance weighting factor f_D , $SR=10$, $\beta=45^\circ$

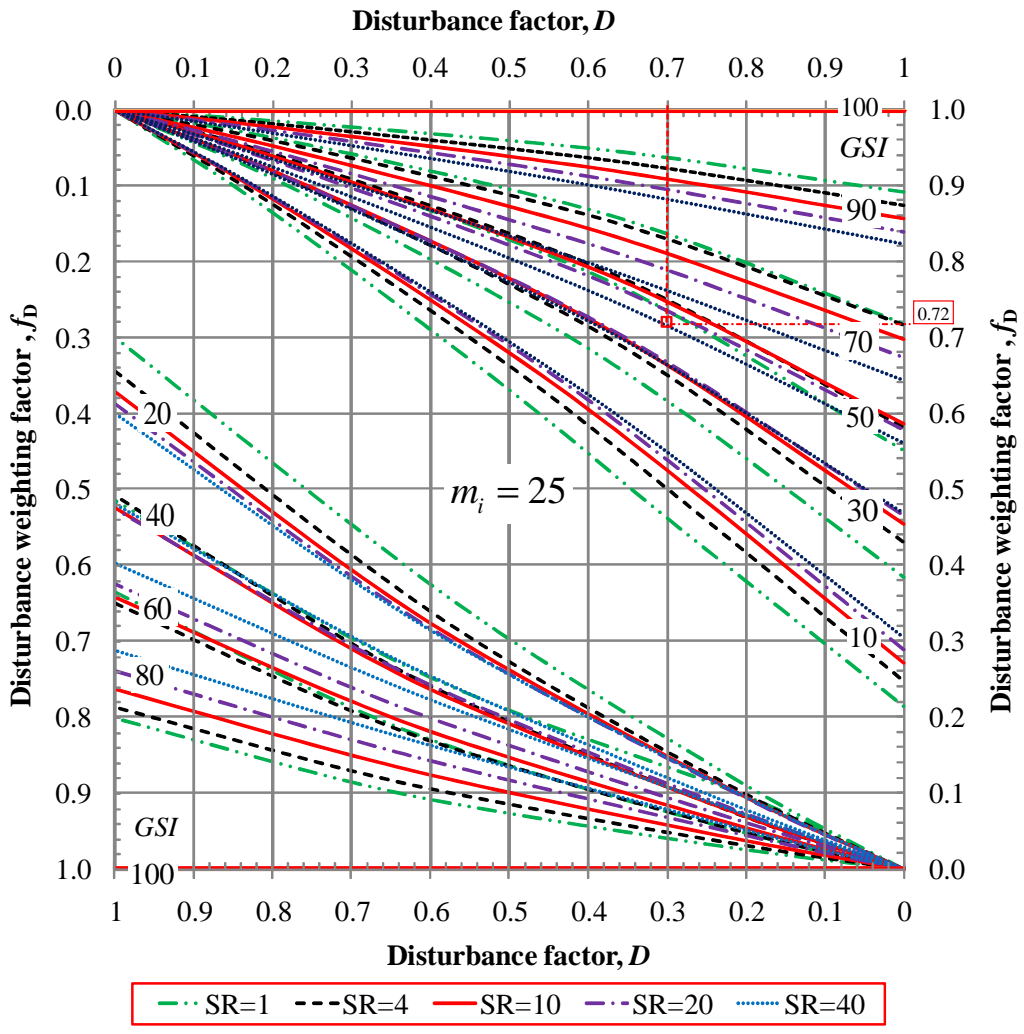
By considering the limit influence of m_i on the estimation of f_D , charts representing the relationship between f_D and D based on $m_i = 5, 15, 25$ and 35 were proposed, as shown in Fig. 10. The use of Fig. 10 to calculate the value of f_D is easy. For example, for a given slope with $GSI=90$, $D=0.7$, $SR=10$ and $m_i=5$, the value of f_D is equal to 0.88 as shown in Fig. 10a.



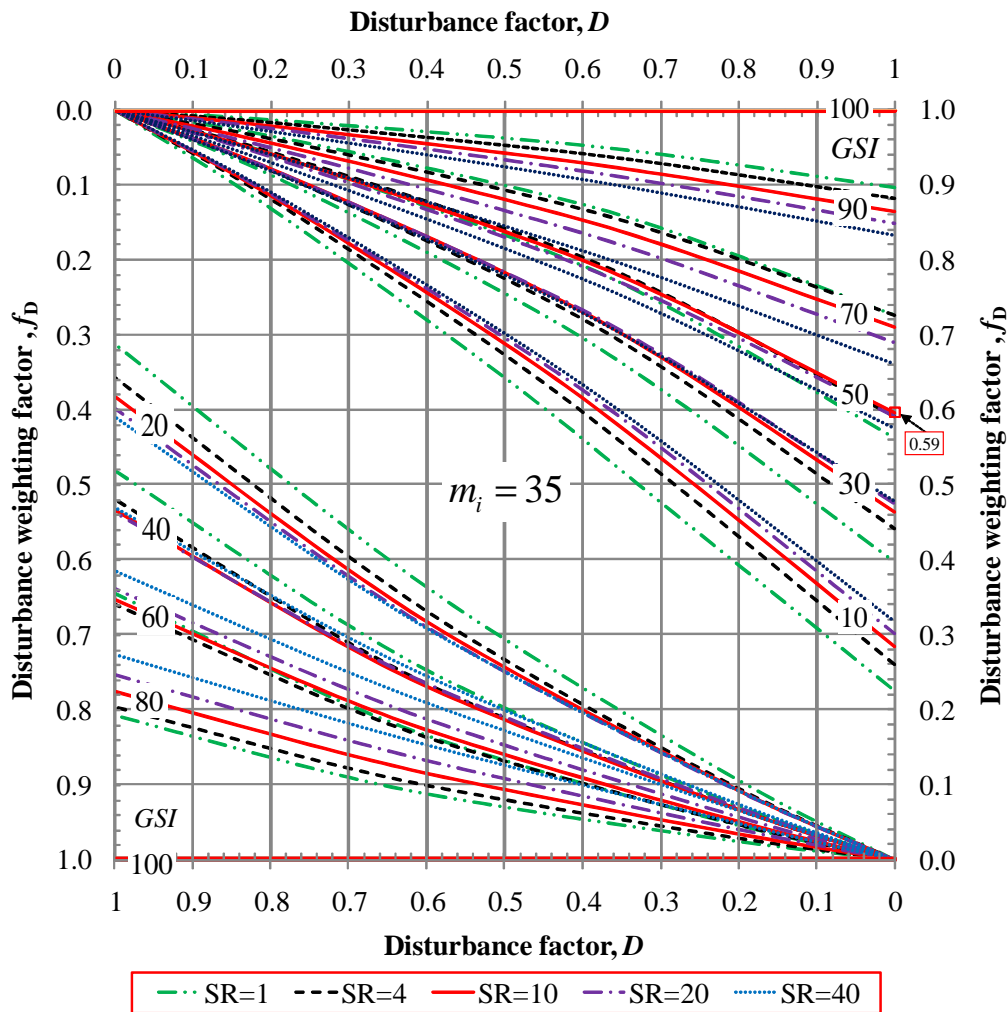
(a)



(b)



(c)



(d)

Fig. 10 Chart for estimating disturbance weighting factor, f_D ($m_i=5, 15, 25, 35$)

3.4 The slope angle weighting factor f_β

The values of FOS_{45° estimated directly from the data in Fig. 5 are based on a slope angle $\beta = 45^\circ$. In order to examine the influence on the FOS of the slope angle, it was necessary to test the slope models using angles of different values. Slope angle β was assigned values ranging from 30° to 75° while the values of the GSI, m_i , D and SR are the same as slope models with $\beta = 45^\circ$.

After hundreds of computer runs using a wide range of rock mass properties and slope geometry, a chart representing the relationship between the slope angle weighting factor f_β and the slope angle β was proposed based on the data $0 < FOS < 4$, which will be applicable for most civil and mining slope cases, as shown in Fig. 11. By adopting a curve fitting strategy, a simplified equation was developed, as shown in Eq. 14.

$$f_\beta = 2.66e^{-0.022\beta} \quad (14)$$

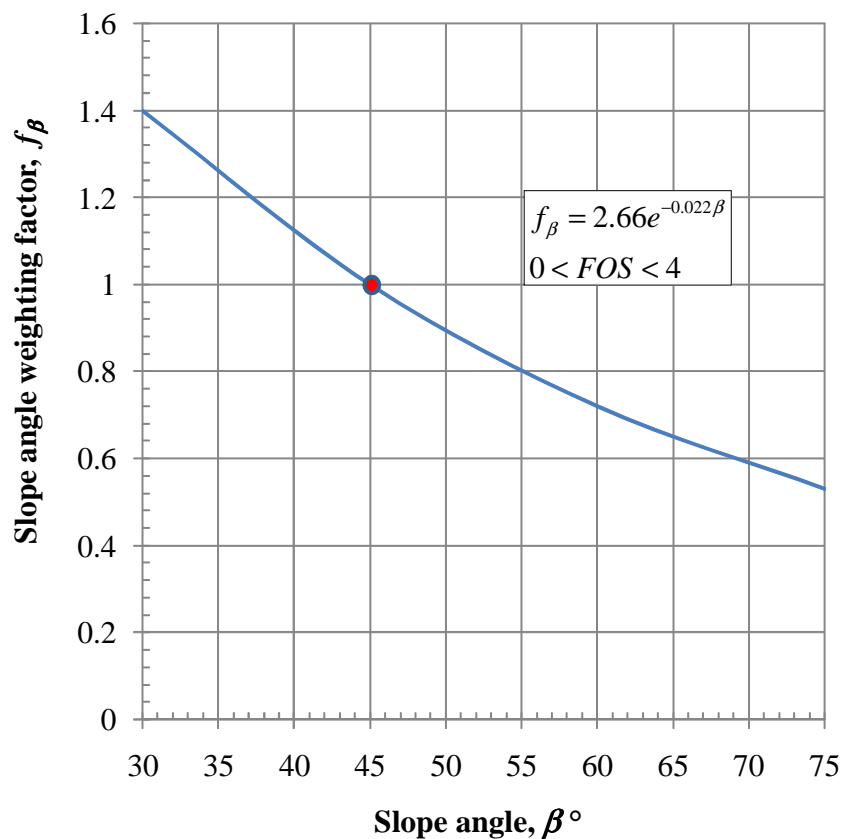


Fig. 11 Slope angle weighting factor chart

Combined with the stability charts (Figs. 5 and 10), the slope angle weighting factor chart or Eq. 14 can be used for estimating the FOS of a slope with various given slope angle β estimated from real cases.

Compared with the values calculated in *Slide 6.0*, the values of the FOS estimated from Fig. 11 show some discrepancy. The prediction performance of Fig. 11 was tested using 1680 sets of data. The discrepancy result shows that 78.6% of the data is lower than $\pm 5\%$, while the absolute average relative error percentage (AAREP) is 3.1%, and the maximum discrepancy percentage (DP_{Max}) is -18.9% as shown in Fig. 12. It was also found that the data with a discrepancy greater than $\pm 10\%$ appears when $GSI > 90$.

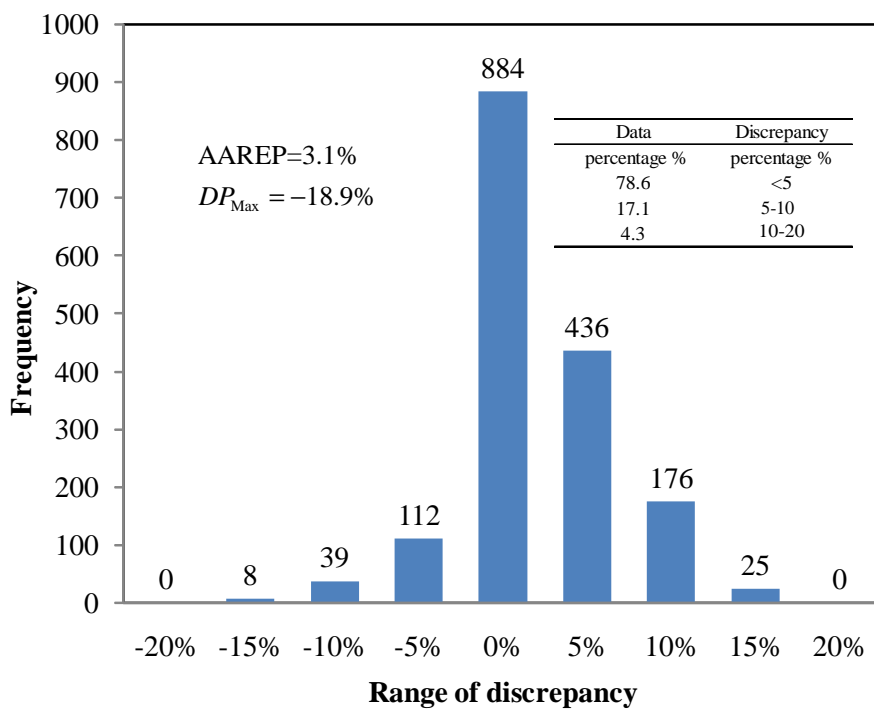


Fig. 12 Discrepancy analysis of the proposed rock slope stability charts

Fig. 11 can also be used in conjunction with the Carranza-Torres [12] slope stability chart shown in Fig. 2, which is based on $\beta = 45^\circ$, for estimating the FOS of a slope with slope angles other than 45° . Example 2 [14] in Table 1, therefore, was reanalyzed using the chart from Fig. 2 together with f_β from Fig. 11. Using the Fig. 2, results in the $FOS_{45^\circ} = 0.62$. Using the data from

Fig. 11, the slope angle weighting factor $f_{\beta} = 0.72$. Finally, the FOS = $f_{\beta} \times \text{FOS}_{45^{\circ}} = 0.72 \times 0.62 = 0.446$, which is slightly different from the FOS = 0.489 calculated using *Slide 6.0*.

3.5 The use of the proposed stability charts

The use of the proposed rock slope stability charts to calculate the FOS of a given slope is quite straightforward. Firstly, for given values of SR, GSI and m_i , the value of $\text{FOS}_{45^{\circ}}$ can be obtained using the stability charts (Fig.5). Secondly, for any given disturbance factor D , the disturbance weighting factor f_D can be obtained from Fig. 10. Thirdly, for the given slope angle β , the slope angle weighting factor f_{β} can be calculated from Eq. 14 or obtained from Fig. 11. Finally, the FOS can be calculated as, $\text{FOS} = f_{\beta} \times f_D \times \text{FOS}_{45^{\circ}}$

Example 2 [14] in Table 1 was again adopted to illustrate the use of the proposed charts. The calculation steps are as follows: Firstly, $m_i = 5$ from Fig. 5a and $m_i = 10$ from Fig. 5b were used to estimate the average value of the FOS for $m_i = 8$. The values of $\text{FOS}_{45^{\circ}}$ for $m_i = 5$ and $m_i = 10$ are 1.5 and 1.8, respectively. Therefore, the average value of $\text{FOS}_{45^{\circ}}$ for $m_i = 8$ was assumed to equal to 1.65. Then, $m_i = 5$ from Fig. 10a and $m_i = 15$ from Fig. 10b were used to estimate the average value of f_D for $m_i = 8$. The values of f_D for $m_i = 5$ and $m_i = 15$ are 0.39 and 0.44, respectively. Thus, the value of f_D for $m_i = 8$ should be located between 0.39 and 0.44. Thirdly, slope angle weighting factor f_{β} for $\beta = 60^{\circ}$ was estimated using the chart (Fig.11) or Eq. 14, with the result $f_{\beta} = 0.72$. Finally, the lower and upper values of the FOS can be calculated. The results were $\text{FOS}_{\text{Lower}} = f_{\beta} \times f_{D\text{-Lower}} \times \text{FOS}_{45^{\circ}} = 0.72 \times 0.39 \times 1.65 = 0.463$ and $\text{FOS}_{\text{Upper}} = f_{\beta} \times f_{D\text{-Upper}} \times \text{FOS}_{45^{\circ}} = 0.72 \times 0.44 \times 1.65 = 0.522$. The result provided by *Slide 6.0* was FOS = 0.489.

4 Case studies for the proposed charts

The following three examples with a wide range of rock properties and slope geometry were used to illustrate the practical application of the proposed rock slope stability charts. The results are shown in Table 5.

Example 1: A small slope consisting of highly fractured rock masses with the following input parameters: $\sigma_{ci} = 2.7\text{MPa}$, $\text{GSI} = 10$, $m_i = 5$, $\gamma = 27\text{kN/m}^3$, $H = 5\text{m}$ and $\beta = 30^\circ$, $D = 0.5$. Example 2: A medium slope consisting of good quality rock masses with the following input parameters: $\sigma_{ci} = 0.625\text{MPa}$, $\text{GSI} = 80$, $m_i = 15$, $\gamma = 25\text{kN/m}^3$, $H = 25\text{m}$ and $\beta = 75^\circ$, $D = 0.3$. Example 3: A large open pit slope consisting of blocky rock masses with the following input parameters: $\sigma_{ci} = 46\text{MPa}$, $\text{GSI} = 50$, $m_i = 35$, $\gamma = 23\text{kN/m}^3$, $H = 250\text{m}$ and $\beta = 60^\circ$, $D = 1.0$. The results show that there is close agreement between the proposed stability chart and the *Slide 6.0* results. The discrepancy percentages for examples 1 to 3 are -3.84%, 1.27% and 0.78%, respectively.

Table 5 Three slope examples analyzed using the proposed stability charts.

Input parameters	Example 1	Example 2	Example 3
σ_{ci} , MPa	2.7	0.625	46
GSI	10	80	50
m_i	5	15	35
γ , kN/m ³	27	25	23
H , m	5	25	250
β , °	30	75	60
D	0.5	0.3	1
Calculated data			
SR: $\sigma_{ci}/\gamma H$	20	1	8
FOS _{45°}	1.1	2.08	3.3
f_D	0.64	0.96	0.59
f_β	1.4	0.53	0.72
Factor of safety			
Proposed charts	0.986	1.058	1.402
<i>Slide 6.0</i>	1.025	1.045	1.391
Discrepancy	-3.84%	1.27%	0.78%

5 Conclusions

New rock slope stability charts for estimating of the stability of rock mass slopes satisfying the GHB criterion have been proposed. The proposed charts can be used to calculate the FOS of a slope directly from the Hoek-Brown parameters (GSI , m_i and D), slope geometry (β and H) and rock mass properties (σ_{ci} and γ).

Firstly, the theoretical relationship between the strength ratio (SR), $\sigma_{ci}/(\gamma H)$ and the FOS has been demonstrated. It is found that when the values of β , GSI , m_i and D in a homogeneous slope are given, the FOS of a slip surface for a particular method of slices is uniquely related to the parameter SR regardless of the magnitude of the individual parameters σ_{ci} , γ and H . Based on the relationship between the SR and FOS, stability charts as shown in Fig. 5 for calculating the FOS of a slope with specified slope angle $\beta = 45^\circ$, $D = 0$ have been proposed.

Secondly, while the disturbance factor D has great influence upon the stability of rock mass slopes, it is, nevertheless, difficult to determine its exact value. Yet a sensitivity analysis of D is probably more significant in judging the acceptability of a slope design than a single calculated FOS with specified D values estimated from the guidelines by [8, 30, 31]. We proposed a disturbance weighting factor f_D as shown in Fig. 10 to show the influence of a range of values of D upon the stability of rock mass slopes.

Thirdly, a slope angle weighting factor f_β has been proposed to show the influence of the slope angle β on slope stability. It should be noted that the chart, as shown in Fig. 11, representing the relationship between f_β and β was proposed based on the data $0 < \text{FOS} < 4$, however, it will be applicable for most civil and mining slope cases.

Combined with stability charts based on $\beta = 45^\circ$, the values of f_β and f_D can be used for estimating the FOS of slopes with various angles in a variety of blast damage and stress relief conditions. The reliability of the proposed charts has been tested against results from *Slide 6.0* using 1680 sets of data representing a wide range of rock mass properties and slope geometries. The results show that there is good agreement between the values of the FOS as calculated from the charts and those produced by *Slide 6.0*, as shown in Fig. 12. The discrepancy of 78.6% of data is lower than $\pm 5\%$, and the absolute average relative error percentage (AAREP) is 3.1%. In addition, it is found that the data with a discrepancy of more than $\pm 10\%$ appear when $GSI > 90$.

The proposed charts are quite simple and straightforward to use and can be adopted as a useful tool for the preliminary rock slope stability analysis.

Acknowledgements

The PhD scholarship provided by China Scholarship Council (CSC) to the first author is gratefully acknowledged. The authors would like to express their gratitude to the editor Prof. Robert W. Zimmerman and anonymous reviewer for their constructive comments on the manuscript. The authors are also grateful to Mrs Barbara Brougham for reviewing the manuscript.

References

- [1] Michalowski RL. Limit analysis and stability charts for 3D slope failures. *J. Geotech. Geoenviron. Eng.* 2010;136:583-93.
- [2] Taylor DW. Stability of earth slopes. *J. Boston Soc. Civil Eng.* 1937; XXIV(3): 337-86.
- [3] Jimenez R, Serrano A, Olalla C. Linearization of the Hoek and Brown rock failure criterion for tunnelling in elasto-plastic rock masses. *Int. J. Rock Mech. Min. Sci.* 2008;45:1153-63.
- [4] Sheorey PR. Empirical rock failure criteria. Rotterdam: Balkema;1997.

- [5] Fu W, Liao Y. Non-linear shear strength reduction technique in slope stability calculation. *Comput. Geotech.* 2010; 37: 288-98.
- [6] Shen J, Priest SD, Karakus M. Determination of Mohr-Coulomb shear strength parameters from Generalized Hoek-Brown criterion for slope stability analysis. *Rock Mech. Rock Eng.* 2012; 45:123-29.
- [7] Hoek E, Brown ET. *Underground excavations in rock.* London: Instn. Min. Metall;1980.
- [8] Hoek E, Carranza-Torres C, Corkum B. Hoek-Brown failure criterion - 2002 Edition. In: *Proceedings of NARMS-TAC, Mining Innovation and Technology.* Toronto; 2002.
- [9] Priest SD. Determination of shear strength and three-dimensional yield strength for the Hoek-Brown criterion. *Rock Mech. Rock Eng.* 2005; 38(4): 299-327.
- [10] Baker R. A second look at Taylor's stability chart. *J. Geotech. Geoenviron. Eng.* 2003; 129 (12): 1102-8.
- [11] Hoek E, Bray JW. *Rock slope engineering.* 3rd edition. London: Instn. Min. Metall; 1981.
- [12] Carranza-Torres C. Some comments on the application of the Hoek- Brown failure criterion for intact rock and rock masses to the solution of tunnel and slope problems. In: G. Barla and M. Barla (Eds.), *MIR 2004 - X Conference on Rock and Engineering Mechanics.* Torino; 24-25 November 2004. p. 285-326.
- [13] Li AJ, Merifield RS, Lyamin AV. Stability charts for rock slopes based on the Hoek-Brown failure criterion. *Int. J. Rock Mech. Min. Sci.* 2008; 45(5):689-700.
- [14] Li AJ, Merifield RS, Lyamin AV. Effect of rock mass disturbance on the stability of rock slopes using the Hoek-Brown failure criterion. *Comput. Geotech.* 2011; 38: 546-58.
- [15] Li AJ, Lyamin AV, Merifield RS. Seismic rock slope stability charts based on limit analysis methods. *Comput. Geotech.* 2009; 36:135-48.
- [16] Zambak C. Design charts for rock slopes susceptible to toppling. *J. Geotech. Eng. Div. ASCE.* 1983;190(8):1039-62.
- [17] Naghadehi M, Jimenez R, KhaloKakaie R, Jalali S. A new open-pit mine slope instability index defined using the improved rock engineering systems approach. *Int. J. Rock Mech. Min. Sci.* 2013; 61: 1-14.

- [18] Steward T, Sivakugan N, Shukla SK, Das BM. Taylor's slope stability charts revisited. *International Journal of Geomechanics*. 2011; 11(4): 348-52.
- [19] Wyllie DC, Mah C. *Rock slope engineering: civil and mining*. 4th edition. New York: Spon Press; 2004.
- [20] Taheri A, Tani K. Assessment of the stability of rock slopes by the slope stability rating classification system. *Rock Mech. Rock Eng.* 2010; 43: 321-33.
- [21] Baker R, Shukha R, Operstein V, Frydman S. Stability charts for pseudo-static slope stability analysis. *Soil. Dynam. Earthquake. Eng.* 2006; 26:813-23.
- [22] RocData 4.0. www.rocscience.com.
- [23] Bishop W. The use of the slip circle in the stability analysis of earth slopes. *Geotechnique*. 1955;5 (1): 7-17.1177
- [24] Li AJ, Cassidy MJ, Wang Y, Merifield RS, Lyamin AV. Parametric Monte Carlo studies of rock slopes based on the Hoek-Brown failure criterion. *Comput. Geotech.* 2012; 45:11-8.
- [25] Slide 6.0. www.rocscience.com.
- [26] Muirwood AM. Tunnels for road and motorways. *Q. J. Eng. Geol.* 1972; 5: 111-26.
- [27] Shen J, Karakus M, Xu C. Direct expressions for linearization of shear strength envelopes given by the Generalized Hoek-Brown criterion using genetic programming. *Comput. Geotech.* 2012; 44: 139-46.
- [28] Phase² 8.0. www.rocscience.com.
- [29] Cai M, Kaisera PK, Uno H, Tasaka Y, Minami M. Estimation of rock mass deformation modulus and strength of jointed hard rock masses using the GSI system. *Int. J. Rock Mech. Min. Sci.* 2004; 41:3-19.
- [30] Hoek E, Diederichs MS. Empirical estimation of rock mass modulus. *Int. J. Rock Mech. Min. Sci.* 2006; 43:203-15.
- [31] Hoek E. Rock mass properties. *Practical Rock Engineering*. 2007. http://www.rocscience.com/hoek/pdf/11_Rock_mass_properties.pdf .

- [32] Sonmez H, Gokceoglu C. Discussion of the paper by E. Hoek and M.S. Diederichs “Empirical estimation of rock mass modulus”. *Int. J. Rock Mech. Min. Sci.* 2006; 43: 671-76.

Chapter 7

Conclusions and Recommendations for Further Work

Rock slope stability is one of the major challenges of rock engineering projects, such as open pit mining. Rock slope failure can affect mining operations and result in costly losses in terms of time and productivity. Therefore, the evaluation of the stability of rock slopes is a critical component of open pit design and operation. The rock slope stability is predominantly controlled by the rock mass strength which is a non-linear stress function. However, when limit equilibrium method (LEM) and shear strength reduction (SSR) method are used to analyze rock slope stability, the strength of the rock mass is generally expressed by the linear Mohr-Coulomb (MC) criterion. It is known that the MC criterion is linear, therefore, it does not agree with the rock mass failure envelope very well.

This research focuses on the application of the Hoek-Brown (HB) criterion, which can ideally represent the non-linear behavior of a rock mass and has been successfully applied in the field of rock mechanics for over 30 years, on the rock slope stability analysis. The major research contributions and outcomes of the thesis are listed as follows:

- A new method that can estimate the HB constant m_i values using only UCS and rock types has been proposed. The reliability of the proposed method has been evaluated using 908 sets of triaxial tests together with our laboratory tests for five common rock types. Results from the comparison have shown that m_i values calculated from the proposed method can reliably be used in the HB criterion for predicting intact rock strength without triaxial test data which require expensive and time-consuming testing procedures. Simplified empirical equations for estimating deformation modulus of rock mass E_m also

have been proposed by adopting Gaussian function to fit the *in-situ* data. It has been demonstrated that the proposed equations fit well to the *in-situ* data compared with the existing equations.

- Analytical solutions that can be used to estimate the instantaneous MC parameters angle of friction ϕ and cohesion c from the HB input parameters (GSI, m_i, D, σ_{ci}) have been proposed. The proposed solutions can be implemented into the LEM to calculate the instantaneous shear strength of each slice of a failure surface under a given normal stress. It also can be used in conjunction with numerical modeling performed by SSR technique to calculate the instantaneous shear strength of elements under various stress states.
- A new non-linear SSR method has been proposed to analysis the stability of 3D rock slopes satisfying the HB failure criterion. This method is based on estimating the instantaneous MC shear strength parameter c and ϕ values from the HB criterion for elements in FLAC^{3D} model. Then, the proposed 3D slope model has been used to analyse the influence of boundary condition on the calculation of FOS using 21 real open pit cases having various slope geometries and rock mass properties. A boundary weighting factor, f_B has been introduced to investigate the correlation of FOS under different boundary conditions. Results have illustrates that the effect of boundary conditions on the FOS values are more obvious for the slope with low slope angle than steep slope. The values of $f_{B,xy}$ and $f_{B,xyz}$ will go up to 1.7 and 1.5 when slope angle is less than 35°. On the other hand, when the slope angle is more than 50° $f_{B,xy}$ and $f_{B,xyz}$ values tend to equal to 1.4 and 1.1, respectively.
- 2D slope stability analysis using LEM has been carried out. The value of FOS for a given slope is calculated based on estimating the instantaneous shear strength of slices of a slip

surface from the HB criterion. By analyzing the stability of various slopes having different geometries and rock mass properties, novel stability charts for assessing the stability of rock mass slopes have been proposed. The proposed charts are able to estimate the FOS for a slope directly from the HB parameters (GSI , m_i and D), slope geometry (β and H) and rock mass properties (σ_{ci} and γ). The proposed charts are simple and straightforward to use and can be adopted as useful tools for the preliminary rock slope stability analysis.

It should be noted that there are some limitations in the current research and further research recommendation are described as follows:

- The proposed empirical equations for predicting m_i and E_m values are based on the analysis of existing database and the reliability of estimation of these empirical equations depends on the quality and quantity of laboratory data. Therefore, the proposed empirical equations are open to further improvement as more testing data become available.
- The current 3D slope stability study is based on simple slope geometry. However, it is known that the slope geometry is more complex in reality. For example, the natural slope often has curvature, and round surface often appeared in open-pit mining design. Therefore, future work is required to consider the effect of complex geometries on 3D numerical model.
- The proposed 2D stability charts do not account for ground water conditions and seismic effects on the slope stability. In some situations, ground water level on the slope and earthquakes can be major factors for slope instability. Thus, further studies needs be conducted to investigate the effects of ground water and seismicity on the slope stability.